LA-2120

LOS ALAMOS SCIENTIFIC LABORATORY
OF THE UNIVERSITY OF CALIFORNIA ○ LOS ALAMOS NEW MEXICO

A PRACTICAL MANUAL ON THE MONTE CARLO METHOD FOR RANDOM WALK PROBLEMS

LEGAL NOTICE

Printed in USA. Price $5.50 Available from the

Office of Technical Services
U. S. Department of Commerce
Washington 25, D. C.

LA-2120
PHYSICS AND MATHEMATICS
(TID-4500, 13th Ed., Suppl.)

LOS ALAMOS SCIENTIFIC LABORATORY
OF THE UNIVERSITY OF CALIFORNIA LOS ALAMOS NEW MEXICO

REPORT WRITTEN: January 1957

REPORT DISTRIBUTED: December 18, 1957

A PRACTICAL MANUAL ON THE MONTE CARLO METHOD FOR RANDOM WALK PROBLEMS

Work done by:
E. D. Cashwell
C. J. Everett
O. W. Rechard

Report written by:
E. D. Cashwell
C. J. Everett

Contract W-7405-ENG. 36 with the U. S. Atomic Energy Commission

ABSTRACT

This report is written to serve as a guide to those persons who, having no previous experience with Monte Carlo methods, wish to apply these methods to their own problems. Particular emphasis is given to techniques which are useful in dealing with problems concerned with the diffusion of particles (and gamma rays) in material media of some complexity, both from a geometrical and a nuclear standpoint. Included as an appendix are brief summaries of a variety of problems of the above-mentioned type to which the methods described herein have been applied successfully.

FOREWORD

The present report is a summary of the Monte Carlo method as it applies to problems involving the interplay of neutrons and photons with bulk matter in geometric systems of varying complexity. It is intended to serve as an introduction and practical guide for the fast-growing group of people who are concerned with such systems.

A brief resumé of some of the unclassified problems successfully treated by the methods here outlined is included as an appendix and may serve to emphasize the practicality and flexibility of these sampling procedures. A similar resumé of some of the classified problems which have been handled is issued separately as LAMS-2121.

The general method was originally developed by Fermi, Ulam and von Neumann; many others have contributed special techniques and devices. No attempt has been made to give all sources in the text, and naturally no claims to originality are made for the procedures included.

CONTENTS

	Page
ABSTRACT	3
FOREWORD	5
CHAPTER I. BASIC PRINCIPLES	11
1. General nature of the problem	11
2. Outline of procedure	12
3. Production of random numbers	15
4. The fundamental principle of Monte Carlo	16
5. Application of the principle	21
CHAPTER II. THE SOURCE ROUTINE	25
1. Introduction	25
2. Particle parameters	27
3. Remarks on units	32
4. Space coordinates for source particles	33
a. Uniform source on an annulus of radii $R_o < R_1$	34
b. Uniform source in a spherical shell	34
c. Parallel-beam source incident on lateral cylindrical surface, or on a sphere	34
d. Isotropic point source external to cylinder	36
5. Direction coordinates for source particles	36
a. Isotropic source; u,v,w direction cosines	36
b. The cosine distribution	38
c. Isotropic and cosine sources in spherically symmetric systems	40
d. Isotropic point source external to cylinder	40
e. General distribution in half of direction-space	42
f. A prejudiced source	43
6. Energy of source particles	45
7. Other source parameters	46
8. Source for α-type calculations	46

Page

CHAPTER III. THE MEAN FREE PATH AND TRANSMISSION 49

1. The cross section concept 49
2. The mean free path 50
3. An example 53
4. "Small" systems and transmission 54
5. The "forced first collision" routine 56
6. Remark on the device in spherical problems 58
7. The transmission in subsequent history 61
8. Prejudiced first collision in "large" systems 61

CHAPTER IV. THE COLLISION OR ESCAPE ROUTINE 63

1. Introduction 63
2. A routine for the spherical shell 65
3. Reorientation formulas for the spherical shell . . . 68
4. Flux problems in spherical geometry 72
5. A routine for the finite cylinder 72
6. The finite cylindrical shell with central hole . . . 74
7. The spherical shell in absolute space 78
8. Slab geometry 80
9. Problems run in cycles of time $\Delta\tau$ 81

CHAPTER V. THE COLLISION ROUTINE FOR NEUTRONS 83

1. Introduction 83
2. Capture and selection of the type of collision . . . 84
3. Elastic collisions in general 89
4. The differential elastic scattering cross section . . 99
5. A routine for elastic scattering 102
6. Differential elastic cross section for the lab. system . 108
7. A weight device for elastic scattering 109
8. Fission 112
9. Inelastic (n-n) collisions in general 114
10. Inelastic (n-n) collisions on heavy nuclei 118
11. Inelastic (n-n) collision with Maxwell distribution . . 119
12. A combined transfer matrix for fissionable nuclei . . 121
13. Collisions shattering a nucleus 124
14. The (n-2n) reaction in deuterium 129
15. An (n-2n) reaction on heavy nuclei 132
16. Capture in a small zone 133
17. Capture by a "point" detector 136
18. Remarks on thermal neutrons 140
19. Remark on determination of photon sources 141

Page

CHAPTER VI. PHOTON COLLISIONS 143

1. Introduction 143
2. Basic concepts and constants 143
3. Compton collisions 144
4. The Klein-Nishina differential cross section 149
5. The photon energy distribution and Compton cross section 150
6. Photoelectric effect and pair production 153

CHAPTER VII. DIRECTION PARAMETERS AFTER COLLISION 155

1. Introduction 155
2. Formulas for the final direction cosines 155
3. Subroutine for the final direction cosines 161
4. Final direction w in slab or spherically symmetric case 163
5. Scattering isotropic in the laboratory system 164

CHAPTER VIII. TERMINAL CLASSIFICATION 165

1. Introduction 165
2. Classification of escapes on number of collisions . . . 165
3. Energy and angle distributions of escape 166

CHAPTER IX. REMARKS ON COMPUTATION 175

1. Scaling 175
2. Debugging 175
3. Special subroutines 177

   a. A random number routine 177
   b. Shifted random numbers 178
   c. A logarithm routine 179
   d. The exponential exp(- x/y) 182
   e. A cosine routine 183

4. A Monte Carlo device for $\sqrt{r}$ 186
5. A Monte Carlo device for the cosine of an equidistributed angle 187

CHAPTER X. STATISTICAL CONSIDERATIONS 189

1. The limit theorem in the Bernoulli case 189
2. Application to the terminal ratios 190
3. The central limit theorem 193
4. Application to problems using weights 195
5. Illustrative examples 197

Page

APPENDIX. SUMMARY OF CERTAIN PROBLEMS RUN ON MANIAC I 204

Introduction 204

Problem 1. Compton collisions in a spherical shell 205

Problem 2. Compton collisions in a solid sphere 205

Problem 3. Neutrons in a spherical shell 206

Problem 4. Energy independent scattering in a cylinder . . 207

Problem 5. Energy dependent scattering in a cylinder . . . 208

Problem 6. Cylindrical shell with parallel source 209

Problem 7. 14 Mev neutrons in a cylindrical shell 210

Problem 8. Cylindrical shell with point source 213

Problem 9. A scintillation counter 215

Problem 10. A "long counter" 216

Problem 11. A problem connected with neutrino detection . . 217

Problem 12. An α determination 219

Problem 13. Neutron flux in air 220

Problem 14. Escape distribution from a carbon slab 221

Problem 15. Escape distribution from a spherical shell . . 221

Problem 16. A rocket motor 222

Problem 17. Photon diffusion in a reactor 225

Problem 18. A thick Zr target problem 226

Problem 19. A thick C target problem 226

Problem 20. Heavy water experiment 227

CHAPTER I

BASIC PRINCIPLES

1. General nature of the problem. All problems treated in the present manual involve estimation of what percentage of particles emanating from a given source, after undergoing specified processes in a material medium of known geometry, can be expected to terminate in certain stipulated categories.

If all relevant probabilities are known for the elementary events in the "life history" of such a particle, the Monte Carlo method is applicable, and indeed is usually the only method available.

Moreover, its technique is pre-eminently realistic, consisting in actually following each of a large number of particles from the source throughout its life history to its "death" in some one of the terminal categories, using the elementary probabilities at each stage of its career in determining its fate.

The present state of development of high-speed digital computers permits the use of samples of a size sufficiently large to ensure satisfactory accuracy in most practical problems.

2. Outline of procedure. In any particular problem, a particle is completely characterized by a set of parameters which are sufficient to determine its (probability) behavior in all situations it may encounter during its history. These always include its position and direction coordinates, and in most cases its energy. Much more will be said about these and other particle parameters in the sequel (the appendix to this report and LAMS-2121).

The Monte Carlo method of dealing with problems of the kind we have indicated breaks up naturally into a well-defined set of subroutines, which we shall briefly describe here, postponing their detailed treatment to subsequent chapters. They are schematized in the following generalized flow diagram (Fig. 1). This is only intended as a general guide to the chapters of the text, and is subject to many revisions, depending on the special circumstances of the problem.

(σ). The proper assignment of all particle parameters to a source particle involves the spatial and angular distribution of the source, and its energy distribution, in case of a non-monoenergetic source.

(β_o). A special routine may be provided to determine the position of first collision in cases of high transmission, where it is desirable to distinguish between this and subsequent collisions.

(β). A general routine is designed to decide whether a particle, starting with known parameters from an arbitrary point of departure, in a particular zone of the system either suffers a collision within this zone or reaches the boundary of this zone on its line of flight without incident. The essential physical concept involved in this decision is

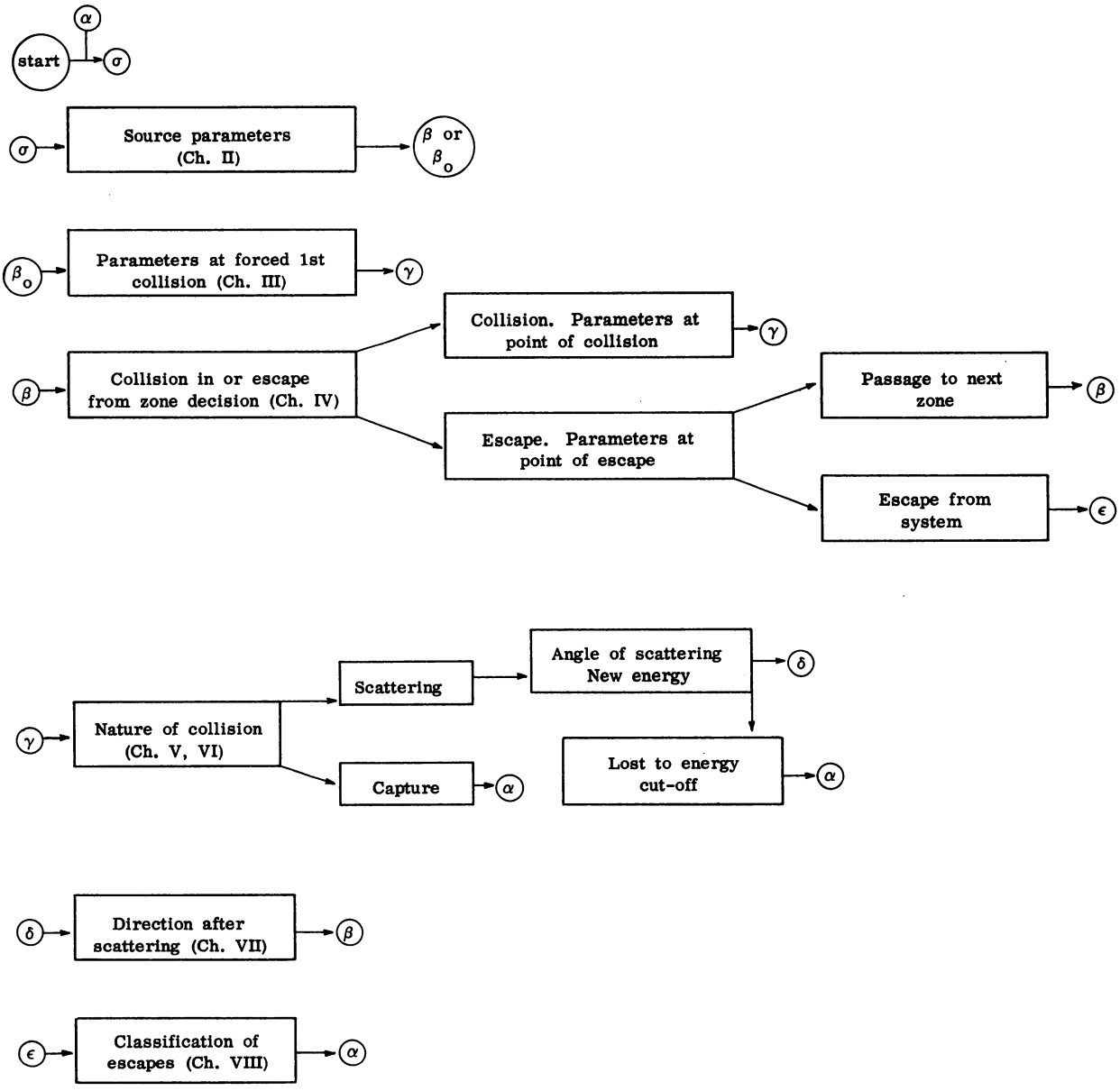

Fig. 1

the mean free path. The subsequent procedure depends on the nature of this decision, as indicated in Fig. 1. The particle parameters at the point of collision or escape are computed before proceeding. In case of escape, one proceeds to (β) or to (ϵ) according as to whether the escape is to an adjacent zone, or from the system.

(γ). The collision routine naturally depends upon the physics of the medium and is subject to the widest variation. Its objective is to decide the exact nature of the collision and the immediate fate of the particle after collision. This includes the eventuality that the particle may terminate its career under the conditions of the problem; if this occurs, a tally is made in the appropriate terminal category counter, and one returns, as in all cases of termination, to an entry (α) which leads to the source routine (σ) for introducing a fresh particle. In the event that the particle is to be followed further, the essential information required before proceeding to (δ) is a knowledge of the laboratory angle of deflection from the line of flight and the energy and "weight" of the particle after deflection.

(δ). A purely geometric routine determines the direction parameters of the deflected particle, and leads to (β). At this point, all particle parameters should be evaluated as they obtain at the point of collision, after deflection.

(ϵ). In the event that escape from the system occurs in the (β) routine, terminal classification is made and one returns to (α).

This is the general scheme of the method as it operates in all problems we propose to discuss. The chapters that follow are designed to elaborate on each of these subroutines in detail, the necessary physical concepts and their preparation for computation being developed as they are needed.

Before this, however, must come a brief discussion of random numbers and the "fundamental principle of Monte Carlo," upon which all else rests.

3. Production of random numbers. It is necessary to have upon call some source of random numbers equidistributed on the interval $0 \leq r < 1$. Ideally, one might spin a wheel of uniform scale, and indeed there exist lists[1,2] of such numbers generated in truly random fashion. There are computational algorithms adapted to digital computers which appear to serve our purpose just as well. One can find descriptions of such methods in the literature,[1,2] together with discussions of the

---

(1) Cf. articles in U. S. Department of Commerce, National Bureau of Standards, Applied Mathematics Series #12, Monte Carlo Method, Washington, D. C., 1951.

(2) The Rand Corporation, A Million Random Digits with 100,000 Normal Deviates, Free Press Publishers, Glencoe, Illinois, 1955.

D. H. Lehmer, Mathematical Methods in Large-Scale Computing Units, Proceedings of a Second Symposium on Large-Scale Digital Calculating Machinery, Harvard University Press, Cambridge, Massachusetts, 1951.

Herbert A. Meyer, ed., Symposium on Monte Carlo Methods, John Wiley & Sons, Inc., New York, 1956.

"tests of randomness" which have been applied to them. We do not enter here upon such questions since the method adopted will probably be dictated by the type of machine used and other practical considerations. A description of the method we have employed will be found in Ch. IX, § 3a, b. We should like to call attention especially to the short paper by von Neumann, cited in footnote (1), which contains some words of wisdom for those who may be troubled by the "state of sin" accompanying the use of deterministic "random numbers."

4. The fundamental principle of Monte Carlo. Suppose that a homogeneous medium consists of nuclei of three different types A, B, and C, and one knows that, in the event of a collision of a neutron in the medium, the probability of collision with type A is .2, with B is .3, and with C is the remaining .5. It is intuitively clear that, if a large number N of random numbers are produced, approximately

$.2\,N$ will fall on the interval $0 \leq r < .2$

$.3\,N$ will fall on the interval $.2 \leq r < .5$

$.5\,N$ will fall on the interval $.5 \leq r < 1$

and that this approximation will improve with increasing N; indeed, this is the salient feature we demand of any scheme of random number production. It is clear therefore how reference to a random number can be used to decide which of the three types of nuclei is hit in the event of a collision.

"tests of randomness" which have been applied to them. We do not enter here upon such questions since the method adopted will probably be dictated by the type of machine used and other practical considerations. A description of the method we have employed will be found in Ch. IX, § 3a, b. We should like to call attention especially to the short paper by von Neumann, cited in footnote (1), which contains some words of wisdom for those who may be troubled by the "state of sin" accompanying the use of deterministic "random numbers."

4. The fundamental principle of Monte Carlo. Suppose that a homogeneous medium consists of nuclei of three different types A, B, and C, and one knows that, in the event of a collision of a neutron in the medium, the probability of collision with type A is .2, with B is .3, and with C is the remaining .5. It is intuitively clear that, if a large number N of random numbers are produced, approximately

$.2\,N$ will fall on the interval $0 \leq r < .2$

$.3\,N$ will fall on the interval $.2 \leq r < .5$

$.5\,N$ will fall on the interval $.5 \leq r < 1$

and that this approximation will improve with increasing N; indeed, this is the salient feature we demand of any scheme of random number production. It is clear therefore how reference to a random number can be used to decide which of the three types of nuclei is hit in the event of a collision.

One of the decisive features of digital computers now existing is their ability to make decisions at high speed, with no limitation on the number of logical possibilities involved. The typical Monte Carlo flow diagram is largely occupied with intricate decision features.

As a first example of how a flow diagram[3] schematizes the procedure in the above example we may note Fig. 2.

More generally, if $E_1, \ldots, E_n$ are n independent, mutually exclusive events with probabilities $p_1, \ldots, p_n$, respectively, and $p_1 + \ldots + p_n = 1$, we will agree that

$$p_1 + \ldots + p_{i-1} \leqq r < p_1 + \ldots + p_i$$

determines E_i. This is the "fundamental principle" insofar as it applies to the discrete case of a finite number of eventualities.

We may use it to furnish a heuristic approach to the continuous case, in which it is desired to determine from a random number one of a continuum of values of a variable x. In this connection it is convenient to bear in mind the fact that the latter case may always be regarded as approximable by a large finite number of distinct cases; indeed, in computation with a fixed number of digits, we are always actually concerned with the discrete approximation.

---

[3] In all flow diagrams of this report we adopt the convention: x^+ means $x \geqq 0$, x^- means $x < 0$. A box containing r always denotes reference to the special subroutine generating the next random number of the sequence.

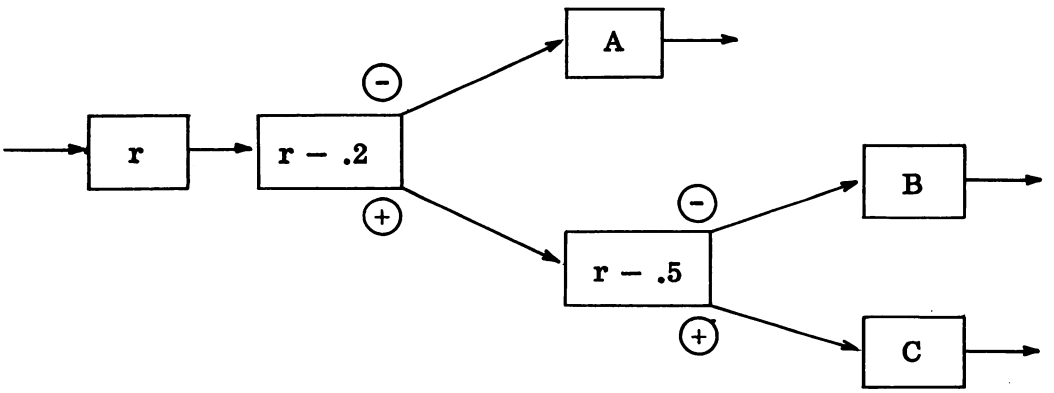

Fig. 2

Suppose that we arbitrarily assign a variable x on the interval $0 \leqq x < n$ to the events $E_1, \ldots, E_n$, with the agreement that $i - 1 \leqq x < i$ represents the event E_i. Let us construct a <u>probability density function</u> $p(x)$ by the definition

$$p(x) \equiv p_i \qquad i - 1 \leqq x < i \qquad i = 1, \ldots, n$$

Thus $p(x)$ will be a step function[4] like that of Fig. 3. Now suppose that we define the <u>probability distribution function</u>

$$P(x) = \int_0^x p(\xi)\, d\xi$$

whose graph is a broken line as indicated in Fig. 4. Note that $P(0) = 0$, $P(n) = 1$. Since $P(i) = p_1 + \ldots + p_i$, we may interpret $P(x)$ to mean the probability of the inequality $\xi \leqq x$, for $x = i$, $i = 1, \ldots, n$.

Moreover, it is clear that the equation

$$r = P(x) = \int_0^x p(\xi)\, d\xi$$

determines x uniquely as a function of r, in such a way that if r is uniformly distributed on the interval $0 \leqq r < 1$, x falls with frequency p_i in the interval $i - 1 \leqq x < i$, thereby determining the event E_i under our agreement.

[4] The figures are drawn for the simple A, B, C example.

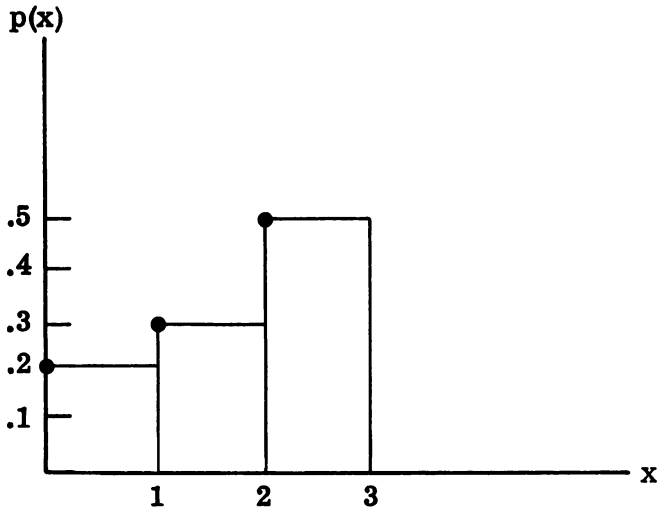

Fig. 3

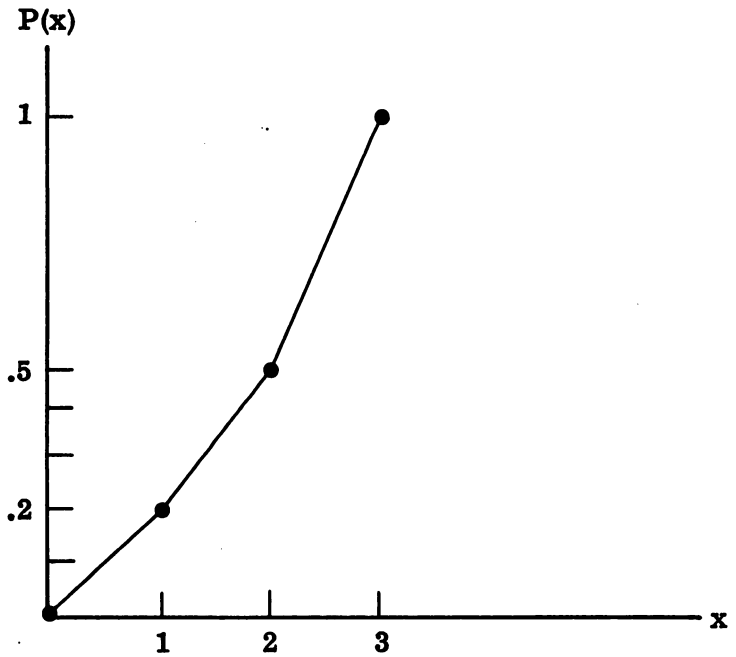

Fig. 4

We may state at once the fundamental principle as it applies to the continuous case: If $p(x)\,dx$ is the probability of x lying between x and $x + dx$, with $a \leqq x < b$, and

$$\int_a^b p(\xi)\,d\xi = 1$$

then

$$r = P(x) = \int_a^x p(\xi)\,d\xi$$

determines x uniquely as a function of r; moreover, if r is uniformly distributed on $0 \leqq r < 1$, then x falls with frequency $p(x)\,dx$ in the interval $(x, x + dx)$.

As a completely trivial first example, consider the case of neutrons that are to be located uniformly on an interval $a \leqq x < b$. We have $p(x)\,dx = dx/(b-a)$, $\int_a^b p(\xi)\,d\xi = 1$, and $r = P(x) = \int_a^x p(\xi)\,d\xi = (x-a)/(b-a)$, whence $x = a+r\,(b-a)$ determines x as a function of the random number r.

5. Application of the principle. It may be noted that the equation

$$r = P(x) = \int_a^x p(\xi)\,d\xi$$

can be expected to give rise to difficult implicit problems, since x must be determined from r. At worst, some successive approximation routine can be provided for the solution of the implicit equation $r = P(x)$ when $P(x)$ is obtainable in closed analytic form. Such time-consuming processes can be obviated in various ways, a few of which we indicate here.

The simplest method, applicable in all cases, even when $P(x)$ is known only in experimental tabular form, consists in subdividing the (a,b) interval, storing accurate values of $P(x_i) \equiv P_i$ for the end points $x_o = a < x_1 < \ldots < x_n = b$ of the subintervals, and using the discrete method for determining the subinterval (x_{i-1}, x_i) on which x falls, together with an interpolation for the actual value of x. If i is the first value of the index for which $r - P_i$ is negative, r being the current random number, we may determine x from one of the formulas

$$x = x_i - \frac{P_i - r}{P_i - P_{i-1}} (x_i - x_{i-1}) \tag{1}$$

$$x = \sqrt{x_i^2 - \frac{P_i - r}{P_i - P_{i-1}} (x_i^2 - x_{i-1}^2)} \tag{2}$$

$$x = \sqrt{x_i^2 - \frac{r - P_{i-1}}{P_i - P_{i-1}} (x_i^2 - x_{i-1}^2)} \tag{3}$$

The linear interpolation in (1) distributes x uniformly on the interval (x_{i-1}, x_i) and is strictly valid only when $p(x)$ is a step function. For sufficiently small subdivisions, (2) or (3) may give better results at the cost of an additional square root and are appropriate when $P(x)$ is concave up or concave down, respectively.

One may contrast the latter formulas (2) and (3) with that resulting from a linear assumption for $p(x)$ on (x_{i-1}, x_i):

$$r = P_{i-1} + p_{i-1}(x - x_{i-1}) + \frac{p_i - p_{i-1}}{x_i - x_{i-1}} \frac{(x - x_{i-1})^2}{2}$$

which is more complicated when solved for x, requires additional storage of the p_i, and uses a trapezoid rule for the P_i.

Very useful also is a device employed by von Neumann, especially when $p(x)$ is readily computable and storage space is at a premium. This consists of "throwing" points (ξ, η) uniformly into the rectangle bounded by the lines $x = a$, $x = b$, $y = 0$, $y = 1$ and rejecting the points lying above the curve

$$y = p^*(x) = p(x)/\max p(x)$$

x being assigned the value ξ whenever (ξ, η) fall below the curve. In many trials, the ratio of the number of points retained with ξ between x and $x + dx$ to the number of points retained altogether will be approximately the ratio of the areas

$$p^*(x)dx \Big/ \int_a^b p^*(\xi)d\xi = p(x)dx \Big/ \int_a^b p(\xi)d\xi = p(x)dx$$

The method is illustrated by the flow diagram of Fig. 5. Obviously the device in this form is impractical if the area under the curve $y = p^*(x)$ is a small fraction of the enclosing rectangle. However, modifications involving other enclosing areas can obviously be devised.

One may also retain only points (ξ,η) above the curve $y = p^*(x)$, assigning the value ξ to x and adjusting the "weight" of the particle by a factor $p(x) \int_a^b (1 - p^*(\xi))d\xi/(1 - p^*(x))$.

Finally, a combination of the two methods may be used, a first random number determining the interval (x_{i-1}, x_i) by reference to the P_i, and the von Neumann device then used on $p(x)$ on this interval. The method is then accurate, and the efficiency high.

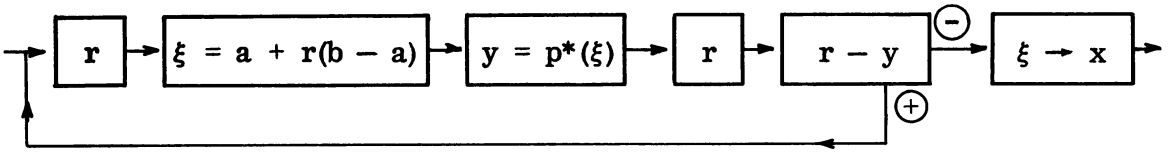

Fig. 5

CHAPTER II

THE SOURCE ROUTINE

1. Introduction. It is the purpose of the present chapter to describe how a problem is initiated by the machine, how "print-outs" are automatically effected, and how the particles are drawn from the source.

Suppose that we let N denote the number of particles already processed, so that $N = 0$ at the start of the problem. After the machine has processed any given number N of particles it will contain in various counters the numbers N_i of these N whose careers have terminated in a set of disjoint, all-inclusive categories C_i. Thus the ratios N_i/N constitute the output of the problem and serve as estimates of the probabilities of a source particle terminating in the various categories C_i. It is ordinarily desirable to print the cumulative totals N_i periodically during the course of the problem, say every N^* particles, so that convergence and "reasonableness" can be observed.

Thus the beginning of a flow diagram usually resembles that in

Fig. 6. It will be noted that N' denotes the number of particles processed since the last print-out, being reset to zero after each print, whereas N cumulates during the entire problem. The computation may be stopped at any time at which the stability of the N_i/N or other statistical considerations indicate that sufficient accuracy has been attained. The (α) entry, as has been mentioned, is that point to which the machine returns after the particle it was following has terminated its career in some one of the categories C_i.

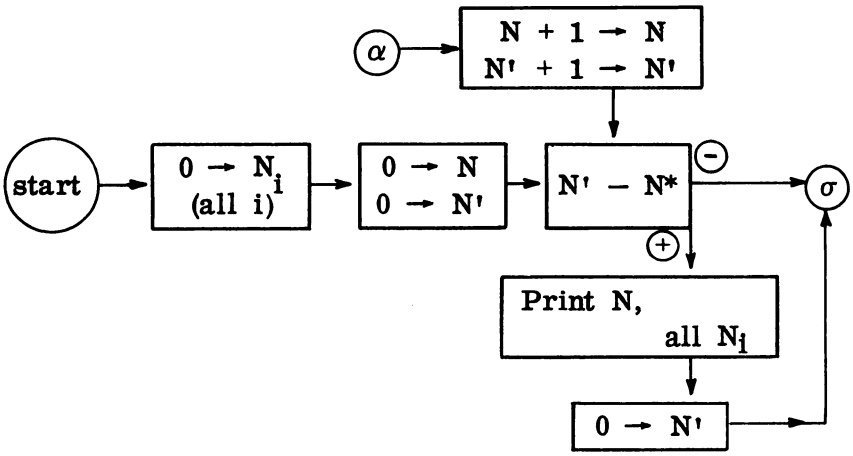

Fig. 6

The (σ) exit leads to that part of the flow diagram devoted to assigning particle parameters to a source particle.

There are two types of storage involved in all machine problems. "Permanent storage" places are reserved for constants like 0, 1, N^*, which do not change their values during the course of the problem, while "dynamic storage" refers to storage positions in the machine which contain values of parameters like N, N', N_i, which are subject to change as the problem progresses.

It is desirable to keep a record of all storage of both kinds introduced into the flow diagram as it is constructed so that none be overlooked, and so that some estimate of the "size" of the problem can be gained as one proceeds. Occasionally it becomes clear that the memory of the machine is being exceeded, and various devices must be introduced for reducing the permanent storage (e.g., by multiple storage) or the length of the code itself.

2. Particle parameters. From a consideration of the physical and geometric features of the problem, one fixes upon a set of particle parameters whose values at any time suffice to completely characterize the particle. We proceed to discuss these in detail.

We shall limit our examples to two types of coordinate systems for space and direction; namely, we shall either employ space coordinates x, y, z, together with direction cosines $u = \cos \alpha$, $v = \cos \beta$, $w = \cos \gamma$ for direction of flight, where α, β, γ are

the angles made by the line of flight with the x, y, z axes, respectively, or (in cases of spherical symmetry only) we shall use the radial distance R of the particle from the center O, together with the cosine $w = \cos \gamma$ of the angle γ which the directed line of flight makes with the positively directed radius vector. These coordinates are indicated in Fig. 7. We may note that $0 \leqq \alpha, \beta, \gamma \leqq \pi$ and on this range the cosines assume all values on the range $-1 \leqq u, v, w \leqq +1$ once and only once. It is also helpful to remember that the direction coordinates (u, v, w) may be regarded as defining a point on the unit sphere $u^2 + v^2 + w^2 = 1$ in direction space U, V, W.

Considerable advantages attend the use of parameters R, w in cases where spherical symmetry warrants it. However, we have found that in more complicated geometries, for example in cylinders, even when symmetry obtains, the use of coordinates indicated by the symmetry is hardly worth while. The main reason for this is that a particle which proceeds from some point of departure to a new place changes its directional coordinates in the latter case. The x, y, z; u, v, w system has the great advantage that u, v, w remains unchanged under linear displacements.

All problems require the use of spatial and directional coordinates. Other parameters are dictated by the nature of the problem.

Most problems are energy dependent; that is to say, the physical processes involved have elementary probabilities which are functions of the particle energy. In such cases we carry an energy parameter E

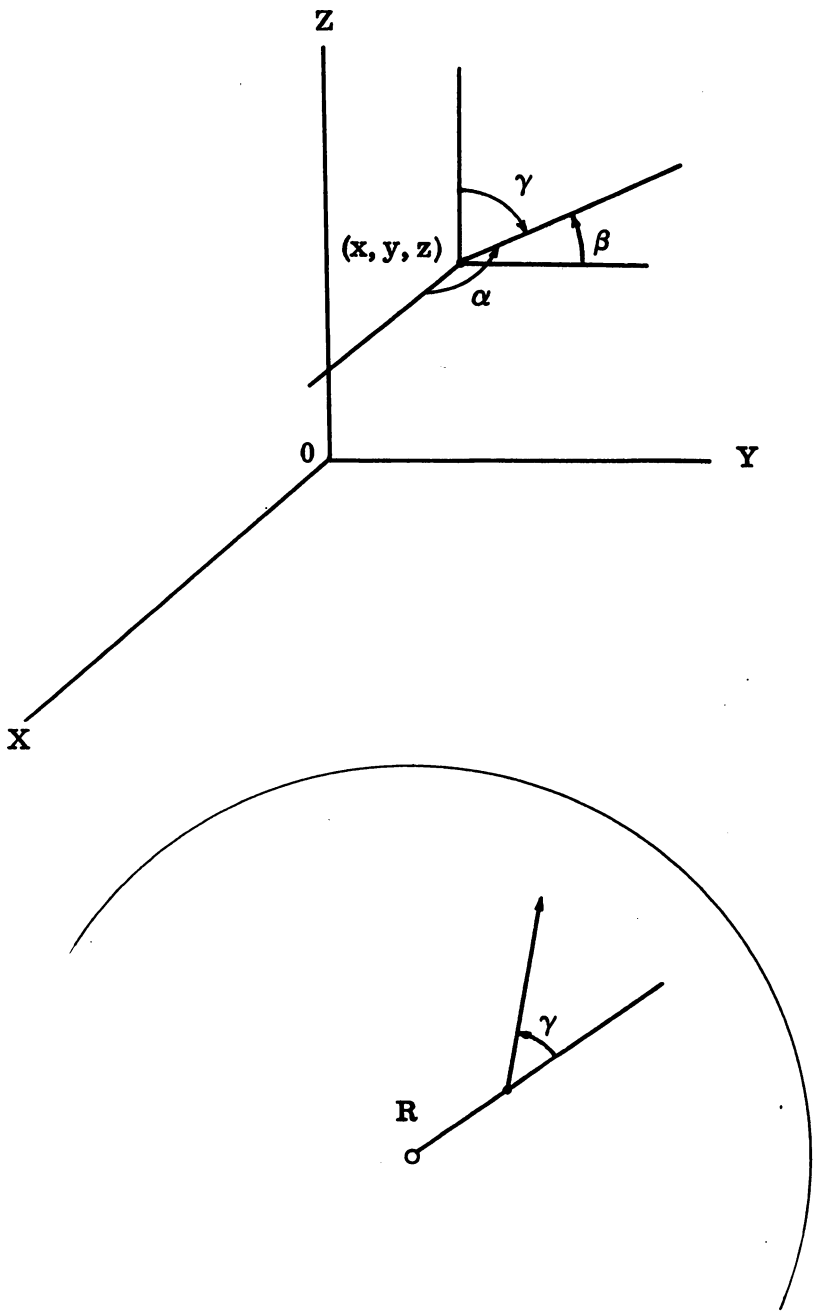

Fig. 7

and usually an energy group index g. Cross sections are usually too complicated as functions of energy to be accurately fitted by simple formulas, so that in practice the whole range of energy involved in the problem is subdivided into suitable groups $g = 1, \ldots, G$ by lower bounds $E_1 > E_2 > \ldots > E_G$, and all necessary functions of energy are tabulated for these intervals.

Moreover, systems encountered in practice are frequently non-homogeneous, being composed of zones $z = 1, \ldots, Z$ of varying densities or of different materials. This usually involves storing physical quantities as functions of z as well as of g. Permanent storage then contains numbers $K_{g,z}$ with two independent indices, which necessitates an additional particle parameter z to indicate the zone presently occupied by the particle.

In problems involving high transmission, capture, fission, (n-2n) reactions or other such features, it is desirable, although not necessary, to introduce a particle parameter W, called its weight, which is initially unity at the source. To illustrate its use, consider a problem in which, upon collision of a neutron with a nucleus, there is a probability p of capture. We have the alternatives of (a) not employing weights, using a random number r in case of collision to determine whether capture occurs or not, by reference to the capture probability p, and if $r < p$, losing the neutron to a capture category, returning to (α); or (b) using a weight parameter W, tallying a weight pW in the capture category deterministically, and continuing

with a neutron of weight (1-p)W, which now scatters on the proper nucleus. In the latter case we lose no trajectories to capture and get a better picture of the capture distribution itself.

Certain problems are concerned with the time a particle takes to travel from the source to its death, which calls for a parameter τ giving the "age" of the particle at all phases of its life. A parameter ν is employed for the number of collisions suffered by a particle in some problems, e.g., in those dealing with thick target corrections.

We include for easy reference a list of these most frequently used particle parameters, and will adhere throughout to the notation indicated here.

Particle Parameters

Space coordinates	x,y,z or R
Direction coordinates	u,v,w or w
Energy	E
Energy group index	g
Zone number	$\mathfrak{z}$
Weight	W
Age	τ
Number of collisions	ν

3. Remarks on units. It is perhaps desirable to mention briefly the matter of units at this point. We use the centimeter-gram-second systems of units, with the following qualifications. (a) Neutron energies are expressed in electron volts (ev), Kev (10^3 ev), or Mev (10^6 ev). For the uninitiated, voltage has dimensions of energy per unit charge; one ev is by definition the energy acquired by an electron which has dropped through a potential difference of one (practical unit) volt. Since the latter is $10^8/c$ of the electrostatic unit of voltage,(5) and the charge on the electron is $e = 4.8025 \times 10^{-10}$ esu, it follows that one ev is $eV = 4.8025 \times 10^{-10} \times 10^8/c = 1.60203 \times 10^{-12}$ erg. (b) The energy of a photon is measured in (dimensionless) units of $m_o c^2$, where m_o is the rest-mass of the electron. This is explained more fully in Ch. VI.

We include here the formula for computation of the time $\Delta\tau$ in seconds for a neutron of energy E Mev to traverse a distance of d cm. Letting $k = 1.60203 \times 10^{-6}$ ergs per Mev, we have in the non-relativistic range of neutron energies(6)

$$Ek = \frac{1}{2} m_1 v^2$$

---

(5) $c = 2.99776 \times 10^{10}$ cm sec^{-1}, the velocity of light in vacuo.

(6) The relativistic kinetic energy is $(m-m_1)c^2$, where $m = m_1/\sqrt{1-\beta^2}$ and $\beta = v/c$. As an exercise one may determine the relative error (1.1%) in computing v from the two formulas when E = 14 Mev, the highest neutron energy involved in the present report, which is thus confined to the non-relativistic range of neutron energies. We do give the relativistic treatment of the Compton effect in Ch. VI, however.

where m_1(gm) is the mass of the neutron and v its speed in cm sec^{-1}. Thus

$$v = \sqrt{2\ E\ k/m_1}$$

Now one "gram atomic mass" of any physical particle contains Avogadro's number $A = 6.0228 \times 10^{23}$ particles. Taking 1.00893 for the atomic mass of the neutron, we have

$$v = k' \sqrt{E(Mev)} \quad cm\ sec^{-1}$$

where $k' = 13.83 \times 10^{8}$ numerically. Thus a 1 Mev neutron travels about 14 meters per microsecond (μ sec). We have then

$$\Delta\tau = k''d/\sqrt{E} \quad sec$$

for the transit time $\Delta\tau$, where $k'' = 7.231 \times 10^{-10}$.

4. Space coordinates for source particles. We have indicated in § 1 of the present chapter how the machine is led from the "start" of the problem to the point (σ) at which it sets up a source particle, or having finished processing a particle, it is returned to (σ) via (α), while in §2 we have discussed the various kinds of parameters as they are carried throughout the career of a particle. We are now

ready to consider how initial values are assigned to these parameters as a particle issues from the source. We hope to give enough examples to indicate the nature of the procedure.

(a). Uniform source on an annulus of radii $R_o < R_1$. Determination of coordinates x,y (cf. Fig. 8). The probability density function $p(R)$ is $2\pi R/\pi(R_1^2 - R_o^2)$, so that the fundamental principle sets

$$r = P(R) = \int_{R_o}^{R} p(R)\, dR = (R^2 - R_o^2)/(R_1^2 - R_o^2)$$

Having thus located the radius R, we note that $p(\phi)\, d\phi = d\phi/2\pi$ so that the next random number determines ϕ by

$$r = \int_{-\pi}^{\phi} \frac{d\phi}{2\pi} = (\phi + \pi)/2\pi$$

We have therefore the routine indicated in Fig. 8.

(b). Uniform source in a spherical shell. The final result is $R = \sqrt[3]{R_o^3 + r(R_1^3 - R_o^3)}$ if spherical symmetry admits use of the single space coordinate R. If x,y,z must be specified, we shall have $x = Ru$, $y = Rv$, $z = Rw$, where (u,v,w) is a point uniformly distributed on the unit sphere $u^2 + v^2 + w^2 = 1$. How such points may be obtained will be discussed in the next section (5a) on direction parameters u, v, w, where the same problem arises.

(c). Parallel-beam source incident on lateral surface of right circular cylinder of radius R_1, height H, or on a sphere of radius R_1.

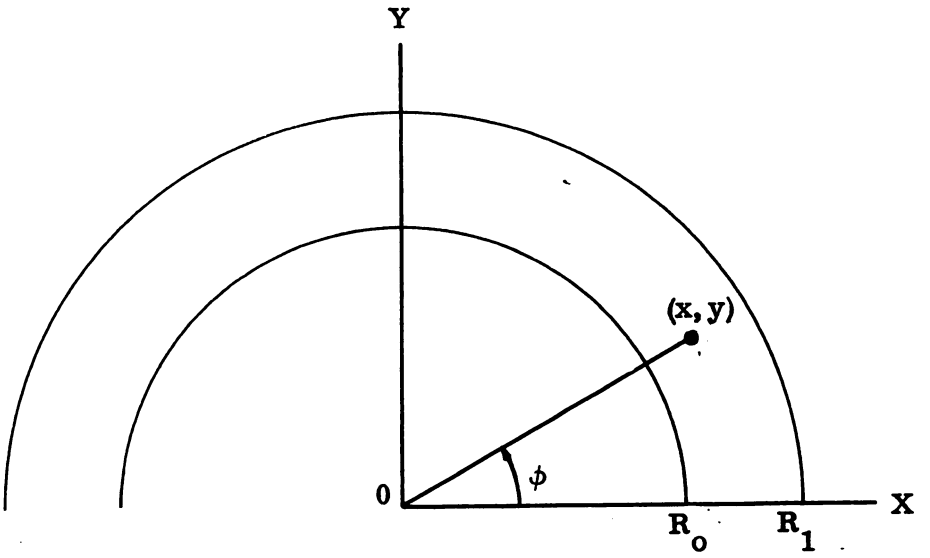

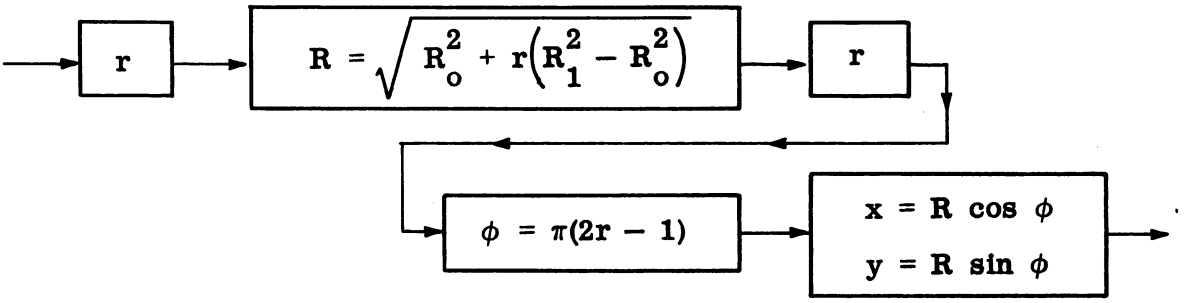

Fig. 8

If the beam is taken in the positive y-direction ($u = 0$, $v = 1$, $w = 0$), and the cylinder in the position shown in Fig. 9, one may use the routine there indicated.

For a similar beam incident on a sphere of radius R_1, we have $x = R_1\sqrt{r}$, $y = -\sqrt{(R_1^2 - x^2)} = -R_1\sqrt{(1 - r)}$, $z = 0$, assuming symmetry about the y axis.

(d). Isotropic point source at distance d_s from right circular cylinder. Here the determination of the x, y, z coordinates of the point of entry to the cylinder is correlated with the direction parameters u, v, w. We therefore postpone this problem to the next section.

5. Direction coordinates for source particles. We next consider the problem of assigning direction cosines u, v, w, or simply w in the spherically symmetric case, to source particles. If the latter are liberated in a material medium, the directions may be expected to be drawn from an isotropic distribution, whereas particles emanating from a surface are naturally limited to half of direction space and usually are distributed in some non-isotropic distribution about the normal to the surface.

(a). Isotropic source; u,v,w direction cosines. The problem involved is tantamount to that of choosing a point (u,v,w) uniformly distributed on the unit sphere $u^2 + v^2 + w^2 = 1$. The element of area for this sphere in spherical coordinates γ, ϕ is $\sin\gamma\, d\gamma\, d\phi = -dw\, d\phi$, where ϕ is the longitude, and we have used γ instead of

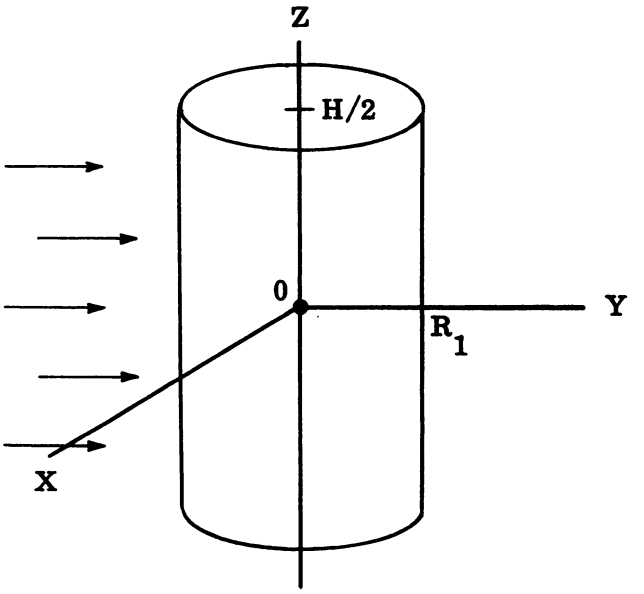

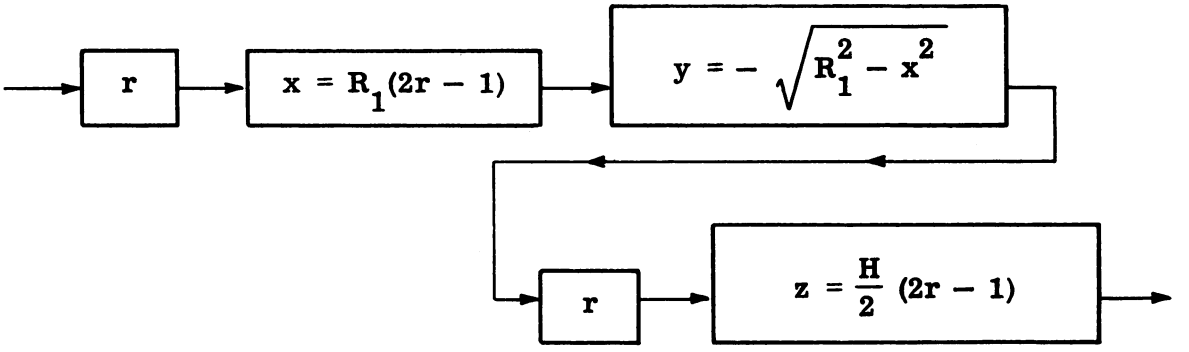

Fig. 9

the traditional θ for the remaining angle since γ has already been introduced for this angle by way of $w = \cos \gamma$ (cf. Fig. 7). The probability density function $p(w)$ is therefore given by $p(w)\, dw = -2\pi \sin \gamma \, d\gamma / 4\pi = \frac{1}{2} dw$. We may therefore first determine w by

$$r = \int_{-1}^{w} \frac{1}{2} dw = \frac{1}{2}(w + 1)$$

and ϕ subsequently by

$$r = \int_{-\pi}^{\phi} p(\phi)\, d\phi = \int_{-\pi}^{\phi} \frac{d\phi}{2\pi} = \frac{1}{2\pi} (\phi + \pi)$$

Reference to Fig. 10 then completes the argument for the isotropic source; we need only remember that $\rho \equiv \sqrt{(u^2 + v^2)} = \sqrt{(1 - w^2)}$.

(b). The cosine distribution.[7] This refers to a point source emanating from a surface. If we agree that the outer normal to the surface at the point has the direction $u = 0$, $v = 0$, $w = 1$, then the cosine distribution has by definition the probability density function $p(w) = 2w$, with $w \geqslant 0$. Thus

$$r = \int_{0}^{w} 2w \, dw$$

---

[7] For a discussion of the way in which the cosine distribution governs particles emanating from a surface one may refer to F. W. Sears, An Introduction to Thermodynamics, the Kinetic Theory of Gases, and Statistical Mechanics, Addison-Wesley Publishing Co., Inc., Cambridge, Massachusetts, 1955. Cf. the chapter on kinetic theory.

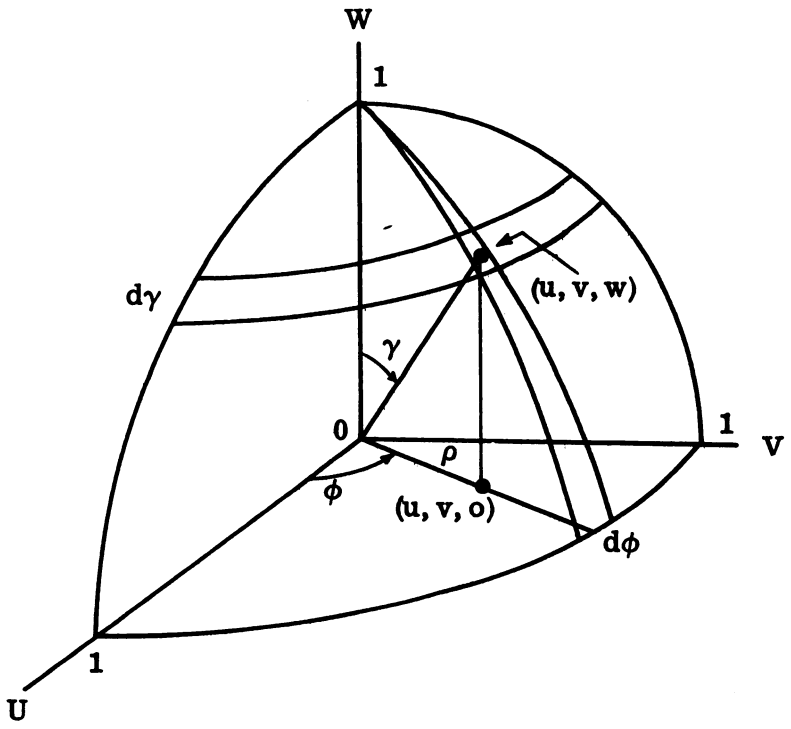

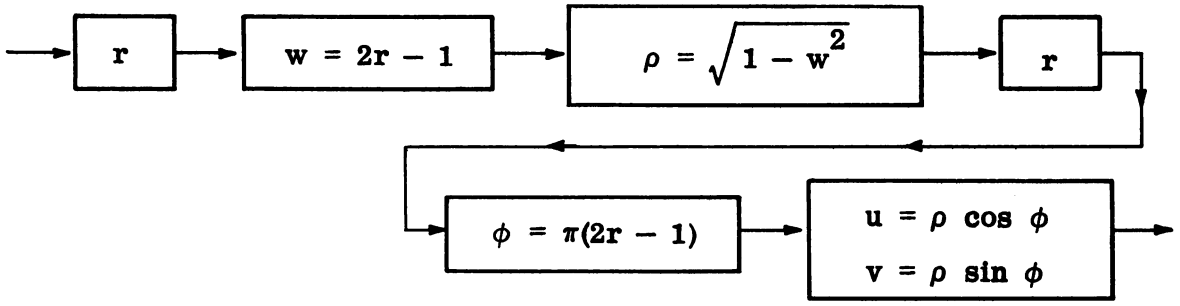

Fig. 10

and $w = \sqrt{r}$ in this case. The flow diagram of Fig. 10 may be used with the replacement of $w = 2r - 1$ by $w = \sqrt{r}$.

(c). Isotropic and cosine sources in spherically symmetric systems. In case spherical symmetry indicates the use of coordinates R, w defined in Fig. 7, we may have to assign the direction parameter w for point sources of the above kinds. Such sources will be located on spherical surfaces, and in case of a cosine source, the latter will be relative to the normal to such a surface, i.e., to the radius vector. It is therefore clear that the formula $w = 2r - 1$ is valid for the isotropic case, while $w = \sqrt{r}$ applies to outwardly directed, and $w = -\sqrt{r}$ to inwardly directed cosine sources.

(d). Isotropic point source at distance d_s from cylinder of radius R_2, height H (cf. Fig. 11). This problem presents some features of interest. Clearly, if we proceed naively to assign direction parameters u, v, w to particles as they leave the source s, using the method of (a) above, most particles will fail to hit the cylinder, the size of which may be greatly exaggerated in the figure. The physical problem is naturally concerned with questions relative to the number of incident particles, not with the problem (an interesting one, incidentally) of what solid angle is subtended at the source by the cylinder. How the latter question may be attacked by Monte Carlo we leave as an exercise. In this connection it is worth mentioning that many purely geometrical problems which present forbidding analytical difficulties are apt to arise in photon problems, and may be (many have been) successfully

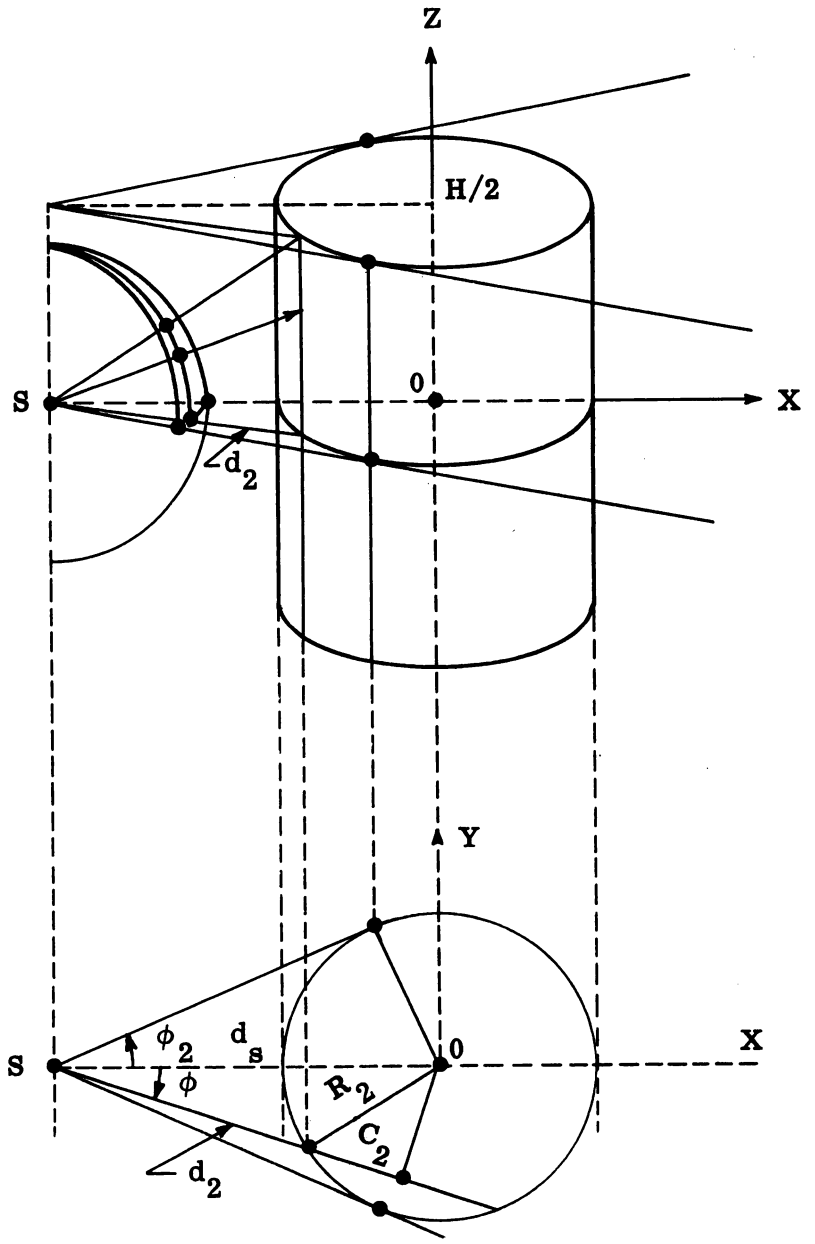

Fig. 11

treated by the simple sampling methods which we are discussing.

To return to our point source, we observe first that the only particles which can hit the cylinder are limited to the wedge defined by the two tangent planes to the cylinder through the source S. This means that directions are limited, in u, v, w space at the source to those with longitude ϕ on the range $-\phi_2 \leqslant \phi \leqslant \phi_2$ where $\phi_2 = \arcsin R_2/d_s$, and ϕ is equidistributed on this range. Moreover, for all those particles issuing from the source between ϕ and $\phi + d\phi$, the direction cosine $w = \cos\gamma$ is limited by the end points of the element of the cylinder determined by ϕ, and on this range w has a constant probability density function, since the element of surface area on the unit sphere is $-dw\, d\phi$.

Now from the figure, the half-chord $c_2 = \sqrt{\left[R_2^2 - (d_s \sin\phi)^2\right]}$, so that the distance $d_2 = d_s \cos\phi - c_2$. Thus for this ϕ, the range of w is $-w_2 \leqslant w \leqslant w_2$, where $w_2 = (H/2)/\sqrt{\left[(H/2)^2 + d_2^2\right]}$. The routine for setting up x, y, z, u, v, w at the point of entry therefore appears as in Fig. 12, where ϕ_2, c_2, d_2, w_2 are given by the above formulas. The last box follows from the fact that

$$z/d_2 = \tan(\pi/2 - \gamma) = \cot\gamma = \cos\gamma/\sin\gamma = w/\rho.$$

(e). General distribution in half of direction-space. Occasionally it is necessary to consider a point source with $w \geqslant 0$ having some experimentally determined distribution in w, which may be given in the form of a table. We may then tabulate $P_0 = 0 < P_1 < \ldots < P_I = 1$, $w_0 = 1 > w_1 > \ldots > w_I = 0$, where P_i is the probability of a cosine

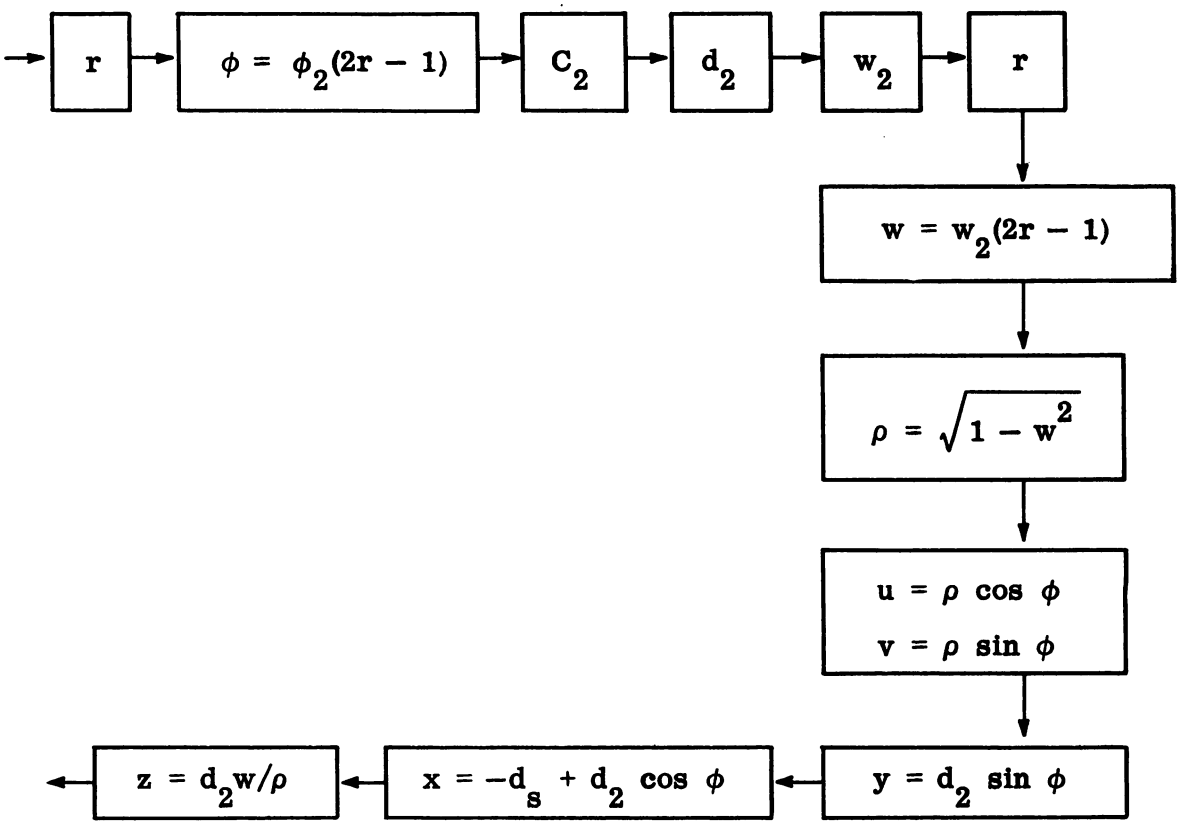

Fig. 12

$w \gtrless w_i$, and proceed as in Fig. 13a (cf. also formulas (2) and (3), Ch. I, §5). When various distributions are to be tried, it is preferable to run a number of different problems, each for a specific w; the results may then be weighted to give terminal percentages for any desired source.

(f). A prejudiced source. It is sometimes desirable to sample certain ranges of source directions more thoroughly than others. To illustrate, suppose that we have an isotropic source, with w uniformly distributed on $-1 \leqslant w \leqslant 1$, but that the position of a counter makes

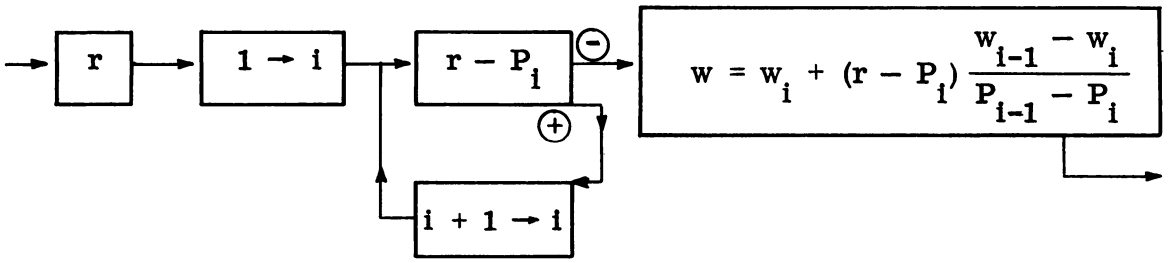

Fig. 13a

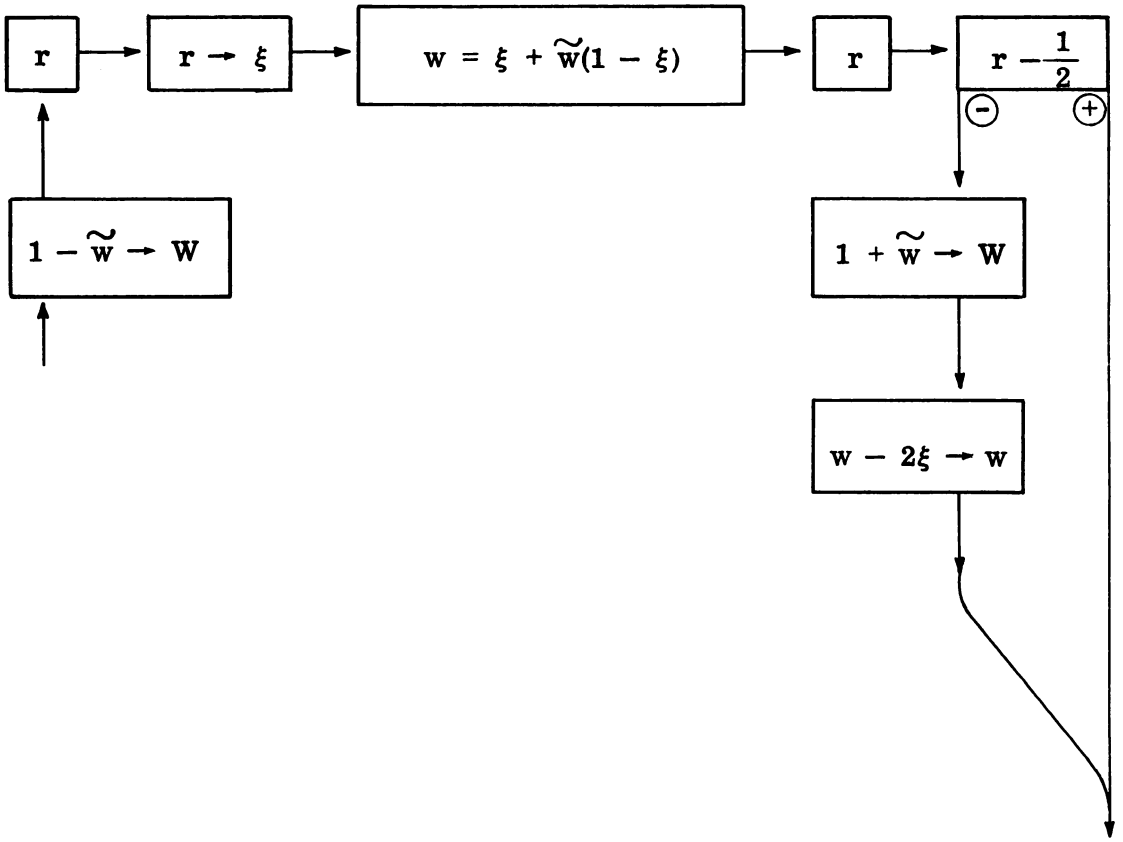

Fig. 13b

more important those particles which leave the source on the range $-1 \leqslant w \leqslant \tilde{w} < 0$. We may then give source particles equal likelihood of starting on this range or its complement, provided we assign weights $(\tilde{w} + 1)$ and $(1 - \tilde{w})$, respectively. In this way about half of all source particles, of relatively smaller weight, originate in the important cone, the total weight processed for N particles having expectation $\frac{1}{2} N(\tilde{w} + 1) + \frac{1}{2} N(1 - \tilde{w}) = N$. The procedure is schematized in Fig. 13b.

6. Energy of source particles. In the case of energy dependent problems, one usually decides upon a set of energy ranges with lower bounds $E_1 > E_2 > \ldots > E_G$, with storage of physical quantities for each of these ranges, E_G being the lowest energy permitted to particles in the problem. Particles which by chance reach lower energies are relegated to a terminal category reserved for such losses. An index $g = 1, \ldots, G$ designates the group number. If the source is monoenergetic, one simply sets $E_o \rightarrow E$, $g_o \rightarrow g$, that is, E and g are assigned the values of the initial energy E_o and the index g_o of the group in which this energy falls; g_o may or may not be unity; one may wish to study the behavior of a series of sources of various initial energies.

If the source particles are not monoenergetic but are chosen from some given energy distribution, one tabulates $P_o = 0 < \ldots < P_G = 1$ together with $E_1 > \ldots > E_G$ and proceeds exactly as indicated

in §5e above, reading g for i, E_g for w_i, and E for w.

7. Other source parameters. The other parameters mentioned in Ch. II, §2, if called for, have the following values at the source: (a) z is set equal to the number of the zone into which source particles enter (which may depend on the values assigned to spatial and directional coordinates, and thus involve a decision routine); (b) the weight W is usually unity at the source; (c) age $\tau = 0$ initially; and (d) $\nu = 0$ for the number of collisions undergone.

8. Source for α-type calculations. In an important class of problems, including those which are designed to determine the rate of growth of a neutron population in a fissionable material, the source consists of a specified number of neutrons $N_{g,z,i}$ in group g, zone z, and direction range i. We will illustrate for the case of a homogeneous sphere of radius R_Z, where these ranges are determined by bounds

$$E_o > E_1 > \ldots > E_G$$

$$0 = R_o < R_1 < \ldots < R_Z$$

$$1 = w_o > w_1 > \ldots > w_I = -1$$

The object of such a problem is the determination of the distribution $N'_{g,z,i}$ in which this initial distribution results at time $\Delta\tau$, and then to use the output $N'_{g,z,i}$ as the input source distribution for the next cycle. A suitable modification of the (α) and (σ) routines is indicated in Fig. 14. The determination of E, R, and w on their ranges may be achieved by appropriate interpolation, or, if preferred, by deterministic assignment of suitable mean values. The initial values of $N_{g,z,i}$ are arbitrary in α-calculations, but are guessed as well as possible to hasten convergence to the limit distribution. The $\bar{g},\bar{z}\ \bar{i}$ refer to the <u>category</u> being processed, and must be distinguished from the neutron parameters g,z, i, which are subject to change while the category from which the neutrons arose is being processed. The feedback of N' for N is subject to suitable renormalization to preserve a reasonable source size.

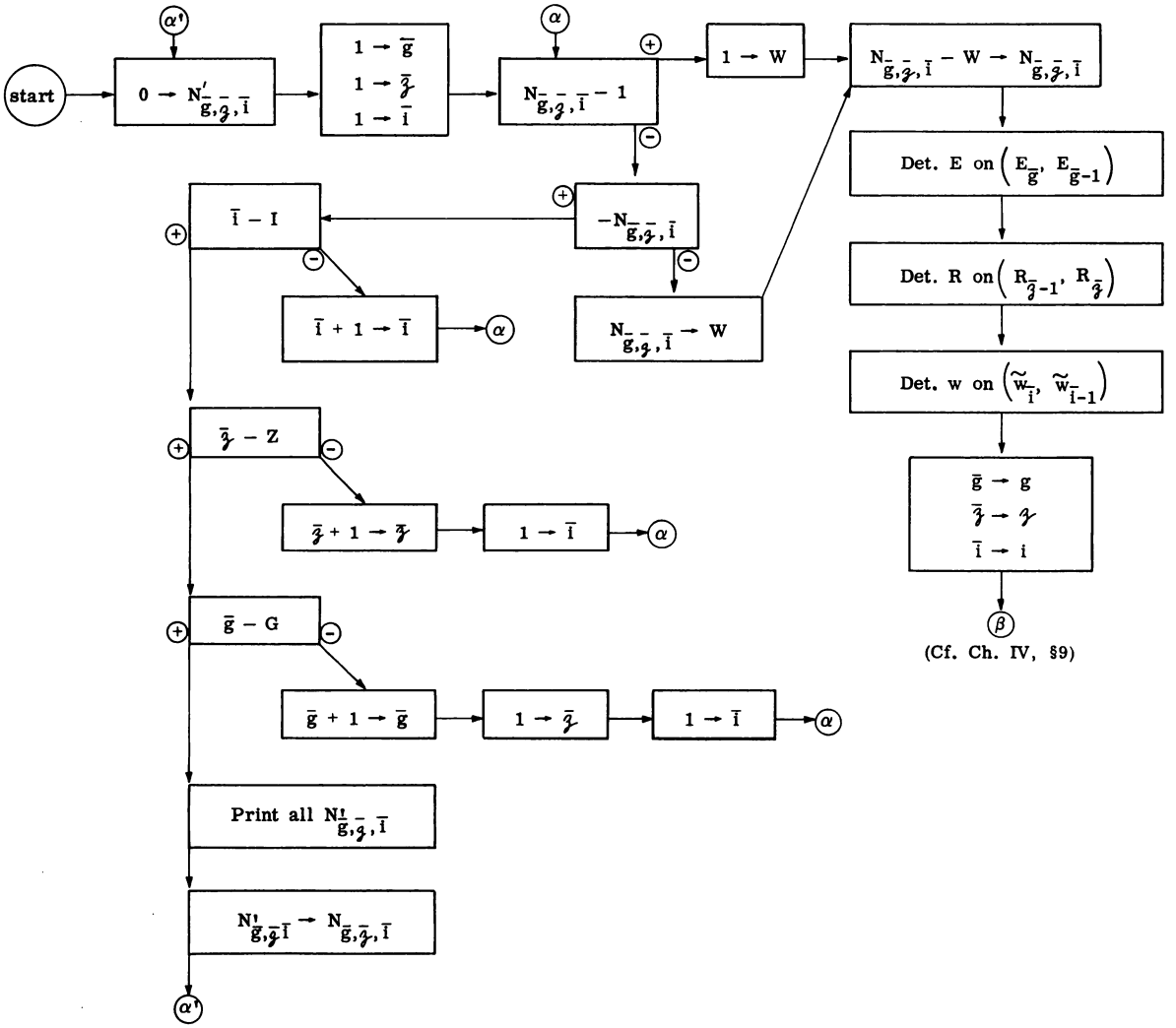

Fig. 14

CHAPTER III

THE MEAN FREE PATH AND TRANSMISSION

1. The cross section concept. The cross section σ of a stationary "target" particle for particles of energy E, relative to a given single process may be thought of as the area presented by the target, assumed stationary in the laboratory system, to a beam of (point) particles of this energy, relative to the laboratory system. If we regard a thin slab of material of area α, thickness $d\ell$, numerical density N (target particles per cm^3), traversed by a parallel beam of particles (of energy E) normal to α, the total area presented to the beam by target particles is $\sigma N \alpha (d\ell)$, assuming $d\ell$ so small that no "shadowing" exists. The fraction of beam-particles undergoing the process in this volume should be $\sigma N \alpha (d\ell)/\alpha$. We, therefore, have the attenuation law

$$dn = -n N \sigma (d\ell)$$

for the number n of particles in the beam, and

$$n = n_o \exp (-N \sigma \ell)$$

represents the number of particles remaining in the beam after traversing a distance ℓ in such a uniform infinite medium, n_o being the number of particles in the beam at $\ell = 0$. Note that we are assuming no other competing processes exist.

It is, therefore, supposed that

$$p(\ell)d\ell = \left[\exp\ (-N\sigma\ell) \right] N\sigma(d\ell)$$

is the probability for a first collision between ℓ and $\ell + d\ell$, and

$$P(\ell) = \int_0^{\ell} \exp\ (-N\sigma\ell)\ N\sigma(d\ell) = 1 - \exp\ (-N\sigma\ell)$$

is the corresponding probability distribution function for a first collision at distance $\leqq \ell$.

2. The mean free path. The average distance λ to first collision is defined as the first moment of the function $p(\ell)$, i.e.,

$$\lambda = \int_0^{\infty} \ell p(\ell)\ d\ell = \int_0^{\infty} \exp\ (-N\sigma\ell)\ N\sigma\ell(d\ell) = 1/N\sigma$$

and is called the mean free path for the process at this energy.

It follows that the Monte Carlo determination of distance ℓ from an arbitrary point of departure to first collision, assuming the medium

homogeneous and infinite must be

$$r = P(\ell) = 1 - \exp(-\ell/\lambda)$$

or

$$\ell = -\lambda \ln (1 - r)$$

Since $1 - r$ is equidistributed on $0 \leq r \leq 1$ if r is, we may use simply

$$\ell = -\lambda \ln r$$

In practice, we are almost always concerned with a complex of different processes, each presenting its own cross section to the beam. Specifically, we may have to deal with a medium containing different types A, B, C, ..., of nuclei; moreover, each type A nucleus may have a variety of different types of cross section, for example, an elastic scattering cross section $\sigma^A(\text{el.})$, an inelastic cross section $\sigma^A(\text{in.})$, a cross section $\sigma^A(\text{fiss.})$ for fission, $\sigma^A(\text{cap.})$ for capture, and so on.

The sum of the cross sections $\sigma^A(\text{el.}) + \sigma^A(\text{in.}) + \ldots$ of all types for a particular nucleus A is called its <u>total</u> cross section $\sigma^A(\text{tot.})$. If the medium contains nuclei of types A, B, C, ... in numerical densities N_A, N_B, N_C, ..., respectively, the "total cross section" for the medium is defined to be

$$\Sigma = N_A \sigma^A(\text{tot.}) + N_B \sigma^B(\text{tot.}) + \ldots$$

Reference to the preceding discussion makes it clear that the the simple $N\sigma$ of that argument should be replaced by Σ in the general case, and the mean free path for the medium is, therefore,

$$\lambda = 1/\Sigma$$

The Monte Carlo method is always concerned with the distance l from point of departure to collision, and only in case of collision, turns to a consideration of the nature of target hit, and the type of process involved. Thus it is always the mean free path $\lambda = 1/\Sigma$ that is used and never the free path for any of the individual processes.

It must be remembered that cross sections are, in general, dependent upon the energy of the particle (picturesquely, the size of the target depends on the speed of the arrow); thus we write $\sigma^A_E(\text{el.})$, ... $\sigma^A_E(\text{tot.})$, Σ_E, and λ_E as functions of energy E, and, in practice, the free path is usually tabulated as λ_g, g = 1, ..., G, where g is the energy group index.

Moreover, in systems consisting of zones of differing composition, we will have an additional zone index on the free path, thus λ^{γ}_g.

3. An example. Consider the problem of determining λ for neutrons of energy E = 3 Mev in a medium of CH_2 of density δ = .92 gm cm^{-3}. At this energy, C has an elastic scattering cross section $\sigma^C(el.)$ = 1.14 barns (1 barn = 10^{-24} cm^2) while H has a similar cross section $\sigma^H(el.)$ = 2.23 barns. No other processes are involved.

The atomic weight of C is 12 and of H is 1, so that the molecular weight of CH_2 is 12 + 2(1) = 14. In one gram molecular weight G of any compound are A = .6 x 10^{24} molecules. The mass of one CH_2 molecule is, therefore, G/A gm. Since 1 cm^3 of CH_2 has mass δ gm, the number of molecules of CH_2 in 1 cm^3 is $N = \delta/(G/A) = \delta A/G = .0394 \times 10^{24}$ cm^{-3}. Hence, the numerical densities of C and H are $N_C = N$, $N_H = 2N$, and $\Sigma = N_C \sigma^C(tot.) + N_H \sigma^H(tot.) = N(\sigma^C(el.) + 2\sigma^H(el.)) = .221$ cm^{-1}. Thus finally $\lambda = 1/\Sigma = 4.52$ cm.

In problems involving many zones of the same material at different densities, it may be necessary to store only the basic nuclear constants, together with zone densities, and provide for the machine to compute its own λ_g^γ when needed, by reference to the stored quantities. For instance, in the preceding example, taking energy dependence into account, we should have

$$\lambda_g^\gamma = 1/\delta_\gamma K_g$$

where

$$K_g = \frac{A}{G}(\sigma_g^C + 2\sigma_g^H)$$

and δ_γ are stored quantities. Such a procedure is time-consuming, especially when it necessitates computation of the probabilities for type of collision upon each collision.

The concept of free path as we have formulated it applies to photons in their interaction with electrons and nuclei as well as to neutrons interacting with nuclei. A discussion of photons will be found in Chapter VI. Throughout the report, except in Chapters V and VI, we speak in a general way of "particles" which may be photons or neutrons.

4. "Small" systems and transmission. Consider a homogeneous medium having mean free path λ for particles of a monoenergetic source. If the distance from source S to the boundary of the system along a given direction is L, then, of a beam of N source particles leaving the source in this direction, $N \exp(-L/\lambda)$ will escape undeterred. It is clear that if the dimensions of such a system are small compared to the free path λ, most source particles will escape. This is especially undesirable if the assignment of source parameters is complicated, and, in any case, requires needlessly large sources to produce an effective sample.

Now there is nothing to prevent us from regarding a single mathematical particle leaving the source in a given direction as representing a large set of W actual particles. Since the output of all problems is a set of ratios N_i/N, where N is the total number

of source particles, the initial value assigned to W may be taken as unity.

We may then argue that, for a particle of weight W (=1) leaving the source in the situation described above, a partial weight W exp $(-L/\lambda)$ is transmitted, the latter weight being tallied in a category T reserved for total transmission (without collision). Then we determine a position of first collision on the interval $0 \leqq \ell \leqq L$ within the medium for the remaining particle of weight $W\left(1 - \exp(-L/\lambda)\right)$ according to the formula $r = P(\ell)/P(L)$, where $P(\ell) = 1 - \exp(-\ell/\lambda)$, as derived in a preceding section. Solving for ℓ, one obtains $\ell = -\lambda \ln\left\{1 - r\left[1 - \exp(-L/\lambda)\right]\right\}$.

If the medium is non-homogeneous, but may be regarded as consisting of a number of zones, each homogeneous in itself, the portion of the line of flight lying within the medium may be decomposed into successive intervals of lengths $L_1, \ldots, L_m$, where L_γ is the segment lying in zone γ with free path λ_γ. The transmission is then clearly $t = \exp(-L_1/\lambda_1) \cdot \exp(-L_2/\lambda_2) \ldots \exp(-L_m/\lambda_m) = \exp -\left\{L_1/\lambda_1 + \ldots + L_m/\lambda_m\right\}$. The probability of a first collision at a distance $\leqq \ell \leqq L$ from the point of origin is, therefore, $1 - \exp(-\rho)$, where ρ is defined by

$$L_1 + \ldots + L_{\gamma-1} < \ell \leqq L_1 + \ldots + L_{\gamma-1} + L_\gamma$$

and

$$\rho = \frac{L_1}{\lambda_1} + \ldots + \frac{L_{\gamma-1}}{\lambda_{\gamma-1}} + \frac{\ell - (L_1 + \ldots + L_{\gamma-1})}{\lambda_\gamma}$$

Thus ρ is the number of free paths represented by ℓ. We therefore may record the weight Wt as transmitted, and force a first collision of the weight W(1 - t) on the line of flight at a distance $\ell \leq L$ by means of the formula

$$r = (1 - e^{-\rho})/(1 - t)$$

Thus $\rho = -\ln[1 - r(1 - t)]$ determines γ by means of the inequalities

$$\frac{L_1}{\lambda_1} + \ldots + \frac{L_{\gamma-1}}{\gamma-1} < \rho \leq \frac{L_1}{\lambda_1} + \ldots + \frac{L_\gamma}{\lambda_\gamma}$$

and ℓ by the equation

$$\ell = L_1 + \ldots + L_{\gamma-1} + \lambda_\gamma \left[\rho - \left(\frac{L_1}{\lambda_1} + \ldots + \frac{L_{\gamma-1}}{\lambda_{\gamma-1}}\right)\right]$$

5. The "forced first collision" routine. We illustrate the use of the device in two typical problems in this and the following section. Consider a parallel-beam monoenergetic source incident on the lateral surface of a cylindrical shell of radii $R_o < R_1$, and height H, composed of homogeneous material having free path λ at this energy. We suppose that the source routine has already assigned to a source particle its parameters at entry, say, u = 1, v = 0, w = 0, and x, y, z (in the manner indicated in Chapter II, §4c), together with $E = E_o$, $g = g_o$, $\upsilon = 0$, and

W = 1. The exit from (σ) should then lead to the (β_o) routine for forced first collision as indicated in Fig. 16, based on the geometric properties of Fig. 15.

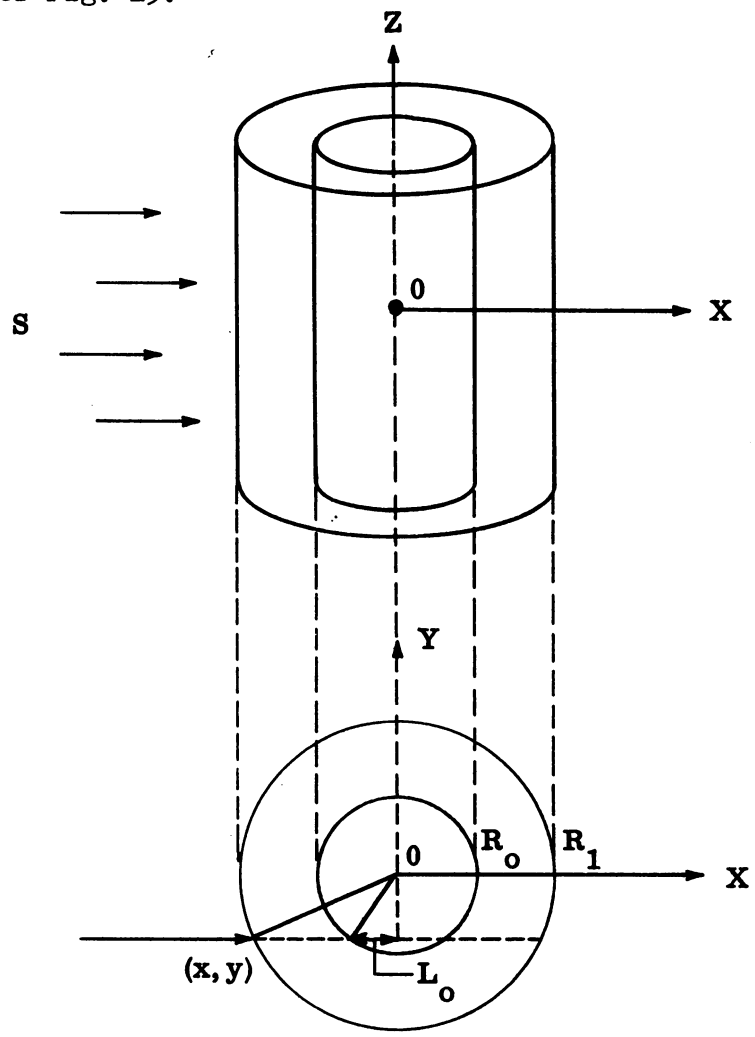

Fig. 15

The procedure naturally depends on whether or not the line of flight crosses the hole. This is the reason for the $|y| - R_o$ decision. The distance L is the total path length of the line of flight lying within the medium. The transmission τ_o is based on the free path for initial energy group g_o. The distance traversed within the medium from point of entry to point of collision is denoted by ℓ. Note that the exit leads to the collision routine (γ) with all parameters as they exist at the point of collision, momentarily before impact.

6. Remark on the device in spherical problems. Although we shall not include an example of the forced first collision device in a system treated with spherical coordinates, we should mention that, if it is used to determine a weight W and a radial distance R_ℓ at the point of first collision,[8] one should exit to an entry such as (γ') discussed in Chapter IV, §3, which sets up the direction w and radius R as they exist at the point of collision, before entering (γ) itself.

As an example of the forced first collision method in a non-homogeneous medium, consider a parallel beam of particles directed vertically upward (u = 0, v = 0, w = 1) and incident on a sphere $x^2 + y^2 + z^2 = R_o^2$ subdivided into spherical homogeneous shells by the radii $R_o > R_1 > \ldots > R_k = 0$, zone η having total mean free path

---

[8] If R,w are the source parameters, and ℓ the distance from source to forced first collision, $R_\ell^2 = R^2 + \ell^2 + 2R\ell w$ in the solid homogeneous case.

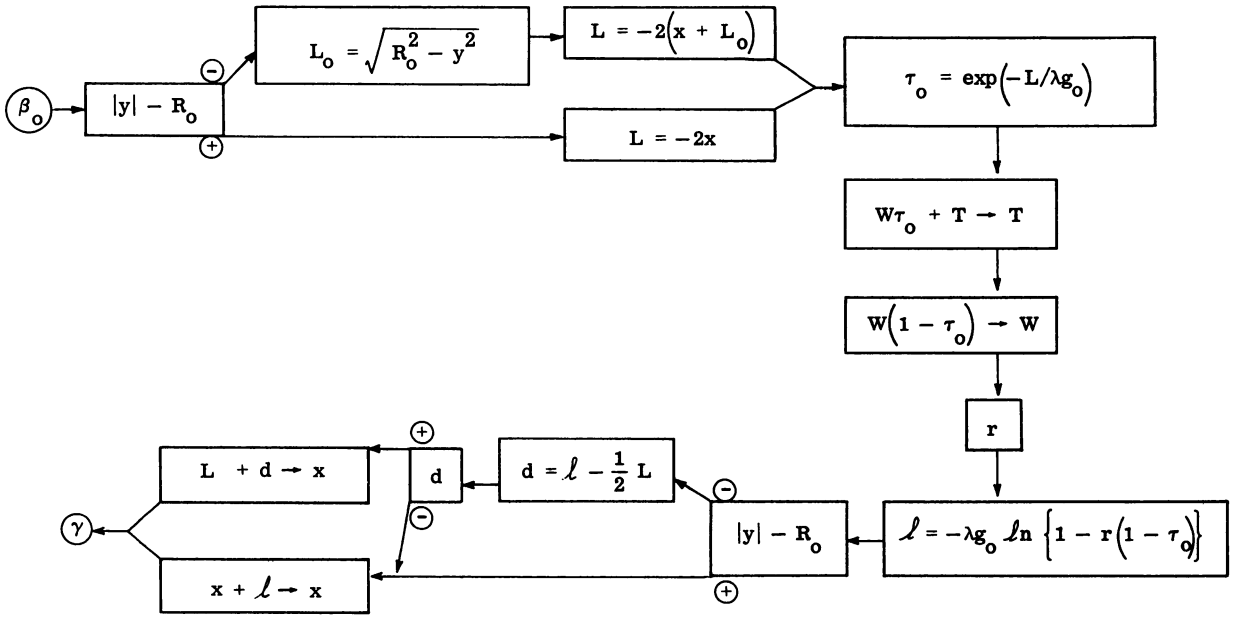

Fig. 16

λ_γ for the incident energy. A set of storage places $\rho_1, \ldots, \rho_k$ are reserved in the machine for the numbers of free paths represented by segments (z',z") of the line of flight in the zones through which it passes. The method is illustrated in Fig. 16a. It is assumed that $x = R_o \sqrt{r}$, $y = 0$ have already been set for the point of entry in the source routine, symmetry obtaining about the z-axis.

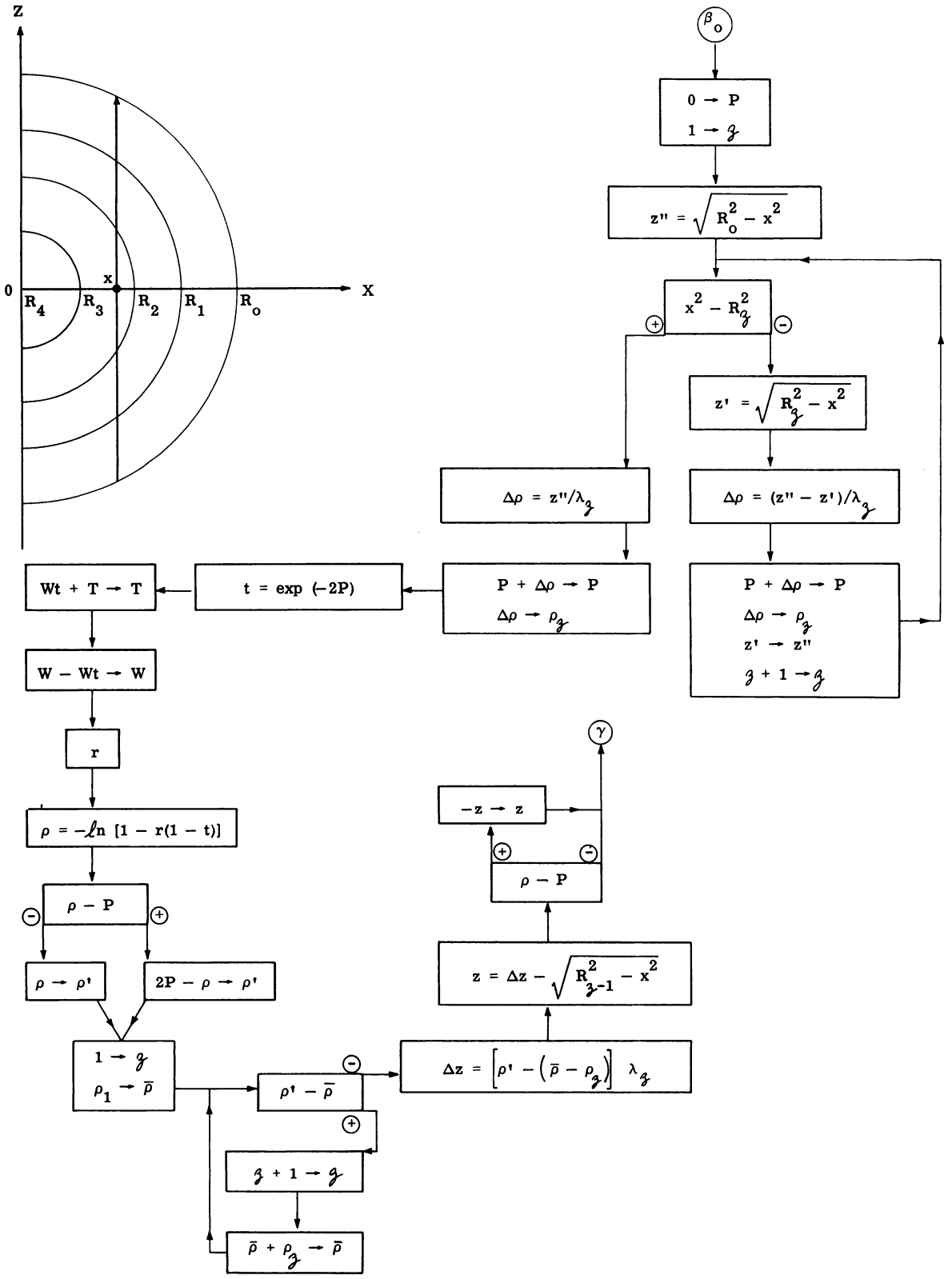

Fig. 16a

7. The transmission in subsequent history. The device of forcing collisions of the non-transmitted weight may, of course, be applied to collisions after the first. If applied consistently to all collisions, then no trajectory ever terminates in escape, and one would ordinarily rely on a weight cutoff for termination. Usually the geometric complexity of paths after first collision renders use of the device for further collisions impractical. We do not consider forced collisions other than the first in the present manual.

8. Prejudiced first collision in "large" systems. In problems concerned with "large" systems, such as those arising in shielding, the transmission must be very small and yet one may have to obtain energy-angle distribution of escape and space distribution of various types of collision (e.g., inelastic collision and radiative capture of neutrons in determining γ-sources) throughout the system. Moreover, the existence of energy cutoffs makes very unlikely the arrival of particles in the farther reaches of the system after many collisions. In such cases, one may overcome the dwindling of first collisions due to the exponential by prejudicing the distribution of first collisions and weighting accordingly.

We illustrate with a simplified example. Consider a thick plane slab of two layers (free paths λ_1, λ_2 at incident energy) bounded by the planes $z = 0$, $z = L_1$, $z = L_2$, with a source directed vertically upward and incident on the surface $z = 0$. One may then determine the

position z of first collision, together with the weight at this point by the scheme of Fig. 16b. Note that the formula $z = rL_2$ distributes first collisions uniformly throughout the slab, while the weighting gives the correct expectation for first collision between z and z + dz, namely,

$$\frac{dz}{L_2} \cdot \frac{L_2}{\lambda_m} e^{-\rho} = e^{-\rho} \frac{dz}{\lambda_m}$$

If N source particles are processed, the expected total weight assigned to these at first collision is then $N(1 - \tau_o)$, where $\tau_o = \exp - \left\{ \frac{L_1}{\lambda_1} + \frac{L_2 - L_1}{\lambda_2} \right\}$ is the transmission.

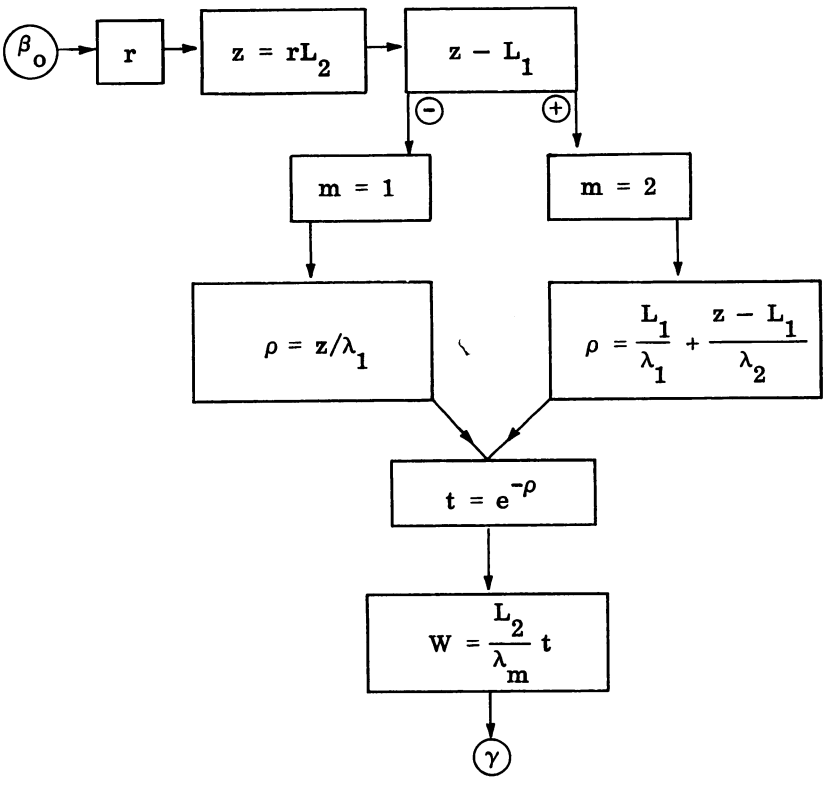

Fig. 16b

CHAPTER IV

THE COLLISION OR ESCAPE ROUTINE

1. Introduction. In the last chapter, we discussed a special routine for "forced first collision." Conceptually, this routine conducts a particle from a special point of departure, namely, the source, to a point of collision within the system, with no escape alternative for the trajectory itself. When this (β_o) routine is used, it is entered only once, namely, directly from the source, and has only one exit, the collision routine (γ).

In all problems, whether this device is used or not, a routine (β) is required which is designed to conduct a particle from a perfectly arbitrary point of departure in an arbitrary zone, at which the particle parameters are known, to its next point of collision within the zone, or to its point of departure from the zone, in the event the boundary is reached without collision. (Cf., however, §9 of this chapter.)

This (β) routine is entered directly from the source, in problems not using the (β_o) device, and in various other situations, namely, as a particle departs from a collision, as it enters a new zone, or

upon re-entry into the same (central) zone, after crossing a central hole, etc.

Aside from the initial determination of the distance ℓ to collision (calculated for an infinite homogeneous medium), this routine is purely geometric, and consists essentially in comparing the distance ℓ with the distance d to the boundary of the zone along the line of flight. If $\ell < d$, space and direction coordinates are set at the point of collision, and one proceeds to (γ). If $\ell \geq d$ the particle is considered to reach the zone boundary. In this case its parameters are set at the boundary point, and one returns to (β).

It is clear that when a problem involves zones of different geometric shapes, several such routines (β_ν), $\nu = 1,2,\ldots$ may be required, each designed for the geometric problem of its own type of sector. In such cases the particle carries an additional parameter which indicates the type of geometric zone it occupies at any given time. Transfer is made from source points, points of collision, and so on to the appropriate (β_ν).

One may also note that, under our procedure, a particle reaching the boundary of a zone is referred back to (β), unless escape from the system is involved, and is then treated anew relative to the zone entered. An alternative procedure using a single random number to determine the eventual position of collision, or escape from the system, by reference to all path segments defined on the line of flight by all zone boundaries may be used but seems clumsier to handle, and we do not

discuss it. The method involved should be clear from the discussion at the end of §4, Chapter III.

2. A routine for the spherical shell. Consider the problem of a particle with parameters R, w, E, g, ζ at a point of departure in a shell of radii $R_{\zeta-1} < R_{\zeta}$. The flow diagram of Fig. 17 will be seen to keep computation at a minimum. Here, R_ℓ is the radial distance to the point of collision in an infinite medium of free path λ_g^{ζ}, t is the tangential distance to the inner boundary from the point of departure at R, and $w_t = -t/R$ is the cosine of the angle γ_t from OR to this tangent (cf. Fig. 18). Reference to the cos γ curve of Fig. 19 shows that, w being negative, $w_t^2 - w^2 < 0$ implies that the line of flight cuts the inner boundary. Moreover, if $R_\ell^2 - R_{\zeta-1}^2$ is non-negative, the sign of $\ell^2 - t^2$ distinguishes between a point of collision on one or the other side of the inner boundary.

It will be seen that for "solid spheres" with no central hole this flow diagram will work automatically if $\zeta = 1$ is the index of the innermost zone, provided $R_o = 0$ be stored together with the other zone radii $R_1 < \ldots < R_Z$. Thus no special (β) routine is required for the central spherical zone. The exits (γ') indicate collision within zone z (cf. the next section).

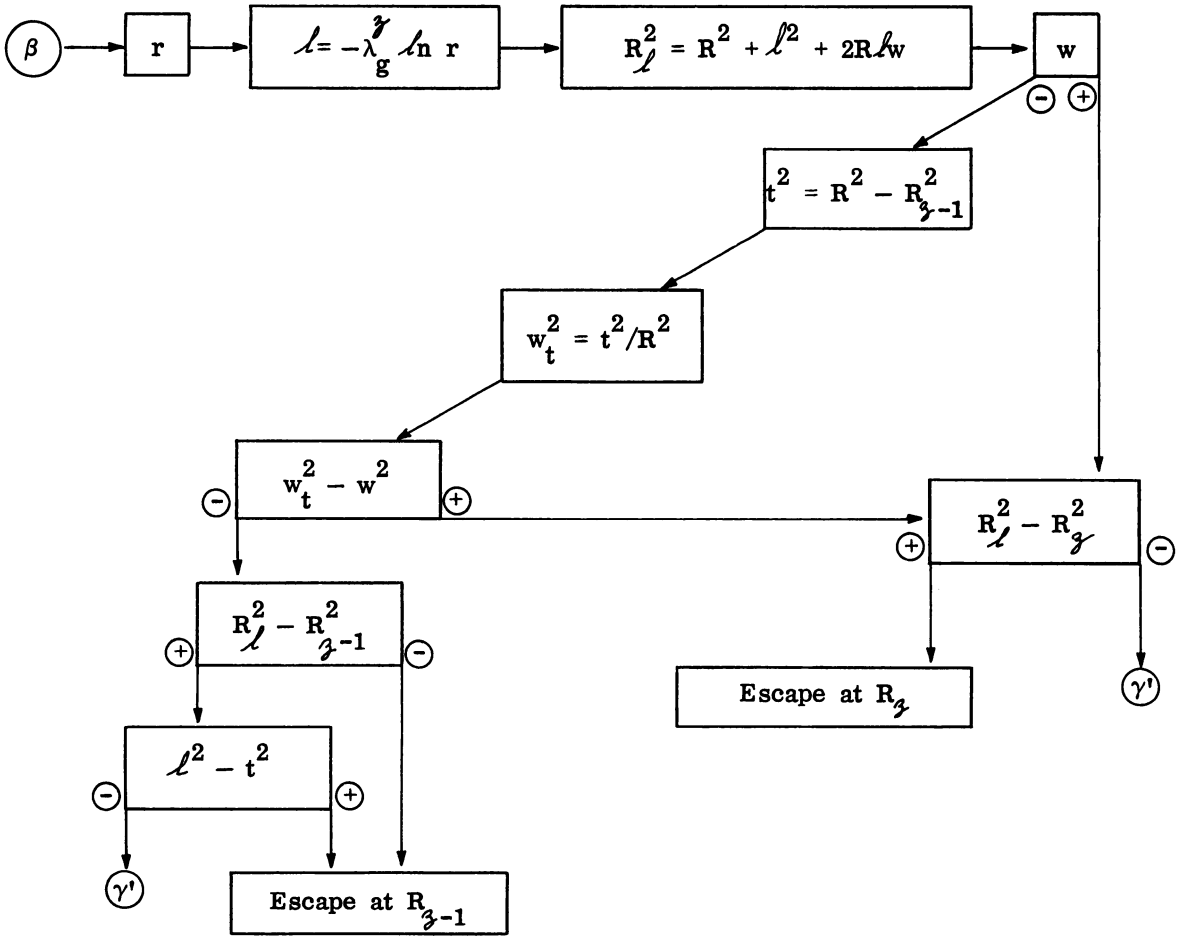

Fig. 17

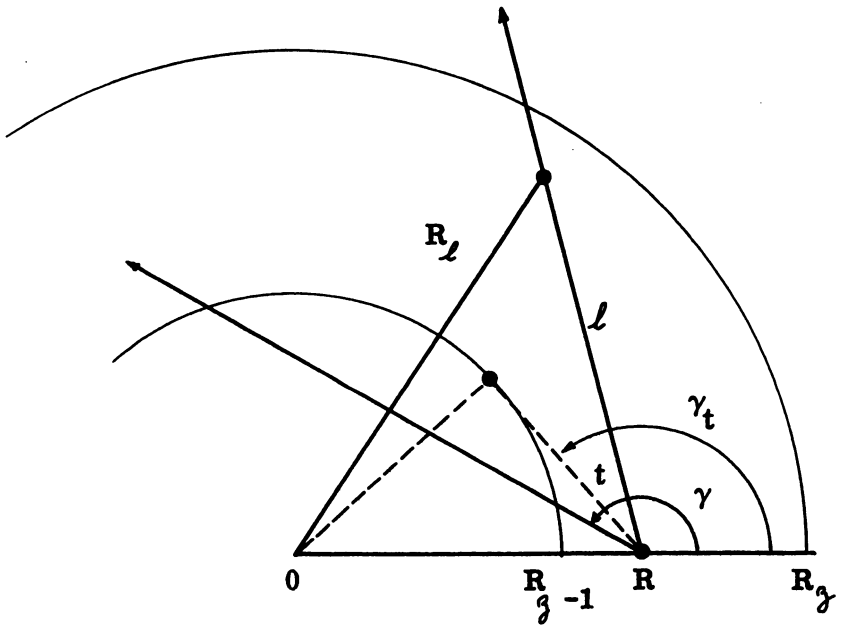

Fig. 18

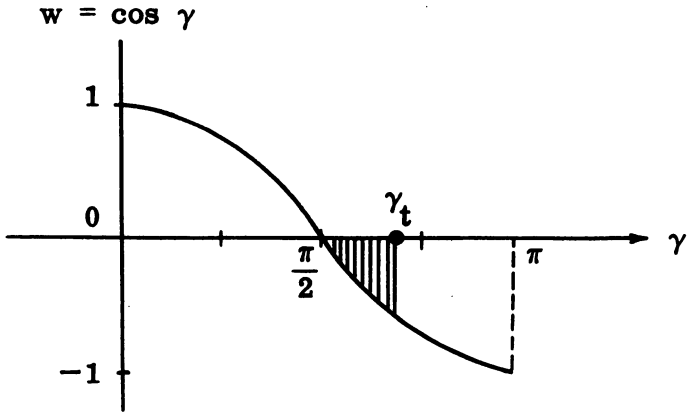

Fig. 19

3. Reorientation formulas for the spherical shell.[9] In case of collision (γ'), one provides a routine for computing the parameters R,w as they exist at the point of collision, before proceeding to (γ) itself. This is indicated in Fig. 20. Moreover, in the event of escape at R_η, we have two alternatives. If $\eta = \mathfrak{N}$, the number of the outermost zone, the particle leaves the system, and one proceeds to (ϵ), while if $\eta < \mathfrak{N}$, the particle enters a new zone $\eta + 1$. Classification of an escaping particle may or may not involve its direction of escape. In the latter case, one may by-pass the reorientation part of the escape routine of Fig. 20 by putting the $\eta + 1 \rightarrow \eta$ and $\mathfrak{N} - \eta$ boxes first. One obtains the w' formula of the latter routine from the relation w' = cos $\gamma' = \sqrt{\left[1 - \sin^2 \gamma'\right]}$ and the law of sines: $\sin \gamma / R_\eta = \sin \gamma' / R$. Note that cos γ' takes the positive square root since an entry to a zone from the inner boundary has acute angle of entry.

Similarly, one obtains $w' = -\sqrt{\left[1 - (R/R_{\eta-1})^2(1 - w^2)\right]}$ for the entry cosine at $R_{\eta-1}$. For solid sphere problems, the escape contingency at $R_{\eta-1}$ occurs only if $\eta > 1$, and involves the substitutions $w' \rightarrow w$, using the latter formula for w', $R_{\eta-1} \rightarrow R$, $\eta - 1 \rightarrow \eta$, and thence passage to (β).

If the central zone $\eta = 1$ is vacuum, escape at R_1 from zone $\eta = 2$ necessitates re-entry of zone $\eta = 2$ after crossing the hole. Thus for the hollow sphere problem, we have the routine of Fig. 21.

---

[9] All the geometric relations involved in the present section are indicated in Fig. 22 and Fig. 23.

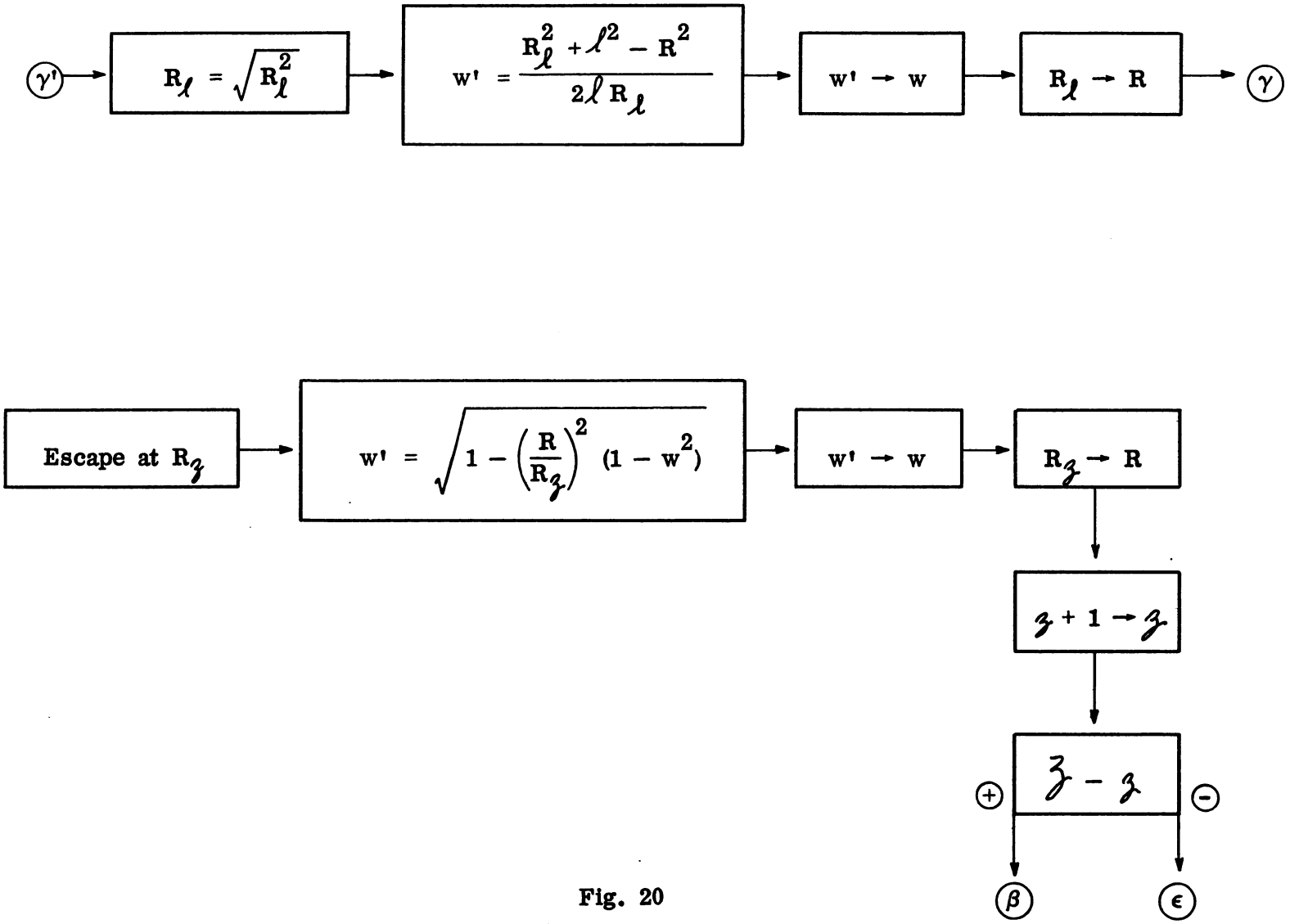

Fig. 20

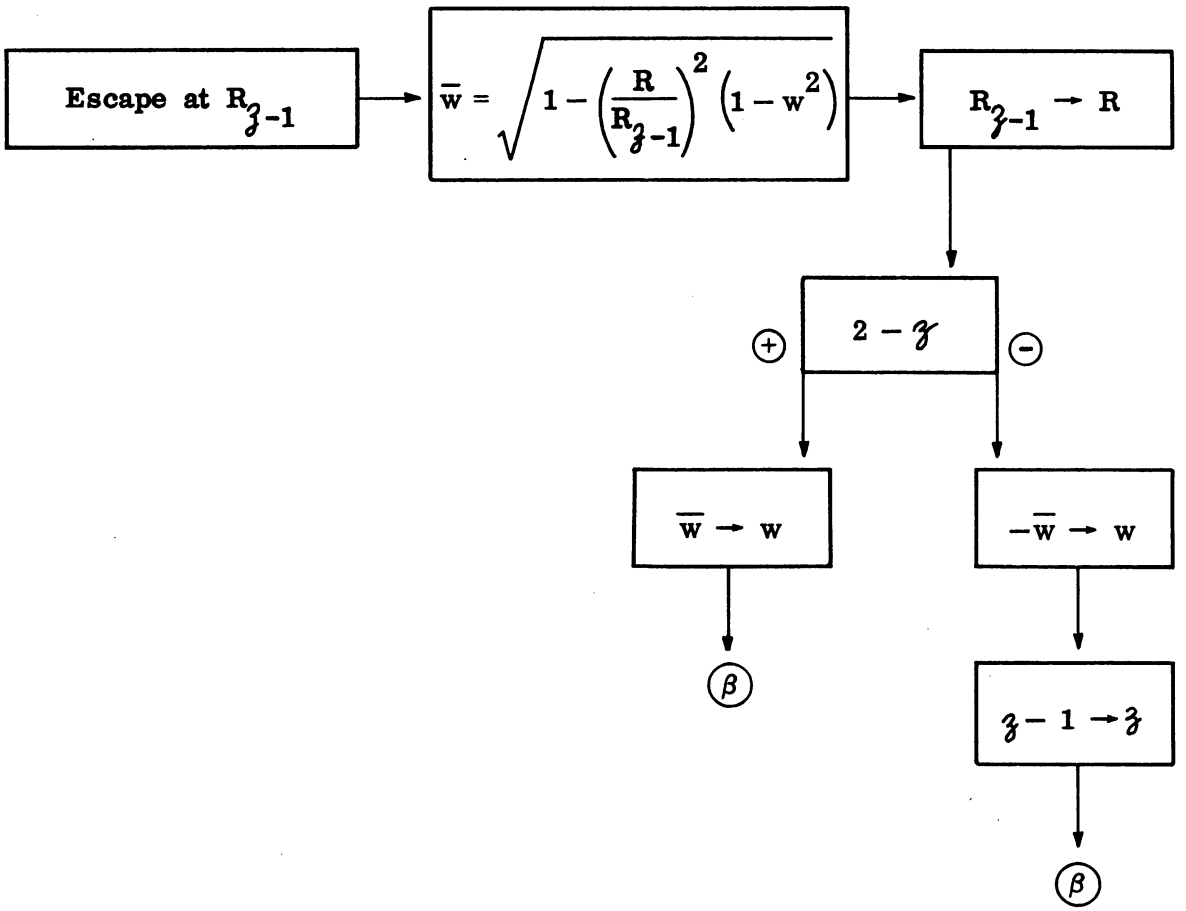

Fig. 21

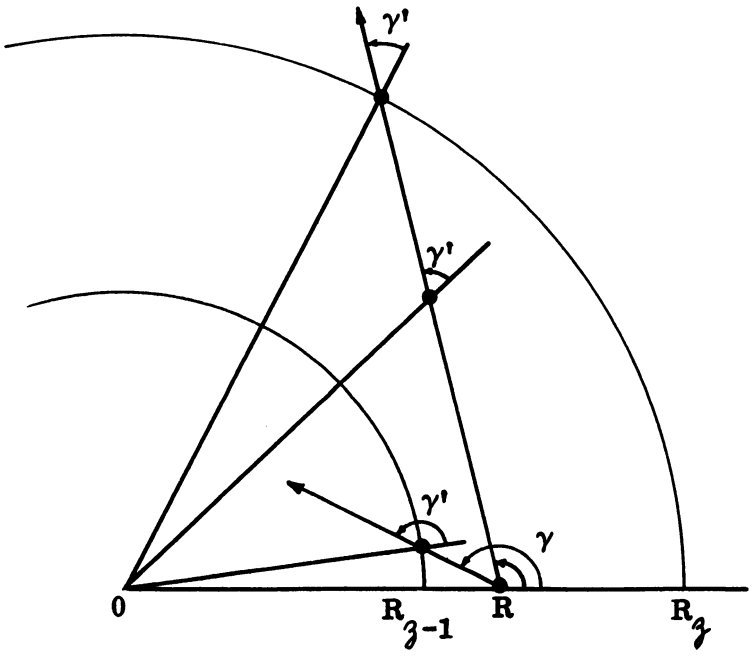

Fig. 22

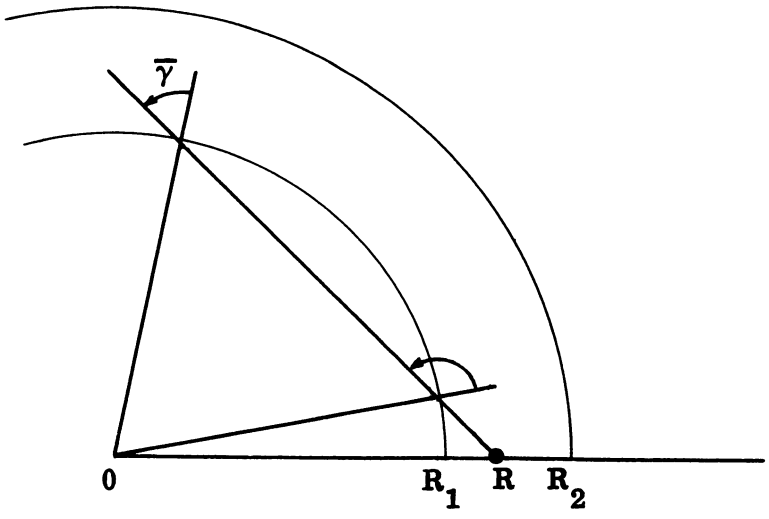

Fig. 23

4. Flux problems in spherical geometry. Certain problems, one of which is that of a central neutron source in homogeneous air, require study of the number of neutrons of energy E which traverse (imaginary) spherical surfaces at varying distances from the source. Such situations may be handled by subdivision of the medium into spherical zones, and incorporating into the "Escape at R_γ and $R_{\gamma-1}$" routines a cumulative tally in counters $N_{\gamma,g}$. These are not terminal categories, except for $\gamma = \bar{\gamma}$ and do not enter into a "sum check," but count all neutrons of all energy groups whenever they cross a spherical boundary R_γ.

5. A routine for the finite cylinder. We consider now the case of a particle with parameters x, y, z, u, v, w, E, g at some point of departure within a finite homogeneous cylinder of radius R_1, height H (cf. Fig. 24). The procedure is indicated in Fig. 25. Note that before entering (γ) in the event of collision, all parameters are stored in the machine as they obtain at the point of collision. The direction coordinates u, v, w are the same at the entry to (γ) as they were at the (β) entry, and do not require new evaluation, as was the case for w in spherical geometry. The exit (ϵ) denotes, as usual, escape from the system and leads to a classification routine for escaping particles. Such routines are discussed in a later chapter.

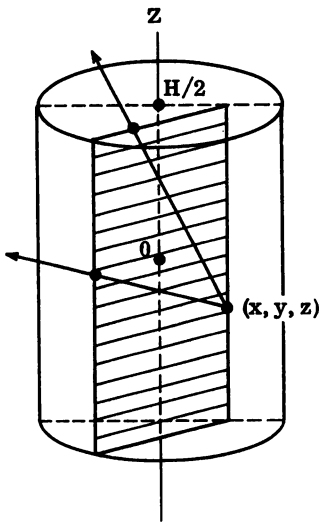

Fig. 24

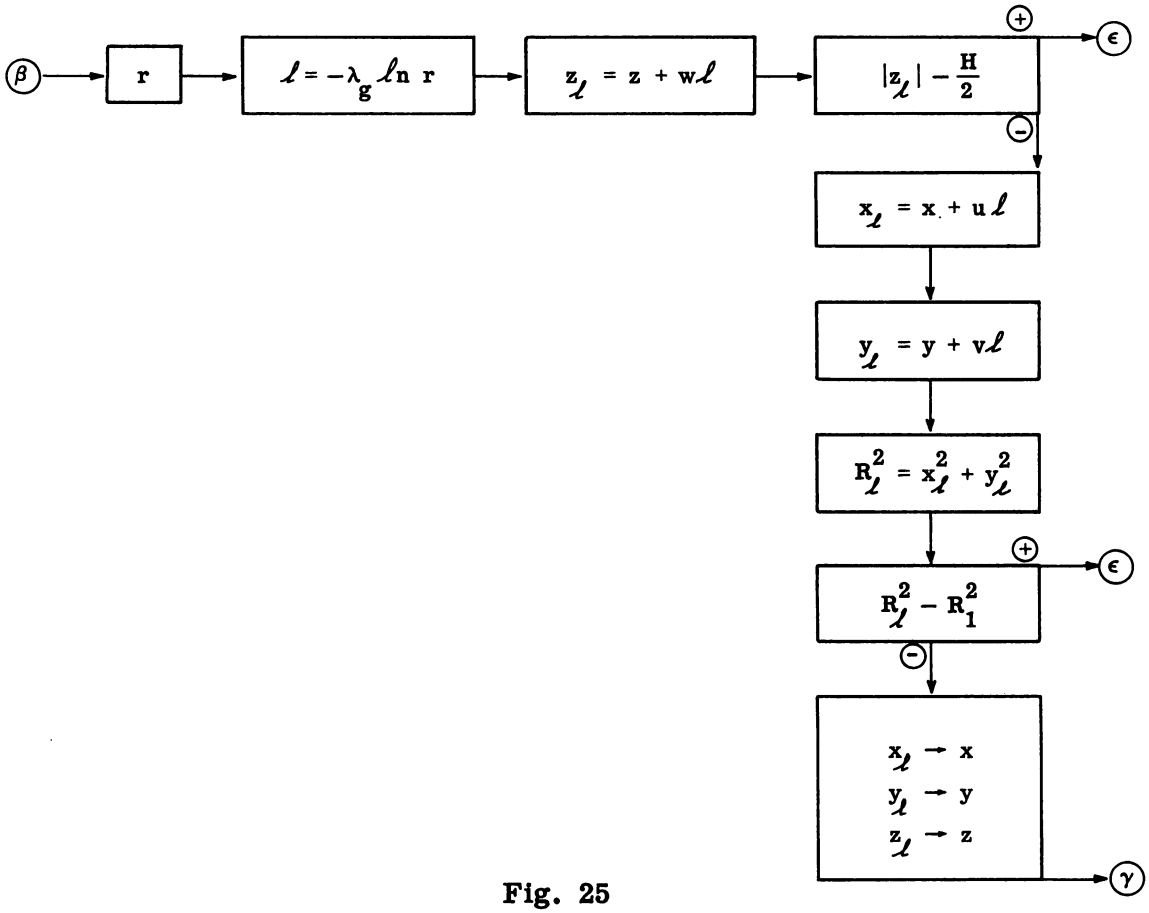

Fig. 25

6. The finite cylindrical shell with central hole. Let x, y, z, u, v, w, E, g be the particle parameters as they obtain at an arbitrary point of departure within a finite cylindrical shell of radii $R_o < R_1$ and height H. The procedure of §5 may be used unless the line of flight $x' = x + ut$, $y' = y + vt$, $z' = z + wt$, $t \geqq 0$ cuts the (infinite) inner cylindrical surface $x^2 + y^2 = R_o^2$ at two real, distinct distances

$$t = \frac{-\delta \pm \sqrt{\Delta_o}}{1 - w^2}$$

where $\delta = ux + vy$ and $\Delta_o = \delta^2 - (1 - w^2)(x^2 + y^2 - R_o^2)$. In the latter case one provides an additional routine as indicated in Fig. 26.

Study of the flow diagram together with Fig. 27 should make the method clear. Note that the case $w = 1$ and the case of a line of flight tangent to the inner cylinder are handled automatically. Nevertheless, some caution may be required at entry to the "t" boxes if $1 - w^2$ is very small. Such a case may be handled easily by a preliminary comparison of $\left[-\delta \pm \sqrt{\Delta_o} \right] - K(1 - w^2)$ with 0, where K is a constant larger than the largest distance within the shell. In case the latter difference is positive, one may consider $|z_t|$ as essentially infinite and may route the flow to the proper box directly, by-passing the explicit computation of t and z_t.

An alternative method which is very convenient when several cylindrical zones are involved is that of Fig. 27a. This has the

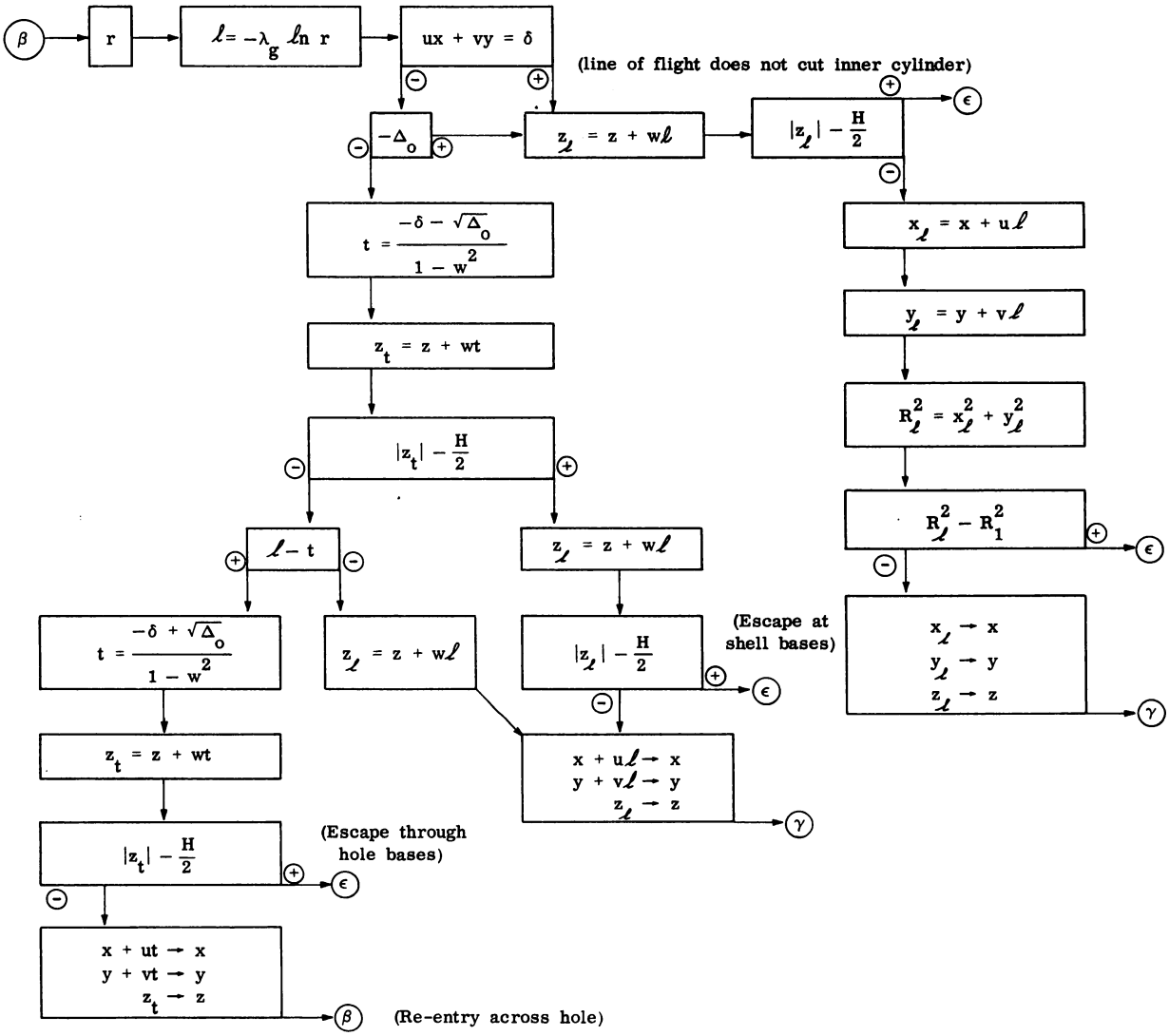

Fig. 26

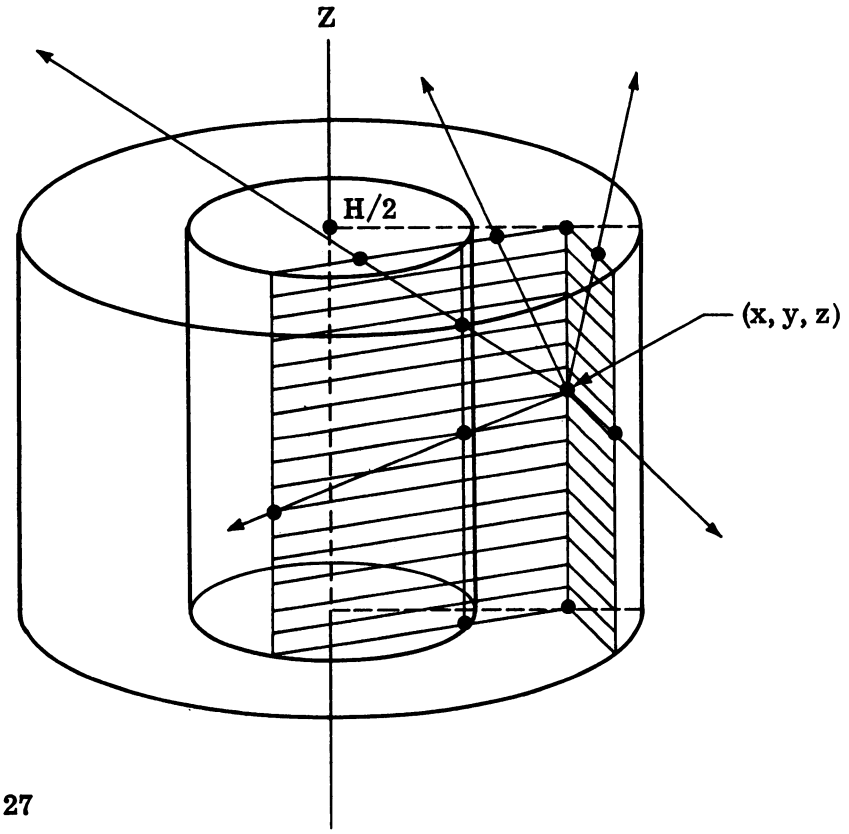

Fig. 27

advantage of effecting the decision between escape or collision with a minimum of square roots, sets up the space parameters at escape position with little repetition of code, and avoids the "infinity decision" referred to above. It is understood that the inner and outer radii $0 \leq R_o < R_1$ and base plane z-coordinates H' and H" are properly set as a particle enters one of the system of zones. Moreover, a parameter $R^2 \equiv x^2 + y^2$ is carried throughout with x, y, z, and an additional $\rho^2 \equiv 1 - w^2$ together with u, v, w. An index X is also used, being set equal to zero at the source. The latter is of a purely computational character.

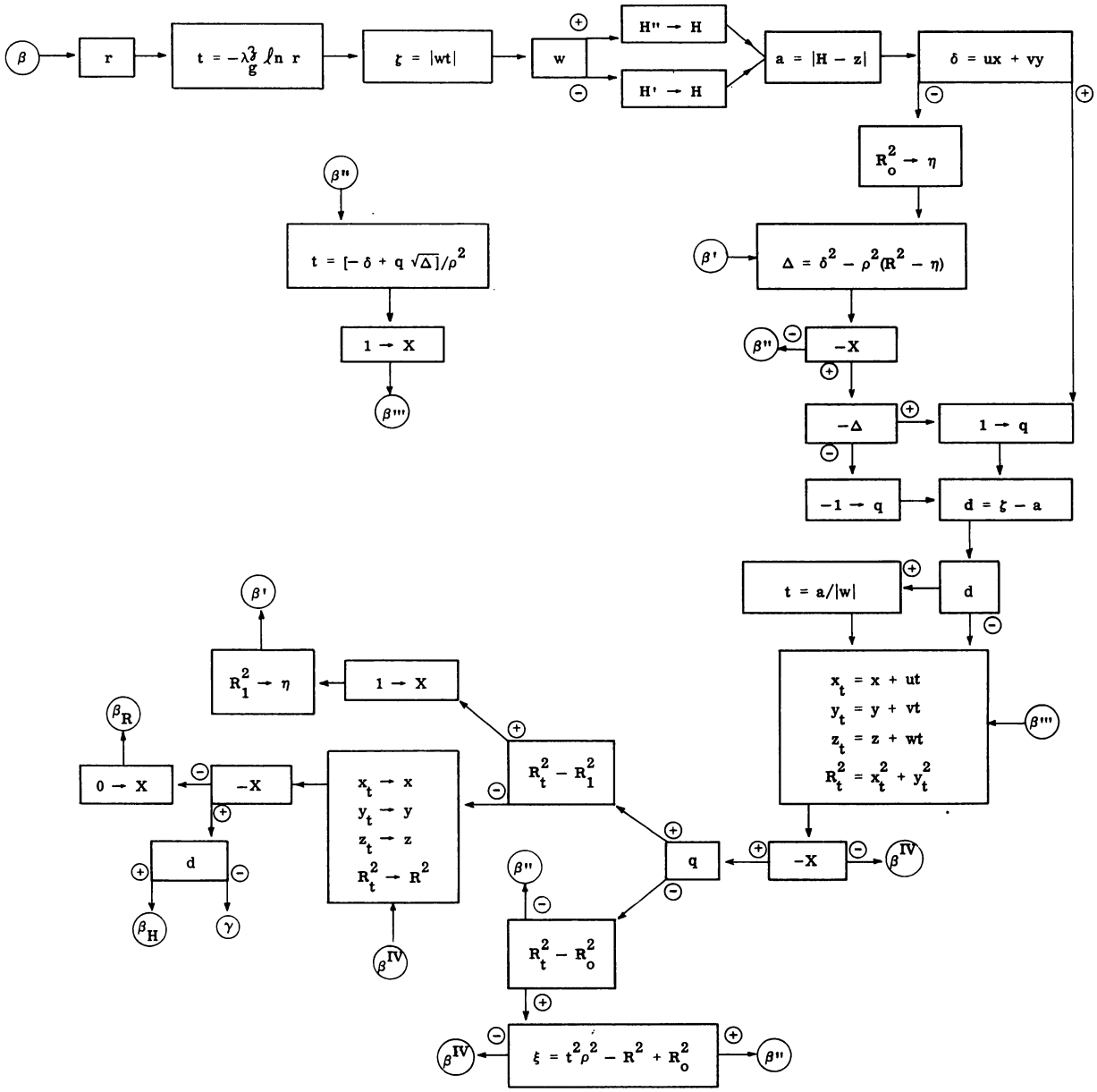

Fig. 27a

It may be helpful to note that q = -1 or q = +1 according to whether the directed line of flight does or does not cut the inner (infinite) surface, while d is "plus" or "minus" according to whether the point of collision is outside or inside the (infinite) base planes. After first transit through the box in which x_t, y_t, z_t, R_t^2 are computed, these quantities refer to the point of intersection of the line of flight with the base plane z = H, when $d \geqq 0$, and to the point of collision when $d < 0$. The exits β_R and β_H indicate escape from the zone through the inner or outer lateral surface, and from one of the bases, respectively. In an actual problem involving several sectors, such exits must lead to rather involved routines for deciding the sector next entered and setting up its geometric parameters R_o^2, R_1^2, H', H", and γ or classifying escape if such is the case.

7. The spherical shell in absolute space. Even when the medium is spherically symmetric, it may be necessary to keep track of the direction of a particle in absolute space, e.g., in case emergent particles are to be classified with respect to their directions relative to a given source direction. In such cases, it is convenient to use x, y, z, u, v, w parameters. The method is similar to that of the preceding section and should require no further explanation. The procedure following a "core hit" depends on the problem and may involve an absorption, passage to an inner zone, or crossing of a central vacuum. We do not elaborate this case further. The procedure is indicated to some extent in Fig. 28.

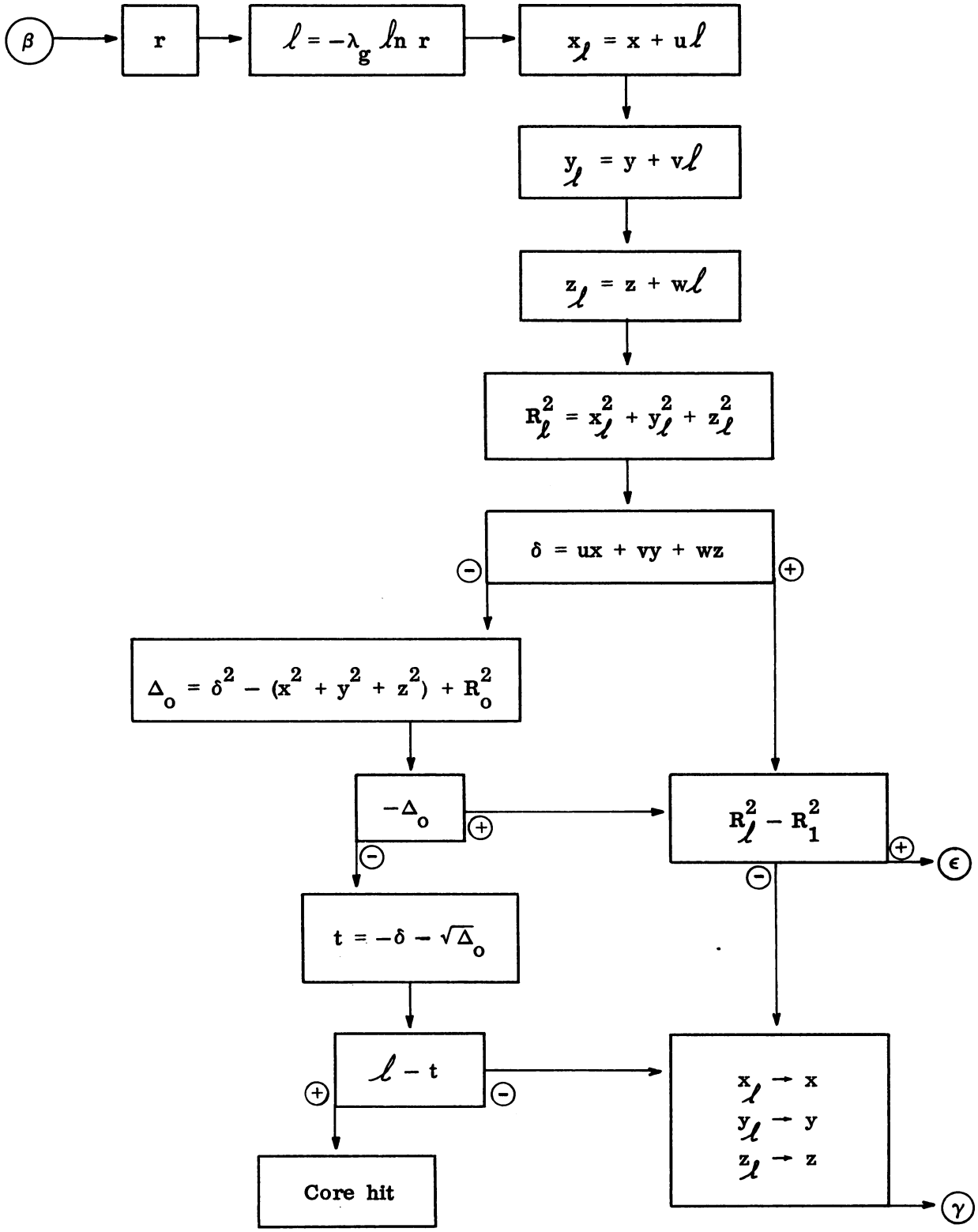

Fig. 28

8. Slab geometry. In problems on plane slabs, the medium can be considered to occupy the region of x, y, z space defined by $Z_o \leqq z \leqq Z_{\bar{z}}$, the coordinate z and the cosine w of the angle γ which the line of flight makes with the positive z-axis being the only relevant coordinates. The slab may consist of zones of different kinds of media, with upper boundaries defined by $Z_1 < \ldots < Z_{\bar{z}}$. The ($\beta$) routine for such a problem may be like that in Fig. 29.

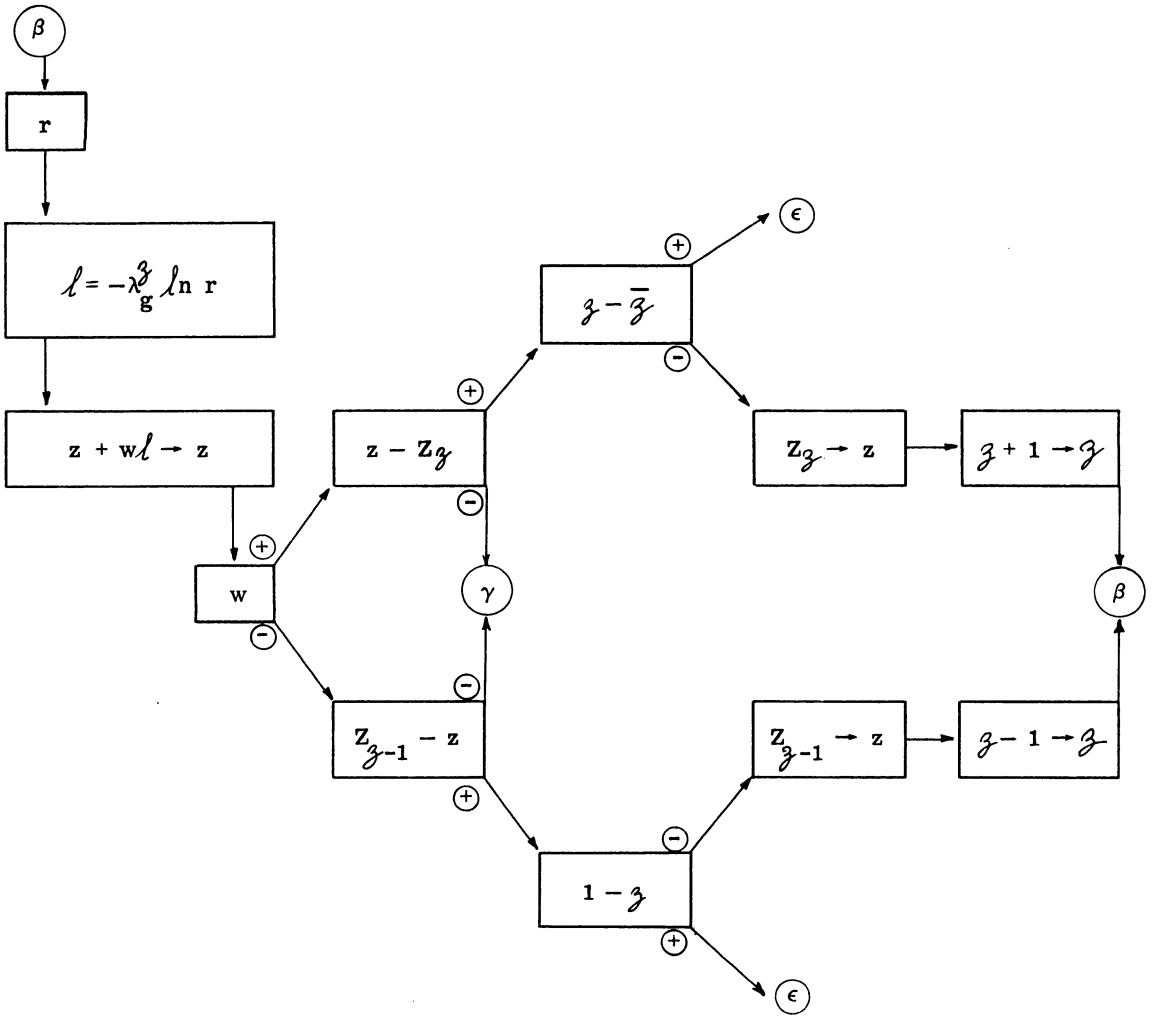

Fig. 29

9. Problems run in cycles of time $\Delta\tau$. In problems involving the distribution of particles (in energy, position, and direction) at a given time $\Delta\tau$ from their origin in some source distribution, a particle is followed until it is lost to some terminal category such as escape, capture, etc., or until the allotted time $\Delta\tau$ has expired. Such problems arise naturally in α-determinations (cf. Chapter II, §8), the computation being performed in successive cycles, the output distribution of each cycle being used as the input of the next. The (β) routine in such cases must be modified so that the essential decision between collision within the zone or arrival at the zone boundary is contingent upon the qualifying condition: "if time permits." Thus, the distance d to collision or boundary must be computed, and the time (cf. Chapter II, § 3)

$$\tau' = \tau + k''d/\sqrt{E}$$

of these events is then compared with cycle time $\Delta\tau$. If $\tau' < \Delta\tau$ one substitutes $\tau' \rightarrow \tau$ and proceeds as usual, whereas, if $\tau' \geq \Delta\tau$, time runs out before the event can occur. One then computes the distance

$$\ell' = (\Delta\tau - \tau)k' \sqrt{E}$$

that the particle can travel in the time remaining, and the position and direction after this distance is traversed. The particle is then classified in an energy, position, and direction category $N_{g,\eta,i}$ and one returns to (α). We include in Fig. 30 an example for a homogeneous sphere with radius R_η. See §§2,3 of the present chapter for (γ') and Chapter II, §8, for (α). (L_B refers to loss from the boundary.)

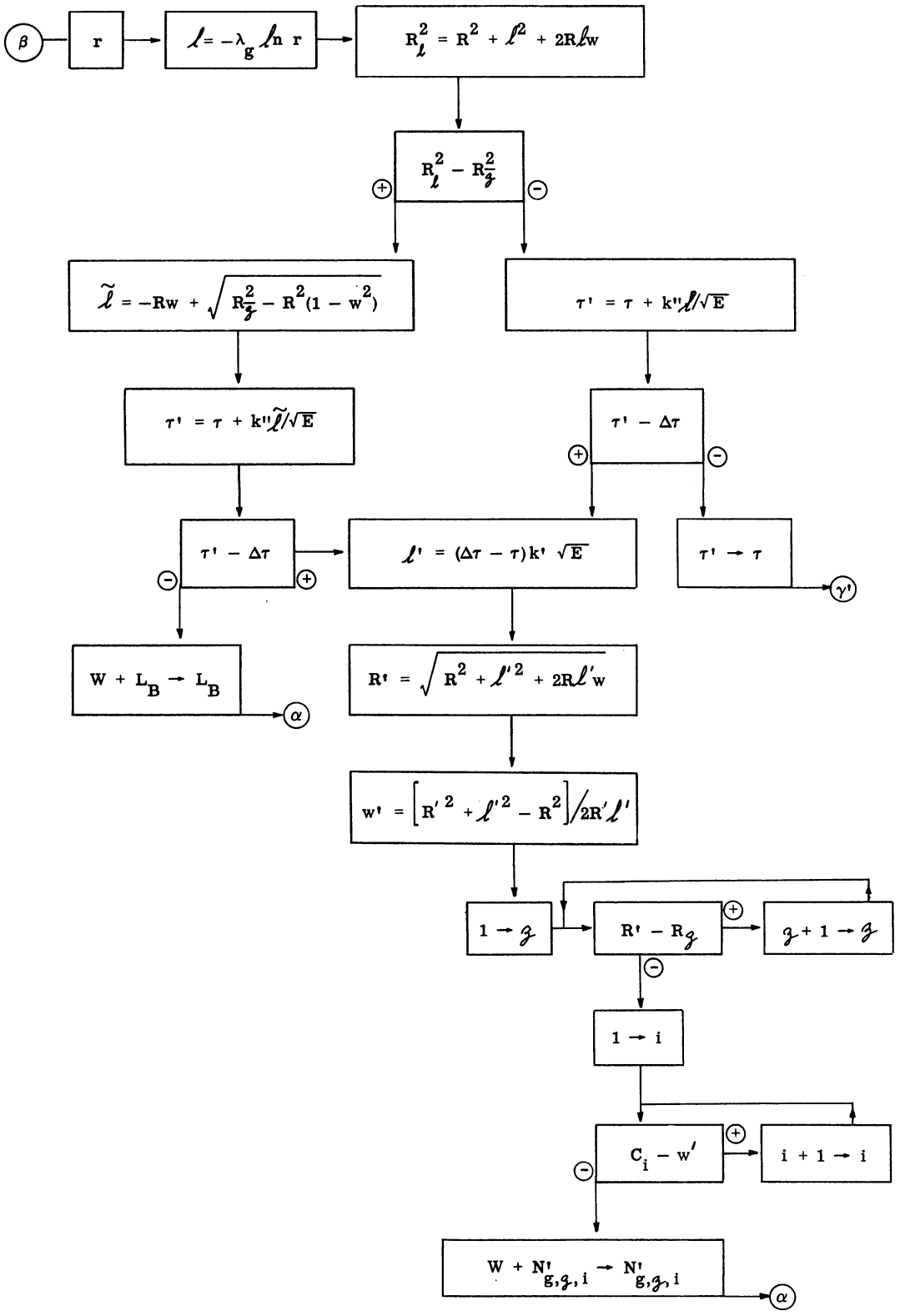

Fig. 30

CHAPTER V

THE COLLISION ROUTINE FOR NEUTRONS

1. Introduction. We have seen in the last chapter how the geometry of the system determines the immediate fate of a particle, on the basis of the equation $\ell = -\lambda \ell n\, r$, as a collision or an escape at the boundary of the zone. The present chapter is devoted to the methods involved in dealing with the former contingency in the case of neutrons colliding with nuclei. In the following chapter, we consider the collision routines for photons.

It may be that the media occupying different zones $\gamma = 1, 2, \ldots, \gamma$ are so diverse in the types of nuclei contained, and thus in the types of neutron processes involved, that it is not worth while to attempt a general code for (γ) covering all contingencies. In such cases, different collision routines (γ_γ) may be provided, each economically adapted to its own type of medium.

The basic object of this chapter and the next is to show how, after collision of a neutron or photon in a given medium, the new E, g, ν, and W are obtained, as well as the cosine of the laboratory angle of

deflection from the incident line of flight. The exit (δ) from the (γ) routine refers to a purely geometric procedure which determines the new direction parameters u, v, w (or simply w) from the incident direction parameters and the laboratory deflection cosine, and thence leads back to (β). The (δ) routine is developed in Ch. VII.

2. Capture and selection of the type of collision. It is impossible to give a perfectly general procedure for the (γ) routine, so diverse are the various types of processes. Each problem must be studied in its own individuality.

If the number ν of collisions is among the neutron parameters, we may begin with

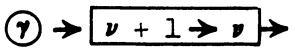

Unless the medium in question consists of only one type of nucleus, and that nucleus has only one type of cross section for neutrons, we must next proceed to decide on the type of nucleus hit, and the type of collision. Recalling the discussion of cross sections (Ch. III, §§ 1,2,3), it is clear that the total area presented to a beam of neutrons of energy group g in the thin slab there defined is $(N_A \sigma_g^A (\text{tot.}) + \ldots) \alpha \, d\ell$. Hence, assuming a collision in the medium, the probability that the collision be with a nucleus of type A is the ratio of areas:

$$N_A \sigma_g^A (\text{tot.}) \ \alpha d\ell / (N_A \sigma_g^A (\text{tot.}) + \ldots) \ \alpha d\ell$$

where the $\alpha d\ell$ may be cancelled.

If one or more of the nuclei A, B, C, ... present admits capture, or some other process which may be regarded as terminal for purposes of the problem (e.g., inelastic collision in monoenergetic problems), we may decide to use a weight parameter W, as discussed previously. (Cf. Ch. II, §2.) It is then economical to store deterministic fractions $\widetilde{C}_g$ of weight captured on collision, where

$$\widetilde{C}_g = [N_A \sigma_g^A (\text{cap.}) + \ldots] / [N_A \sigma_g^A (\text{tot.}) + \ldots]$$

the summations being over nuclear types A, B, ... We should then include at the outset the routine of Fig. 31. Here L_c is a "terminal" category in the sense that capture is a final event in the life of a physical neutron. However, the use of weights prevents the loss of the geometric path being followed and greatly improves the statistics. When weights are used, it is advisable to use a "weight cutoff" W_o, below which weights are negligible, and an additional terminal category L_w, to catch weights falling below the cutoff. This category is terminal in the mathematical sense that one returns to (α) for a new source neutron in case of such a loss, the <u>trajectory</u> terminating at this point. If the weight W of the uncaptured beam exceeds W_o, we

proceed to decide, if necessary, upon which type of nucleus A, B, C, ... the scattering takes place, probabilities being now dependent on the assumption that a non-capture collision occurs.

Suppose for simplicity only two nuclear types A and B are present. For machine purposes, we assign to type A a "type parameter" value e = 1 and to B the value e = 2. We store in addition to the above $\tilde{C}_g$ the probabilities

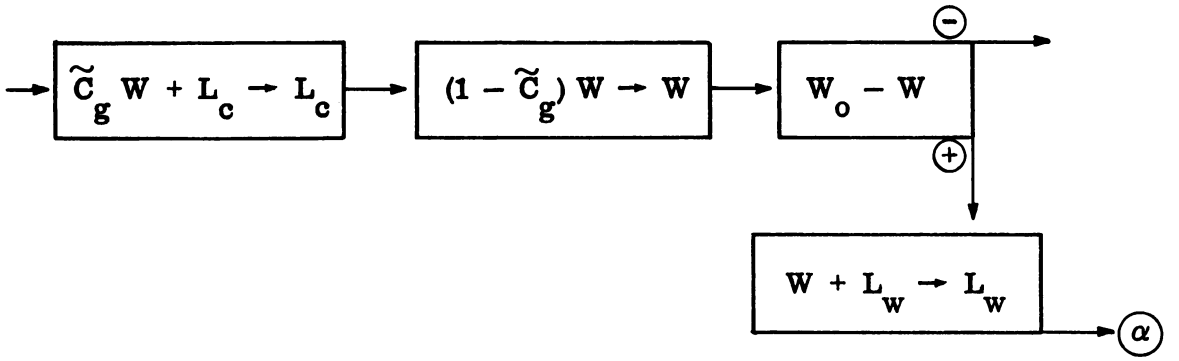

Fig. 31

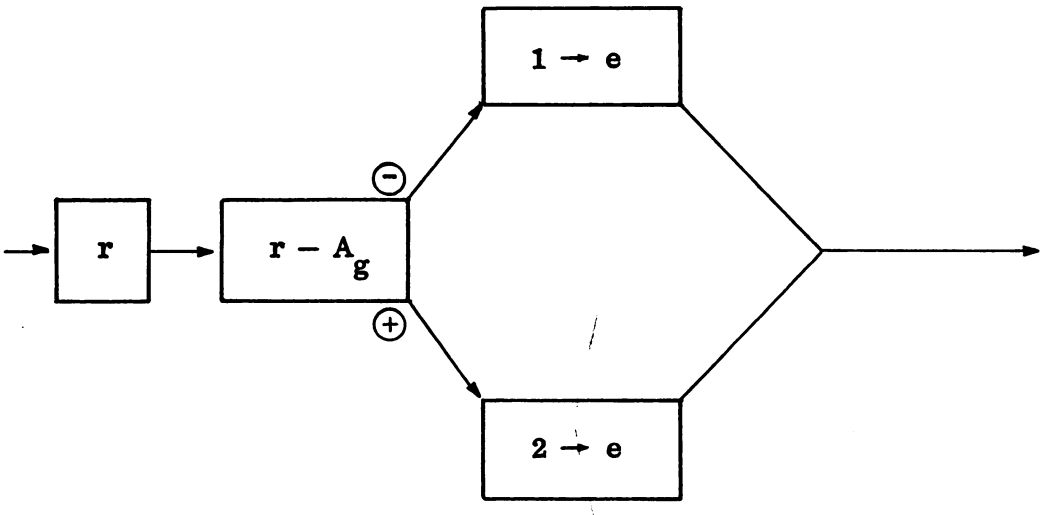

Fig. 32

$$A_g = N_A (\sigma_g^A (\text{tot.}) - \sigma_g^A (\text{cap.}))/[N_A (\sigma_g^A (\text{tot.})$$

$$- \sigma_g^A (\text{cap.})) + N_B (\sigma_g^B (\text{tot.}) - \sigma_g^B (\text{cap.}))]$$

for non-capture collision on type A, and enter the decision routine of Fig. 32 for determination of the parameter e.

We then proceed to routines designed to decide the type of collision on A (e = 1) or on B (e = 2). If the processes involved in the two cases are sufficiently similar one may join the exits of Fig. 32 as shown and go to a common routine which, by use of the variable e, can handle both cases. Otherwise, one provides separate routines for the two types. In any case there is at this point a real disjunction, the neutron hitting one or the other type of nucleus.

It remains to decide which type of collision is undergone, assuming it to be non-capture on nuclear type e. This involves reference of a random number to an additional set of probabilities, the number of which will depend on the number of kinds of processes other than capture which nuclear type e admits.

For example, if e = 1 and A is uranium, we might have three possibilities: elastic scattering, inelastic scattering, i.e., (n-n) reaction with loss of energy, and fission. We should have to store in this case the probabilities

$$\epsilon_g = \sigma_g^A (\text{el.}) / [\sigma_g^A (\text{tot.}) - \sigma_g^A (\text{cap.})]$$

$$\mathcal{I}_g = \left[\sigma_g^A \text{ (el.)} + \sigma_g^A \text{ (in.)}\right] / \left[\sigma_g^A \text{ (tot.)} - \sigma_g^A \text{ (cap.)}\right]$$

and proceed from the box [1→e] of Fig. 32 to the flow diagram of Fig. 33.

It may be preferred, even if capture is to be treated by weights, to first decide on the type of nucleus hit, by reference to the total probabilities

$$N_A \sigma_g^A \text{ (tot.)} / \Sigma_g$$

$$N_A \sigma_g^A \text{ (tot.)} + N_B \sigma_g^B \text{ (tot.)} / \Sigma_g, \quad \text{etc.}$$

and then to store individual capture fractions

$$\sigma_g^A \text{ (cap.)} / \sigma_g^A \text{ (tot.)}$$

for each type of nucleus, allowing the uncaptured weight to undergo one of the remaining processes by use of probabilities such as $\mathcal{E}_g$ and $\mathcal{I}_g$ above.

If capture is not treated by weights, but is regarded as an event terminating the trajectory, the procedure of this section is modified in the obvious way, and we do not include it.

In any event, at the present stage of the flow diagram, we should have effected the decision of the type of nucleus hit, and the type of collision undergone by the incident neutron, with assignment, if necessary, of a nuclear parameter e, and adjustment of the neutron weight.

The possibilities include, of course, return to (α) if capture or weight cutoff terminates the career of the neutron in question.

We proceed to discuss routines for various individual processes commonly encountered in practice.

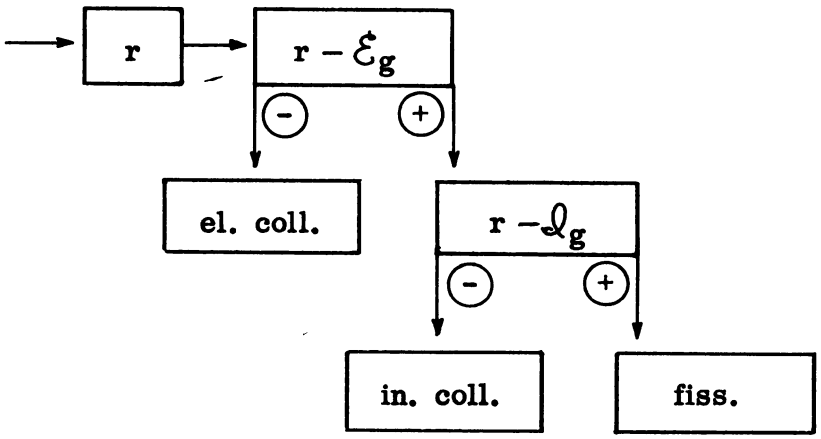

Fig. 33

3. Elastic collisions in general. We discuss in this section the collision between two particles, assuming conservation of momentum and energy. We reserve capitals for vectors, and make the following conventions: $R = (x,y,z)$ denotes the position vector of a point in the laboratory system, $V = \dot{R} = (\dot{x},\dot{y},\dot{z})$, the velocity vector of the point R. If $R_i = (x_i,y_i,z_i)$ are the position vectors of a set of point masses

m_i, $i = 1, \ldots, n$, and $m = \Sigma m_i$ is their total mass, then $R = m^{-1}\Sigma m_i R_i$ defines the position of the center of mass of these particles. We also recall that if $A = (a_1, a_2, a_3)$, $B = (b_1, b_2, b_3)$ are any two vectors, their inner product is $AB = \Sigma a_i b_i$, $A^2 = \Sigma a_i^2$, the norm of A is defined as $|A| = \sqrt{A^2}$, and the cosine of the angle θ between A and B is given by $\cos \theta = AB/|A| \cdot |B|$.

Now consider two point masses m_1 and m_2, with laboratory velocity vectors V_1 and V_2, respectively. The total momentum of the system is the vector $P = \Sigma m_i V_i$, its total kinetic energy is the scalar $k = \Sigma \frac{1}{2} m_i V_i^2$, and its total mass is $m = \Sigma m_i$. Since the equation $mV = \Sigma m_i V_i$ holds for the velocity V of the center of mass, we have always $P = mV$.

It is customary to define the velocities, total momenta, and kinetic energies, relative to the center of mass, by the equations

$$V_i' = V_i - V$$

$$P' = \Sigma m_i V_i'$$

$$k' = \Sigma \frac{1}{2} m_i V_i'^2$$

We find from these definitions the following relations between absolute and relative quantities:

$$\begin{cases} P = \Sigma m_i V_i = \Sigma m_i (V + V_i') = mV + P' \\ \\ k = \Sigma \frac{1}{2} m_i V_i^2 = \frac{1}{2} \Sigma m_i (V + V_i')^2 = \frac{1}{2} mV^2 + VP' + k' \end{cases}$$

or, since $P = mV$,

$$\begin{cases} P' = 0 = m_1 V_1' + m_2 V_2' \\ \\ k = \frac{1}{2} m V^2 + k' \end{cases}$$

Note that the first of these equations states that, relative to the center of mass, the particles always travel on the same straight line with oppositely directed velocities.

We assume now a collision between these two particles, adopting the notations indicated below for the relevant quantities before and after collision:

Before	After
V_i	W_i
P	Q
k	ℓ
V	W
V_i'	W_i'
P'	Q'
k'	ℓ'

and restate the fundamental relations

$$P' = 0 = Q' \tag{1}$$

$$P = m\,V \qquad\qquad Q = m\,W \tag{2}$$

$$k = \frac{1}{2}\,m\,V^2 + k' \qquad \ell = \frac{1}{2}\,m\,W^2 + \ell' \tag{3}$$

Now the defining relations for elastic collision are

$$P = Q$$

$$k = \ell$$

Since $P = Q$ and $P = mV$, $Q = mW$, we have $V = W$, which states that the center of mass of the system proceeds unperturbed by the collision. This equality, together with the equations (3), and the fact that $k = \ell$, implies that $k' = \ell'$, that is to say, the relative kinetic energy is unchanged.

Now $P' = 0$ in general, and we have therefore the equations $m_1V_1' = -\,m_2V_2'$, $m_1^2V_1'^2 = m_2^2V_2'^2$, and $m_1^2V_1'^2 - m_2^2V_2'^2 = 0$, with identical results for the relative velocities W_1', W_2' after collision.

Hence the equations

$$\begin{cases} \frac{1}{2}\,m_1\,V_1'^2 + \frac{1}{2}\,m_2\,V_2'^2 = k' \\ \\ m_1^2\,V_1'^2 - m_2^2\,V_2'^2 = 0 \end{cases}$$

are satisfied by $V_1'^2$, $V_2'^2$ and also (since $k' = \ell'$) by $W_1'^2$ and $W_2'^2$. Since the determinant of the linear system is $-\frac{1}{2}(m_1 m_2^2 + m_1^2 m_2) \neq 0$, the solution is unique and $W_1'^2 = V_1'^2$, $W_2'^2 = V_2'^2$.

We have, therefore, the following very simple picture (cf. Fig. 34), in the center of mass system, of elastic collision.

The upper part of Fig. 34 indicates the relations we have derived: The center of mass velocity is unchanged, the relative incoming (and outgoing) velocities are collinear and oppositely directed, and the relative speeds are unchanged. The dashed lines are coplanar, as are the solid lines; however, the two planes they determine are not necessarily the same.

The conditions for elastic scattering do not determine the angle of scattering, as defined (say) by the angle ψ_1' from W to W_1' (nor the angle between the two planes referred to above). This must be given in the form of a distribution law which depends in our case upon the neutron energy and the nucleus hit. Such distributions will be discussed in the next section. Our immediate object is the derivation of formulas for the angles ψ_i of scattering in the laboratory system, that is, the angles between W and the W_i, and for the kinetic energies $\ell_i = \frac{1}{2} m_i W_i^2$ of the two particles in the laboratory system, as functions of an arbitrary angle ψ_1'.

We first consider the W_i^2:

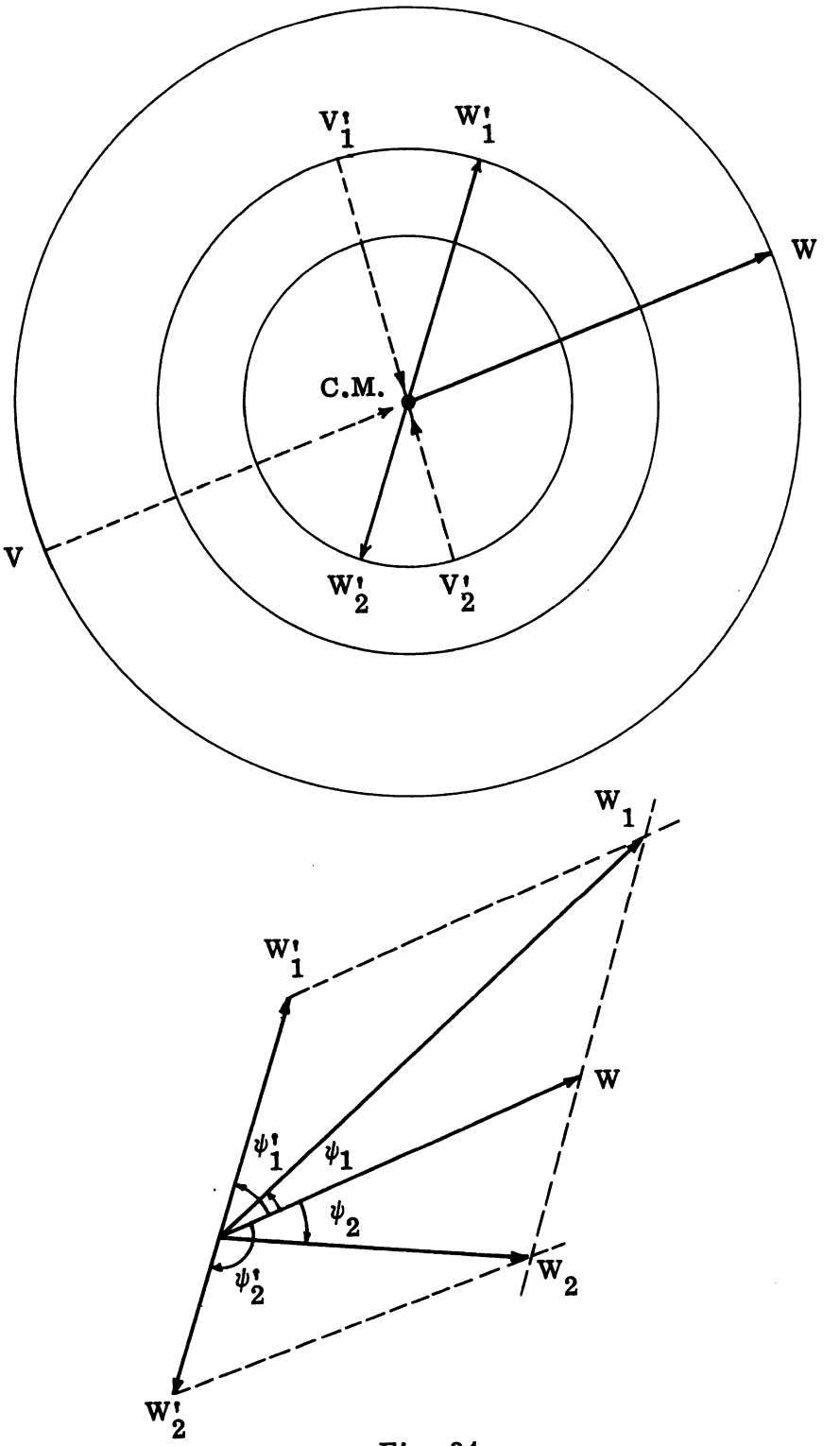

Fig. 34

$$W_1^2 = (W + W_1')^2 = (V + W_1')^2 = V^2 + 2VW_1' + W_1'^2 = V^2 + V_1'^2 + 2|V||W_1'| \cos \psi_1'$$

$$= V^2 + V_1'^2 + 2|V||V_1'| \cos \psi_1'$$

$$W_2^2 = (W + W_2')^2 = (V + W_2')^2 = V^2 + 2VW_2' + W_2'^2 = V^2 + W_2'^2 + 2|V||W_2'| \cos \psi_2'$$

$$= V^2 + V_2'^2 - 2|V||V_2'| \cos \psi_1'$$

Next, we compute the $\cos \psi_i$:

$$\cos \psi_1 = VW_1/|V||W_1| = V(W + W_1')/|V||W_1| = V(V + W_1')/|V||W_1|$$

$$= (V^2 + VW_1')/|V||W_1| = (V^2 + |V||W_1'| \cos \psi_1')/|V||W_1|$$

$$= (|V| + |V_1'| \cos \psi_1')/|W_1|$$

$$\cos \psi_2 = VW_2/|V||W_2| = V(W + W_2')/|V||W_2| = V(V + W_2')/|V||W_2|$$

$$= (V^2 + VW_2')/|V||W_2| = (V^2 + |V||W_2'| \cos \psi_2')/|V||W_2|$$

$$= (|V| - |V_2'| \cos \psi_1')/|W_2|$$

where the $|W_i|^2$ are given above. These formulas provide the general solution to our problem. In most cases the energies of neutrons are sufficiently greater than the (thermal) velocities of nuclei to admit the assumption that the latter are effectively stationary in the laboratory system.

We proceed therefore to specialize to the case of neutrons of mass m_1, laboratory velocity V_1 scattering on nuclei of mass m_2, velocity $V_2 = 0$. In this case we have

$$mV = m_1V_1 + m_2V_2 = m_1V_1, \qquad |V| = m^{-1}m_1|V_1|$$

$$V_1' = V_1 - V = V_1 - m^{-1}m_1V_1 = m^{-1}m_2V_1$$

$$V_2' = V_2 - V = -V = -m^{-1}m_1V_1$$

Substitution gives us

$$W_1^2 = V_1^2\left\{m^{-2}m_1^2 + m^{-2}m_2^2 + 2m^{-2}m_1m_2\cos\psi_1'\right\}$$

and hence, if $\ell_1 = \frac{1}{2}m_1W_1^2$, $k_1 = \frac{1}{2}m_1V_1^2$ are the (laboratory) energies of m_1 after and before collision, we obtain

$$\ell_1/k_1 = m^{-2}\left\{m_1^2 + 2m_1m_2 + m_2^2 - 2m_1m_2 + 2m_1m_2\cos\psi_1'\right\}$$

$$= 1 - 2m^{-2}m_1m_2 + 2m^{-2}m_1m_2\cos\psi_1'$$

It is convenient to introduce the quantities $A = m_2/m_1$, $\bar{r} = (A-1)^2/(A+1)^2 = (m_1 - m_2)^2/(m_1 + m_2)^2 = 1 - 4m^{-2}m_1m_2$, $S = \frac{1}{2}(1 + \bar{r}) = 1 - 2m^{-2}m_1m_2$, and $T = \frac{1}{2}(1 - \bar{r}) = 2m^{-2}m_1m_2$, obtaining finally

$$\ell_1 = k_1(S + T\cos\psi_1')$$

Moreover,

$$\cos \psi_1 = |V_1| \left\{ m^{-1} m_1 + m^{-1} m_2 \cos \psi_1' \right\} / |W_1|$$

$$= \left\{ m^{-1} m_1 + m^{-1} m_2 \cos \psi_1' \right\} / \sqrt{\left\{ m^{-2} m_1^2 + m^{-2} m_2^2 + 2m^{-2} m_1 m_2 \cos \psi_1' \right\}}$$

$$= \left\{ 1 + A \cos \psi_1' \right\} / \sqrt{\left\{ 1 + A^2 + 2A \cos \psi_1' \right\}}$$

Although we make no use of them in the sequel, we include for completeness the results for the scattered nucleus m_2

$$\ell_2 / k_1 = T \left\{ 1 - \cos \psi_1' \right\} = 2T \sin^2 \left(\frac{\psi_1'}{2} \right)$$

and $\cos \psi_2 = \sqrt{\frac{1}{2} (1 - \cos \psi_1')} = \sin \left(\frac{\psi_1'}{2} \right)$, which the reader may verify as an exercise.

The salient results of this section are the formulas

$$E' = E (S_e + T_e \mu)$$

$$a = \left\{ 1 + A_e \mu \right\} / \sqrt{\left\{ 1 + A_e^2 + 2A_e \mu \right\}}$$

where we agree on the following definitions:

m_e = mass of nucleus of type e

m = mass of neutron

$A_e = m_e / m$

$\overline{r}_e = (A_e - 1)^2 / (A_e + 1)^2$

$S_e = \frac{1}{2} (1 + \overline{r}_e)$

$T_e = \frac{1}{2} (1 - \overline{r}_e)$

E = neutron energy before scattering

E' = neutron energy after scattering

} laboratory system

$\mu = \cos \psi_1'$

ψ_1' = angle of deflection in center of mass system from original line of flight (coincident with V = W since $V_2 = 0$)

$a = \cos \psi_1$

ψ_1 = angle of deflection in laboratory system from original line of flight

The constants A_e, S_e, T_e are nuclear (energy independent) constants, the subscript e, if required, being set in the routine of the preceding section.

It may be noted that in the case of scattering on hydrogen, we may assume A = 1, and the formulas become simply $\bar{r} = 0$, $S = T = \frac{1}{2}$, $E' = \frac{1}{2} E (1 + \mu)$, and $a = \sqrt{\frac{1}{2}(1 + \mu)}$. Several remarks are of interest here: (a) we have the relation $E' = Ea^2$; (b) scattering on hydrogen is always forward in the laboratory system, viz., $a = \cos \psi_1 \geq 0$; (c) $a = \cos \psi_1 = \sqrt{\frac{1}{2}(1 + \cos \psi_1')} = \cos (\psi_1'/2)$ implies $\psi_1 = \psi_1'/2$; (d) the formula $a = \sqrt{\frac{1}{2}(1 + \mu)}$ should be used for hydrogen, since the general formula is indeterminate at $\mu = -1$; (e) if scattering on H is isotropic in the center of mass system (a good assumption, incidentally), we have $\mu = 2r - 1$, and $a = \sqrt{r}$, which shows that the laboratory scattering is in the cosine distribution. (Cf. Chapter II, §5b.)

Finally we observe that for "heavy" elements (A_e large) we have the following approximate results: $\bar{r}_e = 1$, $S_e = 1$, $T_e = 0$, $E' = E$, $a = \mu$. If these relations are of acceptable accuracy, one may ignore the energy change and determine a directly instead of μ by the methods of the

next section. In this connection one should refer to Chapter VII, §5, for the case of scattering isotropic in the laboratory system.

4. The differential elastic scattering cross section. We have seen in the last section that the preservation of total momentum and kinetic energy characterizing the elastic scattering process does not serve to determine the angle ψ_1' of scattering in the center of mass system, but does determine the new energy E' of the scattered neutron and its deflection cosine a in the laboratory system in terms of a given $\mu = \cos \psi_1'$.

The determination of μ is governed by a physical distribution function $\sigma_E^e(\Omega)$, whose units are barns per steradian, and which depends upon the scattering nucleus e and the energy E of the incident neutron. Specifically, $\sigma_E^e(\Omega)\, d\Omega$ is defined as the cross section (in the sense of Chapter III, §1) presented to incident neutrons of energy E by a nucleus of type e for the process of scattering in the center of mass system at an angle in the $d\Omega$ neighborhood of the direction Ω with the incident line of flight. Thus by definition,

$$\int \sigma_E^e(\Omega)\, d\Omega = \sigma_E^e(\text{el.})$$

the integration being over the entire surface of the unit sphere in direction space U, V, W, and $\sigma_E^e(\text{el.})$ being the (total) elastic scattering cross section for the element e at energy E. In terms of spherical coordinates (azimuthal angle φ, polar angle ψ_1', Fig. 35), we have

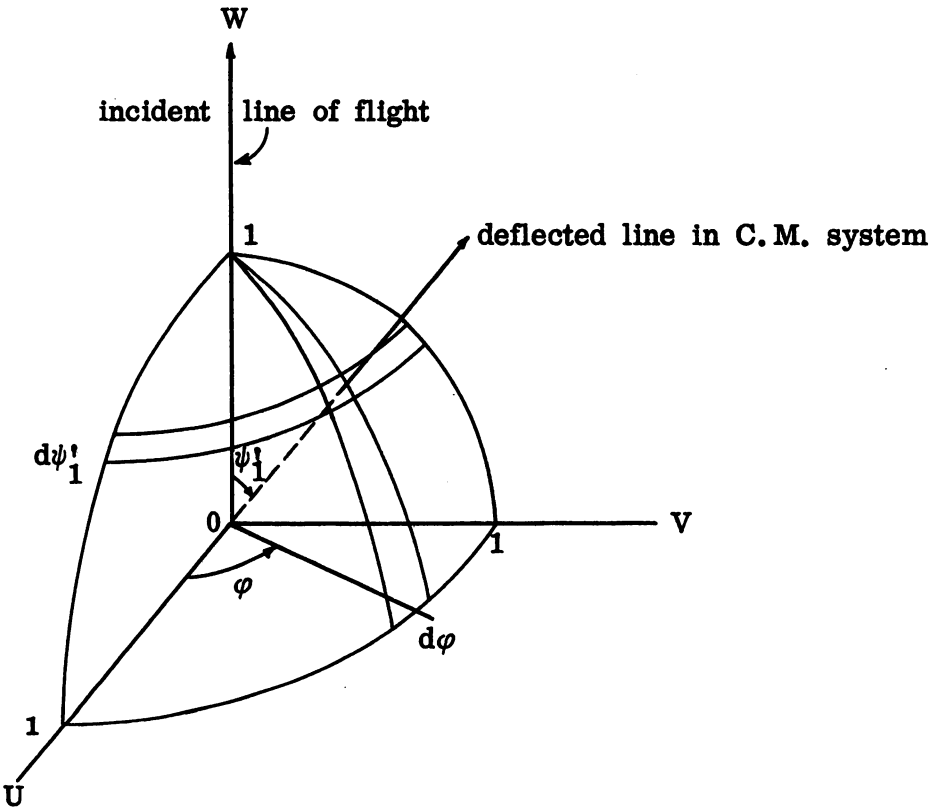

Fig. 35

$$\int_{\psi_1'=0}^{\pi} \int_{\varphi=0}^{2\pi} \sigma_E^e (\psi_1', \varphi) \sin \psi_1' \, d\varphi \, d\psi_1' = \sigma_E^e (\text{el.})$$

In all problems of the text σ_E^e is independent of φ and we have

$$2\pi \int_0^{\pi} \sigma_E^e (\psi_1') \sin \psi_1' \, d\psi_1' = \sigma_E^e (\text{el.})$$

or, in the form usually given,

$$2\pi \int_{-1}^{1} \sigma_E^e (\mu) \, d\mu = \sigma_E^e (\text{el.})$$

It follows that $p_E^e (\mu) = 2\pi \sigma_E^e (\mu) / \sigma_E^e (\text{el.})$ is the probability density function for elastic scattering at the direction ψ_1' from the line of flight in the center of mass system.

Hence, the Monte Carlo procedure sets

$$r = \int_{-1}^{\mu} p_E^e (\mu) \, d\mu \qquad (-1 \leqq \mu \leqq 1)$$

for the determination of μ from the random number r.

5. A routine for elastic scattering. Suppose that elastic scattering on the (light) element e is isotropic in the center of mass system. This means that the function $\sigma^e(\mu)$ is a constant, and the final formula of the preceding section gives simply $\mu = 2r - 1$. In such a case, we should enter a routine like that in Fig. 36. Here E_G represents the "energy cutoff," namely, the last of the lower bounds $E_1 > E_2 > \ldots > E_G$ of the energy groups adopted. Energies falling below this necessitate classification of the corresponding weight in a terminal category L_E reserved for loss to energy cutoff. The loop on $E_g - E$ begins by comparing the new energy E with the lower bound E_g of the group which the neutron occupied before scattering, since elastic scattering cannot raise the energy. Note also that $E_G - E < 0$ at entry to this loop ensures its termination at some $g \geq G$. If $E_G > 0$, the previous $E - E_G$ decision is mandatory. The formulas for E' and a are fully discussed in the preceding §3. As remarked there, the procedure for the special case of hydrogen is simpler and is indicated in the lower half of Fig. 36. For the case of scattering isotropic in the laboratory system, we again refer to Chapter VII, §5. This applies approximately to the case of heavy elements with an isotropic law in the center of mass system.

The (δ) of Fig. 36 refers to a routine for fixing the final laboratory direction parameters of the scattered neutron (cf. Chapter VII) before returning to (β).

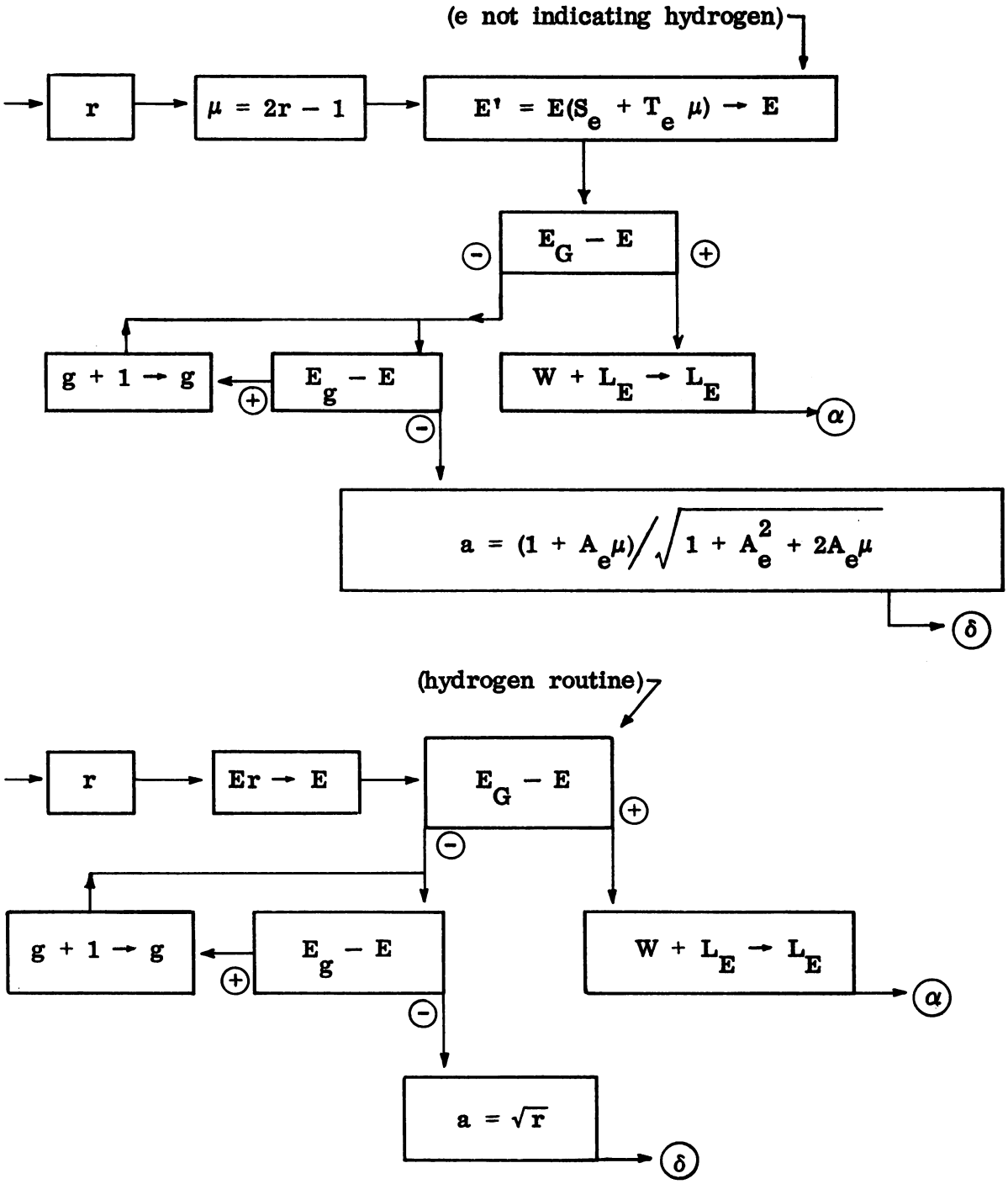

Fig. 36

Most elements have more complicated differential cross section functions, usually characterized by preferential forward (and sometimes backward) scattering, an effect which tends to increase with higher incident energies. The problem of choosing μ from such a distribution is essentially that (already discussed in Chapter II, §5) of selecting the direction parameter w from a given source distribution.

If the problem can be restricted to a single energy, or to relatively few energy groups[10] over each of which the differential function $\sigma_E(\mu)$ may be considered constant, one may well store tables for the probabilities $P_{g,j}$ of scattering at cosines $\mu \geq \mu_j$, where $\mu_1 > \mu_2 > \ldots > \mu_J = -1$ are suitably chosen bounds of subintervals of the cosine range, and the

$$P_{g,j} = \int_{\mu_j}^{1} p_g(\mu)\, d\mu$$

are pre-computed by numerical integration and stored. The routine for determining μ is then that of Fig. 13, where we read j for i, $P_{g,j}$ for P_i, μ_j for w_i, and μ for w.

Aside from its demands on storage space, this is subject to the errors of interpolation, which may be difficult to minimize in cases of

---

[10] These need not coincide with nor be as numerous as the energy groups reserved for free path and scattering-type probabilities. It is not unusual to carry two or even three different sets of energy classifications with corresponding indices g, h,... as neutron parameters.

very forward scattering.

If the original curves $\sigma_E^e(\mu)$ can be simply fitted, the simplest scheme may be the von Neumann device (Chapter I, §5). We should then have a formula for the function

$$\sigma^*(e, E, \mu) = \sigma_E^e(\mu) \Big/ \left\{ \max \sigma_E^e(\mu) \text{ on } -1 \leqq \mu \leqq 1 \right\}$$

and use the routine of Fig. 5 with $a = -1$, $b = 1$, $p^* = \sigma^*(e, E, \mu)$, reading μ for ξ.

Occasionally, the function $\sigma^*(e, E, \mu)$ may be fitted easily for each energy E as a function of μ, say,

$$\sigma^*(e, E, \mu) = A_E^e + B_E^e \mu + C_E^e \mu^2 \qquad -1 \leqq \mu \leqq 1$$

but the coefficients may prove intractable as functions of E. In such a case we may be able to store the coefficients

$$A_g^e, B_g^e, C_g^e$$

for each of a reasonable number of energy groups, and use the routine of Fig. 5 as indicated above, the machine computing $\sigma^*(e, g, \mu) = A_g^e + B_g^e \mu + C_g^e \mu^2$ from μ and the stored coefficients.

Finally, and in the worst cases, it may be necessary to store a table of values of $\sigma^*_{m,n} = \sigma_{m,n} \Big/ \left\{ \max_{m,n} \sigma_{m,n} \right\}$, where $\sigma_{m,n} = \sigma(\mu_m, E_n)$ is the differential cross section for a particular element (we drop the index e temporarily) evaluated at a suitable set of values $\tilde{\mu}_o = 1 > \ldots > \tilde{\mu}_M = -1$ and $\tilde{E}_o > \ldots > \tilde{E}_N$, where E_o is at least

the highest energy encountered in the problem, and $\tilde{E}_N = E_G$ the least such energy. The energies and cosines used for this purpose may be hand-picked, and need not coincide with those used for other purposes elsewhere in the problem. We store a table of the form

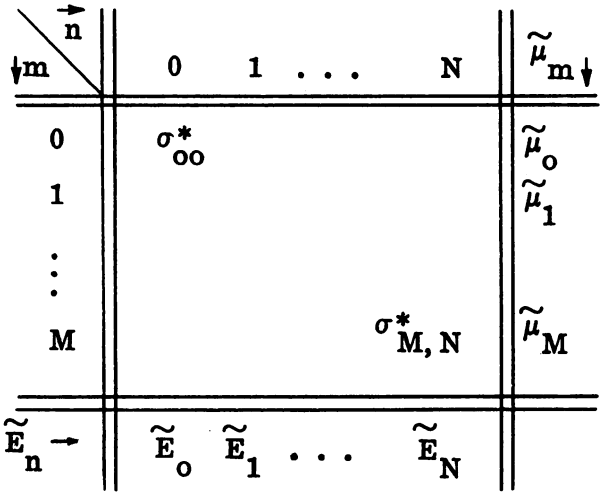

Fig. 36a

and resort to the double interpolation routine of Fig. 37.

However we may determine μ, the routine should lead to a determination of E and g after collision and the deflection cosine a for the laboratory system as indicated in Fig. 36.

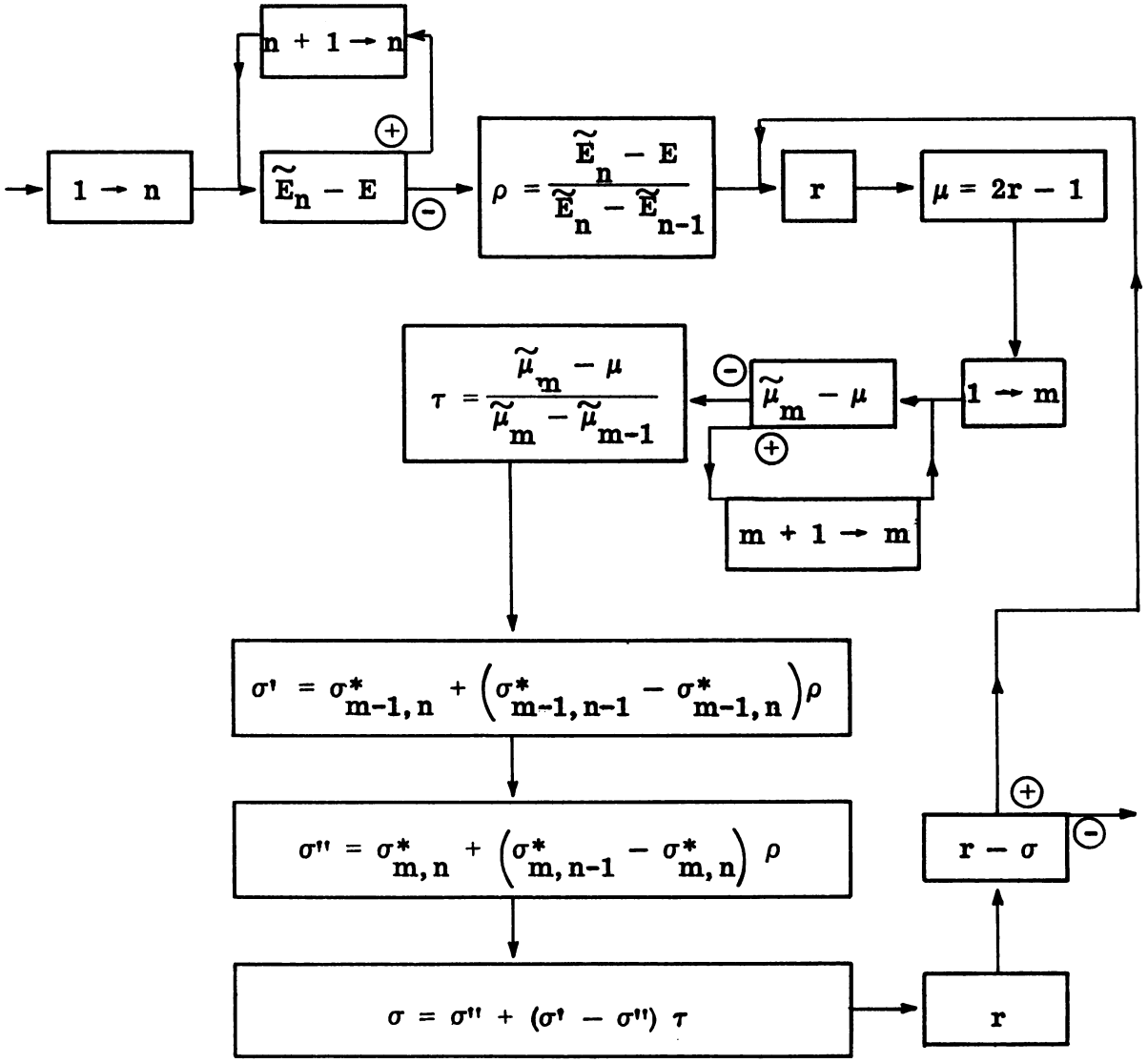

Fig. 37

6. Differential elastic cross section for the laboratory system. If a differential cross section $\sigma_L(a)$ is given for elastic scattering relative to the laboratory cosine $a = \cos \psi_1$, one may choose between the following two alternatives.

(a) One may employ $\sigma_L(a)$ directly to determine a, just as the center of mass differential cross section $\sigma(\mu)$ was used to determine μ. It is then necessary to use the formula

$$\mu = A^{-1} \left\{ -(1 - a^2) + (\operatorname{sgn} a) \sqrt{(1 - a^2)^2 - (1 - a^2) + a^2 A^2} \right\} \quad (4)$$

to determine the corresponding center of mass cosine μ, which is needed in computing the new energy $E' = E(S + T\mu)$.

The above formula is obtained by solving the equation

$$a = (1 + A\mu) / \sqrt{[1 + A^2 + 2A\mu]} \quad (5)$$

for μ in terms of a. The (sgn a) choice of sign on the radical is dictated by the following considerations: From equation (5) it is clear that the sign of a is always that of $1 + A\mu$. In solving equation (5) for μ we obtain

$$1 + A\mu = a^2 \pm \sqrt{[(1 - a^2)^2 - (1 - a^2) + a^2 A^2]}$$

so that the sign of the right side must always be that of a. It is clear graphically that for the function $f(a) = a^2 \pm \sqrt{g(a)}$ to have the sign of a, it is necessary and sufficient that one use the upper branch for $a > 0$ and the lower for $a < 0$.

Formula (4) may be rewritten in the form

$$\mu = -\frac{b^2}{A} + a\sqrt{1 - \frac{b^2}{A^2}}$$

where $b^2 = 1 - a^2$.

(b) Alternatively, we may use the defining relation

$$\sigma(\mu)\, d\mu = \sigma_L(a)\, da$$

to compute the center of mass function $\sigma(\mu)$ in advance, and then use the usual procedures of §5 directly. This may be done by means of the formulas

$$\sigma(\mu) = \sigma_L(a(\mu))\frac{da}{d\mu}$$

where $$a(\mu) = (1 + A\mu)/\sqrt{[1 + A^2 + 2A\mu]}$$

and $$\frac{da}{d\mu} = [A^2(A + \mu)]/[1 + A^2 + 2A\mu]^{3/2}$$

7. A weight device for elastic scattering. In problems involving many collisions in a medium admitting elastic scattering on light elements, it may prove worth while to avoid loss of trajectories, which are usually followed through many collisions, to the energy cutoff E_G. These losses may be obviated by the following device, which makes further strategic use of weights.

We have seen that the relation between emergent and incident energies

in such collisions is $E' = E(S + T\mu)$, where μ is the center of mass deflection cosine, chosen randomly by the equation

$$r = \int_{\mu}^{1} p_E(\mu)\, d\mu = P_E(\mu)$$

Now, for a given incoming energy $E > E_G$, the least emergent energy is $E'_{min} = E(S - T)$. If this exceeds E_G, the energy cutoff for the problem, one proceeds as usual, with no possibility of loss to energy. However, if $E(S - T) \leqq E_G$, that is to say, if $E \leqq E_G/(S - T) \equiv E^*$, there exists a critical cosine μ_c, depending on E, such that $E(S + T\mu_c) = E_G$, with $-1 < \mu_c < 1$, and

$$f = f(\mu_c) = \int_{-1}^{\mu_c} p_E(\mu)\, d\mu$$

represents the probability of scattering with μ on $-1 \leqq \mu \leqq \mu_c$ with the resulting energy $E' < E_G$. Moreover, assuming $\mu \geqslant \mu_c$

$$r = \int_{\mu}^{1} p_E(\mu)\, d\mu \Big/ \int_{\mu_c}^{1} p_E(\mu)\, d\mu \equiv Q_E(\mu)$$

is the proper Monte Carlo formula for determination of the cosine on the range $\mu_c \leqq \mu \leqq 1$, with a resulting energy $E' \geqq E_G$. We may therefore proceed as in Fig. 38.

For the simple case of scattering isotropic in the center of mass system, we have the formulas $f = \frac{1}{2}(1 + \mu_c)$, $\mu = Q_E^{-1}(r) = 1 - r(1 - \mu_c)$, $\mu = P_E^{-1}(r) = 1 - 2r$.

Finally, we note that a neutron being followed by this method

automatically has weight $W > 0$ and energy $E > E_G$, if the random number $r = 1$ does not actually occur in our sequence.

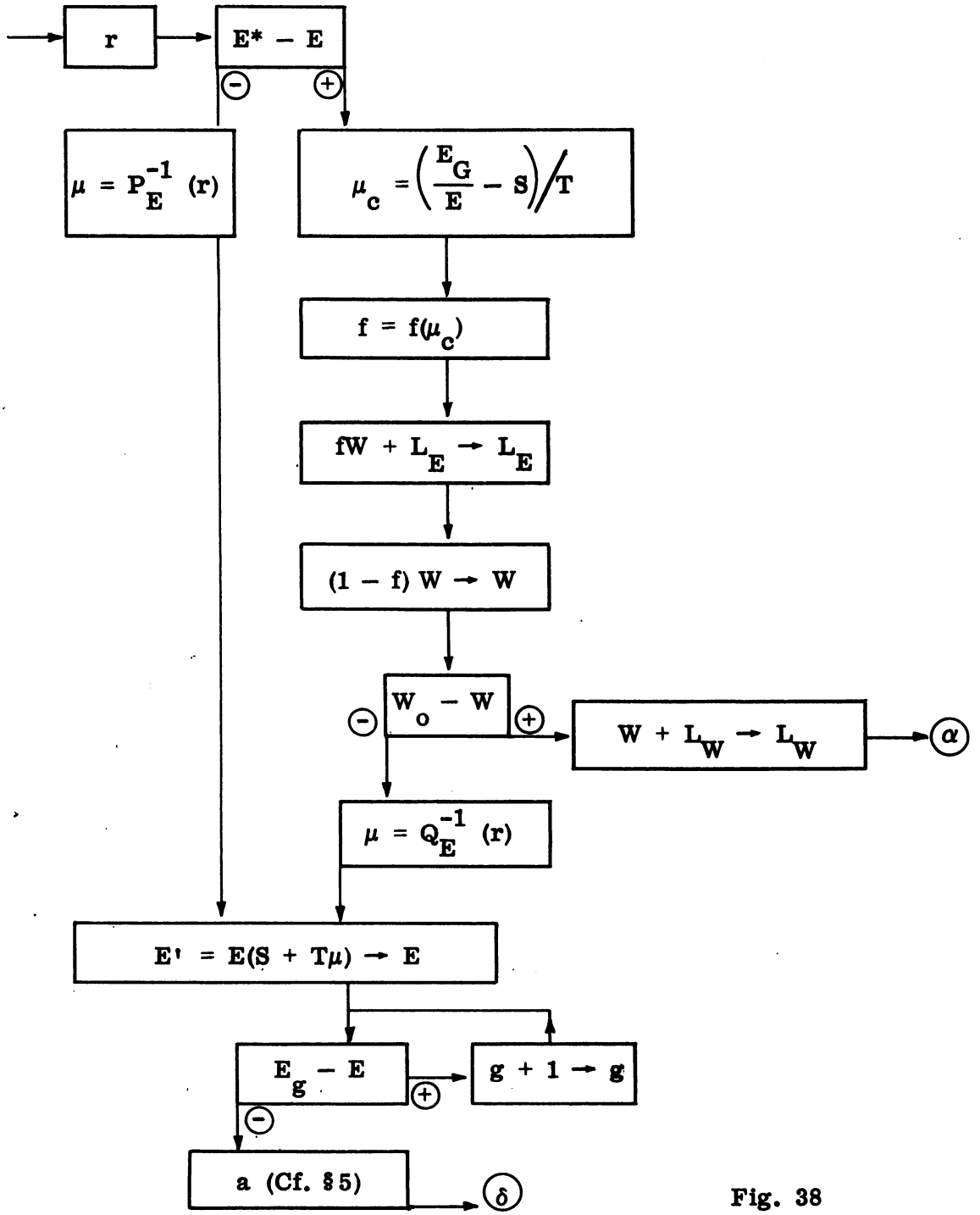

Fig. 38

8. Fission. Suppose that a neutron causes fission of some (heavy) nucleus, resulting in the production of an average number ν_o of neutrons with energies of release independently distributed in a given fission spectrum, and whose emergent direction distributions are isotropic in the laboratory system.

It is possible to invent a probability distribution $p(n)$ with $\nu_o = \Sigma n\, p(n)$, decide on the number n of progeny in a given fission by chance, and follow these n neutrons individually. This may be done even in supercritical systems if recourse is had to time cycles and census taking. However, this is unnecessary and undesirable. We may instead follow a single neutron, of weight ν_o times that of the incident neutron, chosen from the fission spectrum of energies, and directed isotropically. This may reduce fluctuations, enormously simplifies the code, and decreases machine running time.

Suppose that $f(E)\,dE$ is the probability of fission energy E between E and $E + dE$. We choose a set of energy intervals with bounds $\tilde{E}_o > \tilde{E}_1 > \ldots > \tilde{E}_H$, where $\tilde{E}_o$ is the highest significant fission energy and $\tilde{E}_H$ the energy cutoff for the problem. These $\tilde{E}_h$ need not agree with bounds of energy groups used for other purposes. Define

$$F_h = \int_{\tilde{E}_h}^{\tilde{E}_o} f(E)dE$$

We may then refer to Fig. 39. Note that if the $\tilde{E}_h$ are different from the E_g used for (say) storing free paths λ_g, one must determine the index g, beginning the loop with $g = 1$ since fission can

raise energy above the incident energy E in group g. The exit ($\bar{\delta}$) refers to the routine of Chapter VII, §5, for scattering isotropic in the laboratory system.

In some problems, designed to find the distribution, say, in a number of cylindrical shell zones defined by radii $R_1 < R_2 < \ldots < R_m$ and heights $H_1 < H_2 < \ldots < H_n$, of fissions resulting from a given spatial distribution of fissions, fission is a terminal event, and counters $N_{i,j}$ are reserved for the number of neutrons terminating in fission in radial zone i, height zone j. In the event of fission we should then follow the simple classification routine of Fig. 40, rather than that of Fig. 39.

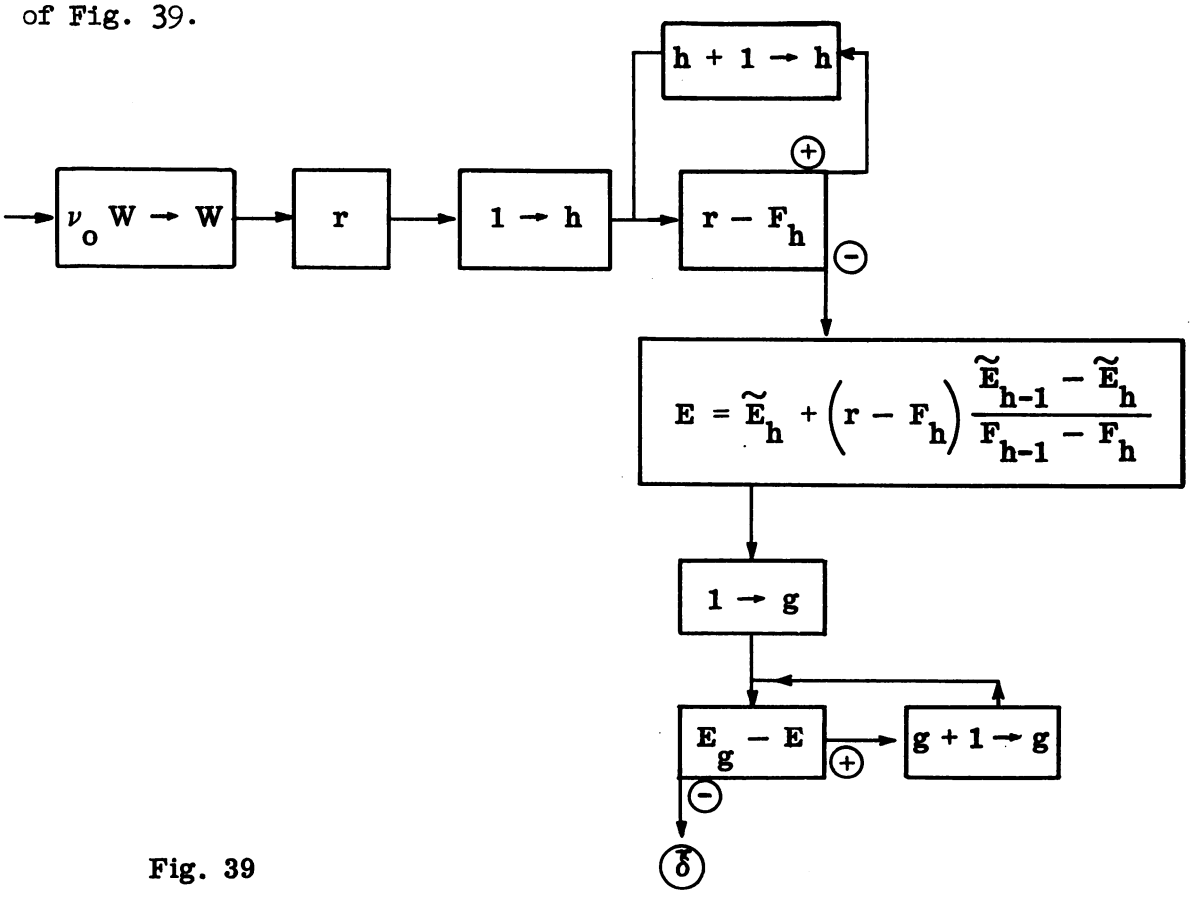

Fig. 39

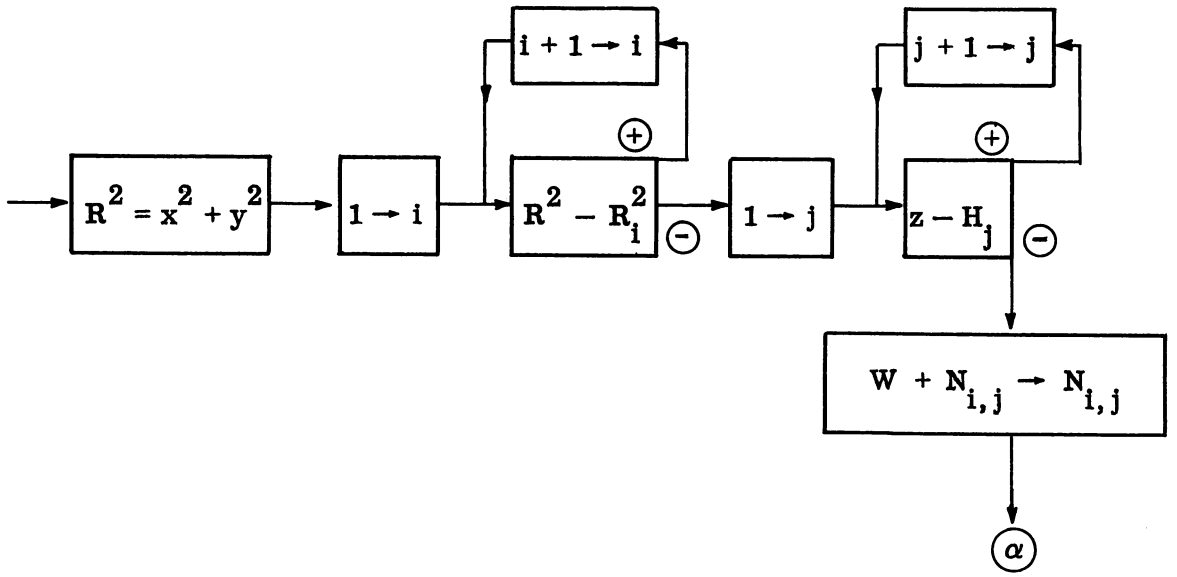

Fig. 40

9. Inelastic (n-n) collisions in general. Using the notation and procedure of §3 of this chapter, we now discuss a type of collision in which an incident neutron of kinetic energy $k_1 = \frac{1}{2} m_1 V_1^2 = E$ strikes a nucleus of mass m_2, imparting to the latter a known energy of excitation ϵ, and emerging with an energy $\ell_1 = \frac{1}{2} m_1 W_1^2 = E'$. We obtain again the fundamental relations

$$P' = 0 = Q' \tag{6}$$

$$P = mV \qquad Q = mW \tag{7}$$

$$k = \frac{1}{2} mV^2 + k' \qquad \ell = \frac{1}{2} mW^2 + \ell' \tag{8}$$

The momentum and energy conservation laws now read

$$P = Q$$

$$k = \ell + \epsilon$$

however, and we find $V = W$ as before, but now

$$k' = \ell' + \epsilon$$

We find again that the equations

$$\begin{cases} \frac{1}{2} m_1 W_1'^2 + \frac{1}{2} m_2 W_2'^2 = \ell' \\ m_1^2 W_1'^2 - m_2^2 W_2'^2 = 0 \end{cases}$$

determine $W_1'^2$ and $W_2'^2$ uniquely, the difference being only that ℓ' is not simply k' but $k' - \epsilon$. Thus the <u>speeds</u> of departure of m_1 and m_2 in the center of mass system are uniquely determined, although they are not simply the <u>incident</u> relative speeds as before. The angle ψ_1' must be determined according to some physically determined distribution law, and from this the laboratory energy and deflection cosine may be computed.

We will derive the relevant formulas. First, solving the above system for $W_1'^2$, $W_2'^2$, suppose that we first rewrite the system for $V_1'^2$, $V_2'^2$:

$$\begin{cases} \frac{1}{2} m_1 V_1'^2 + \frac{1}{2} m_2 V_2'^2 = k' = \ell' + \epsilon \\ m_1^2 V_1'^2 - m_2^2 V_2'^2 = 0 \end{cases}$$

in the form

$$\begin{cases} \frac{1}{2} m_1(V_1'^2 - \epsilon_1) + \frac{1}{2} m_2(V_2'^2 - \epsilon_2) = \ell' \\ m_1^2(V_1'^2 - \epsilon_1) - m_2^2(V_2'^2 - \epsilon_2) = 0 \end{cases}$$

where $\epsilon_1 = 2m_2\epsilon/m_1 m$, $\epsilon_2 = 2m_1\epsilon/m_2 m$, and $\frac{1}{2} m_1\epsilon_1 + \frac{1}{2} m_2\epsilon_2 = \epsilon$, $-m_1^2\epsilon_1 + m_2^2\epsilon_2 = 0$. We see at once that

$$W_1'^2 = V_1'^2 - \epsilon_1 \; ; \; W_2'^2 = V_2'^2 - \epsilon_2$$

We deal only with the neutron m_1. Computing W^2 as before in terms of $\cos\psi_1'$, we obtain

$$W_1^2 = (W + W_1')^2 = (V + W_1')^2 = V^2 + W_1'^2 + 2|V||W_1'| \cos\psi_1'$$

$$= V^2 + V_1'^2 - \epsilon_1 + 2|V| \sqrt{(V_1'^2 - \epsilon_1)} \cos\psi_1'$$

and for $\cos\psi_1$, the laboratory deflection cosine,

$$\cos\psi_1 = VW_1/|V||W_1| = V(W + W_1')/|V||W_1| = V(V + W_1')/|V||W_1|$$

$$= (V^2 + VW_1')/|V||W_1| = (V^2 + |V||W_1'| \cos\psi_1')/|V||W_1|$$

$$\doteq (|V| + |W_1'| \cos\psi_1')/|W_1| = (|V| + \sqrt{V_1'^2 - \epsilon_1} \cos\psi_1')/|W_1|$$

Again specializing to the case $V_2 = 0$, $V = m^{-1}m_1 V_1$, $V_1' = m^{-1}m_2 V_1$, we obtain

$$W_1^2 = m^{-2}m_1^2 V_1^2 + m^{-2}m_2^2 V_1^2 - \epsilon_1 + 2m^{-1}m_1|V_1| \cos\psi_1' \sqrt{(m^{-2}m_2^2 V_1^2 - \epsilon_1)}$$

$$= |V_1|^2 \left\{ m^{-2}m_1^2 + m^{-2}m_2^2 - (\epsilon_1/V_1^2) + 2m^{-2}m_1 m_2 \cos\psi_1' \sqrt{1 - (m^2\epsilon_1/m_2^2 V_1^2)} \right\}$$

and therefore

$$\ell_1/k_1 = m^{-2}\left\{m_1^2 + 2m_1m_2 + m_2^2 - (m^2\epsilon_1/V_1^2) - 2m_1m_2 + 2m_1m_2\cos\psi_1'\sqrt{1-(m^2\epsilon_1/m_2^2V_1^2)}\right\}$$

$$= (1 - 2m_1m_2/m^2) - (\epsilon_1/V_1^2) + 2m_1m_2m^{-2}\cos\psi_1'\sqrt{1 - (m^2\epsilon_1/m_2^2V_1^2)}$$

But $\epsilon_1 = 2m_2\epsilon/m_1m$, so that $m^2\epsilon_1/m_2^2V_1^2 = m\epsilon/m_2k_1 = m\epsilon/m_2E$, and hence, finally, replacing ℓ_1 by E' and k_1 by E

$$E' = E\left\{S - \left(\frac{m_2^2}{m^2}\right)(m\epsilon/m_2E) + T\cos\psi_1'\sqrt{1 - (m\epsilon/m_2E)}\right\}$$

Moreover,

$$\cos\psi_1 = (m^{-1}m_1|V_1| + \cos\psi_1'\sqrt{(m^2m_2^2V_1^2 - \epsilon_1)})/|W_1|$$

$$= |V_1|\left\{m^{-1}m_1 + m^{-1}m_2\cos\psi_1'\sqrt{1 - (m^2\epsilon_1/m_2^2V_1^2)}\right\}/|W_1|$$

or

$$\cos\psi_1 = \frac{m^{-1}m_1 + m^{-1}m_2\cos\psi_1'\sqrt{1 - (m\epsilon/m_2E)}}{\left\{m^{-2}m_1^2 + m^{-2}m_2^2 - \left(\frac{m_2^2}{m^2}\right)(m\epsilon/m_2E) + 2m^{-2}m_1m_2\cos\psi_1'\sqrt{1 - (m\epsilon/m_2E)}\right\}^{1/2}}$$

Finally

$$\cos\psi_1 = \frac{1 + A\cos\psi_1'\sqrt{1 - (m\epsilon/m_2E)}}{\left\{1 + A^2[1 - (m\epsilon/m_2E)] + 2A\cos\psi_1'\sqrt{1 - (m\epsilon/m_2E)}\right\}^{1/2}}$$

Now the reaction can occur only if $\ell' = k' - \epsilon \geq 0$; since $k' = \Sigma\frac{1}{2}m_iV_i'^2 = \frac{1}{2}\left\{m_1m_2^2m^{-2} + m_2m_1^2m^{-2}\right\}V_1^2 = m_2m^{-1}E$, the condition is simply

$E \geqq m\, m_2^{-1} \epsilon$. If we define this critical energy as ϵ_c, we may write

$$E' = E\left\{S - \left(\frac{A}{1+A}\right)^2 \left(\frac{\epsilon_c}{E}\right) + T \cos \psi_1' \sqrt{1 - (\epsilon_c/E)}\right\}$$

$$\cos \psi_1 = \frac{1 + A \cos \psi_1' \sqrt{1 - (\epsilon_c/E)}}{\left\{1 + A^2 \left[1 - (\epsilon_c/E)\right] + 2A \cos \psi_1' \sqrt{1 - (\epsilon_c/E)}\right\}^{1/2}}$$

About these formulas we make the following remarks: (a) For $\epsilon_c = 0$, they reduce, as they should, to those for elastic scattering, (b) for $\epsilon_c > 0$ and A large (heavy nuclei), they become approximately $E' = E - \epsilon$ and $\cos \psi_1 = \cos \psi_1'$, as we should expect.

It must also be pointed out that a nucleus may have various excited states each with its own excitation energy ϵ, and a corresponding inelastic cross section $\sigma_E(\epsilon)$ for neutrons of energy $E \geqq (m/m_2)\epsilon = \epsilon_c$. For light nuclei these must be dealt with individually, using the above formulas with the appropriate ϵ_c.

For heavy nuclei, the states may be well separated in some cases, and may be dealt with individually, using the simple relations of remark (b) above. If, however, the excited states are very close together, one resorts to such methods as those of the following two sections.

10. Inelastic (n-n) collisions on heavy nuclei. If the states of the nucleus are closely packed on the energy scale, it is customary to give a table of experimentally determined probabilities $P_{h,h'}$ for

an incident neutron of energy group h to produce in (n-n) reaction a neutron of energy $E' \geqq \widetilde{E}_{h'}$, where $h' \geqq h$, and $\widetilde{E}_o > \ldots > \widetilde{E}_H$ is a suitable set of lower bounds for energy. One may then proceed to determine the energy E' in the usual way by use of a random number and linear interpolation, as in Fig. 41, which is drawn for the case of isotropic scattering in the laboratory system, and therefore exits to $(\bar{\delta})$ (Chapter VII, §5). Note that the $P_{h,h'}$ form a triangular matrix, with $P_{h,h'}$ non-zero only for $h' \geqq h$, and $P_{h,H} = 1$, $h = 1, \ldots, H$.

Some inaccuracy is unavoidable in such a method, since, strictly speaking, $P_{h,h'}$ is a function not only of the group h, but of the energy E in this group.

11. Inelastic (n-n) collision with Maxwell distribution. Consider an (n-n) collision of a neutron of energy $E < \bar{E}$ with a heavy nucleus for which it may be assumed that the emergent energy E' probability density function is proportional to

$$n(E') = E' \exp(-E'/T) \qquad 0 \leqq E' \leqq E$$

where $T = \alpha\sqrt{(E/\bar{E})}$, α being a given constant.

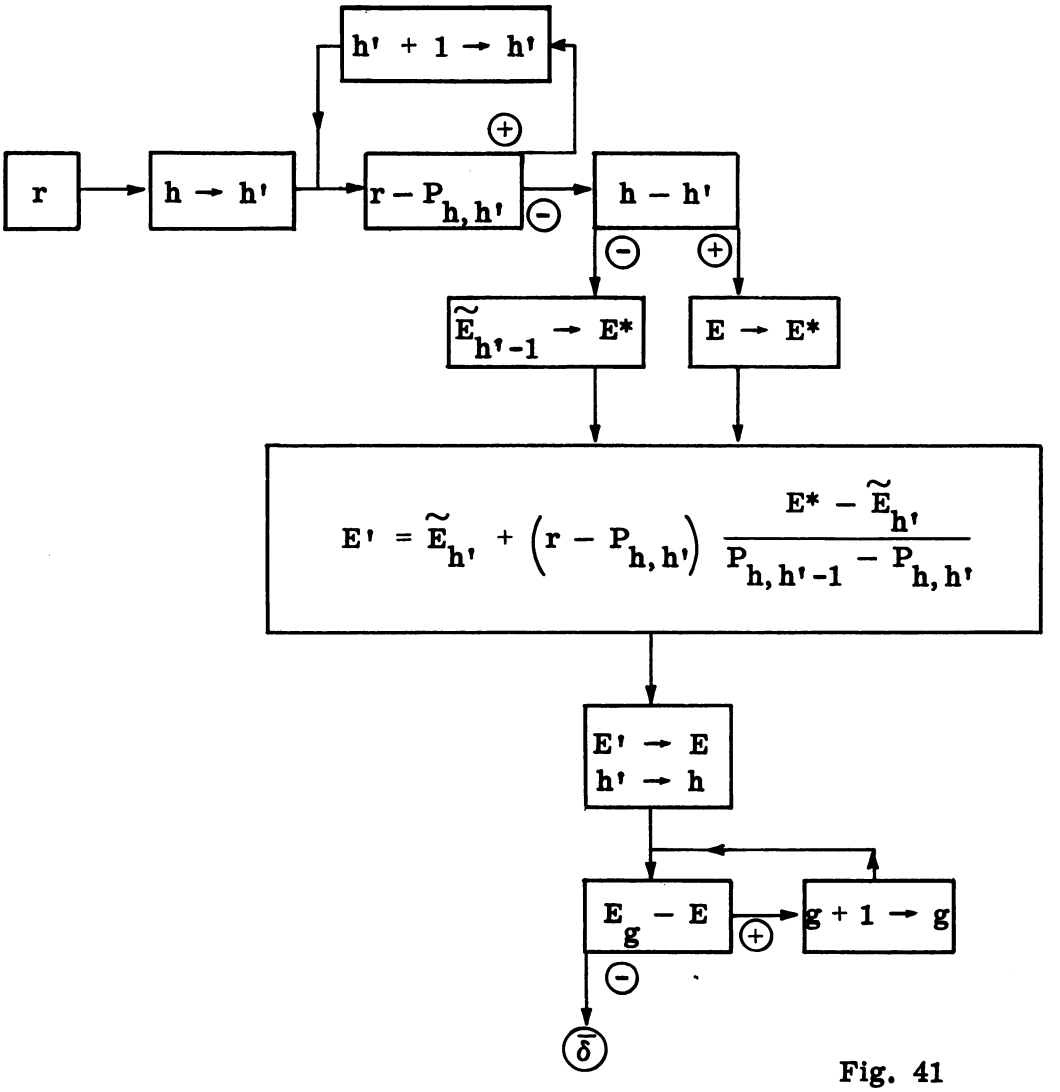

Fig. 41

If $A(E) = \int_0^E E' \exp(-E'/T)\, dE'$

we have

$$P_E(E')\, dE' = (1/A(E))\, E' \exp(-E'/T)\, dE'$$

and the Monte Carlo principle involves determination of E' from E and r by means of

$$r = \int_0^{E'} P_E(E')\, dE'$$

The solution for E' is difficult and we use instead the device of Chapter I, § 5. The latter requires the function

$$p^*(E') = n(E')/\max N(E')$$

the maximum being for the range $0 \leqq E' \leqq E$. Now the maximum of $n(E')$ is at $E' = T$, and we may use this provided $T = \alpha\sqrt{(E/\bar{E})} < E$, which means that the incident energy E shall exceed $\alpha^2/\bar{E}$. Let us suppose for simplicity that $\alpha^2/\bar{E} < E_G$, the energy cutoff (as is usually the case). We have then

$$p^*(E') = (\frac{e}{T})\, E' e^{-E'/T} \leqq 1$$

for all incident energies E on the range $E_G < E \leqq \bar{E}$ and we may proceed in the usual way, with $E' = rE$, etc.

12. A combined transfer matrix for fissionable nuclei. If the nature of a problem involving a fissionable nucleus does not demand keeping the individual types of collision separate (for example, for purposes of tabulating capture, fission, etc.) and if the neutrons emerging from each type of collision are all emitted isotropically in the laboratory system, a much simpler method can be used to great advantage, in place of the several individual procedures indicated in previous sections. Let us adopt the following notations, in addition to the usual σ_h(cap.), σ_h(el.), σ_h(in.), σ_h(fiss.), σ_h(tot.):

$p(h,h')$= probability of scattering from group h to group h' (inelastic collision)

ν_o = average number of emergent neutrons per fission

$f(h')$ = probability of fission neutron energy in group h'

$\delta_{h,h'}$ = Kronecker δ function, with value 1 for $h=h'$, 0 otherwise

Now, assuming a collision of a neutron of group h with the nucleus, it is clear that the expected number $\bar{\nu}_{h,h'}$ of neutrons emerging from the collision in group h' is

$$\bar{\nu}_{h,h'} = \left\{\sigma_h(\text{cap.}) \cdot 0 + \sigma_h(\text{el.})\delta_{h,h'} + \sigma_h(\text{in.})p(h,h') + \sigma_h(\text{fiss.})\, f(h')\nu_o\right\}/\sigma_h(\text{tot.})$$

Thus, the total expected number of neutrons per collision is

$$\bar{\nu}_h = \sum_{h'=1}^{H} \bar{\nu}_{h,h'} = \left\{\sigma_h(\text{el.}) + \sigma_h(\text{in.}) + \sigma_h(\text{fiss.})\nu_o\right\}/\sigma_h(\text{tot.})$$

Hence, the probability of an emergent neutron from such a collision being in group h' is

$$q_{h,h'} = \bar{\nu}_{h,h'}/\bar{\nu}_h$$

We may therefore store a table of $Q_{h,h'} = \sum_{k=1}^{h'} q_{h,k}$ $h = 1,\ldots, H$, $h' = 1,\ldots, H$, and $Q_{h,o} = 0$, $h = 1,\ldots, H$, as shown below, and proceed according to Fig. 42.

h \ h'	0	1	2 . . .	h' . . .	H
1	0				1
2	0				1
⋮	⋮				⋮
h	0			$Q_{h,h'}$	1
⋮	⋮				⋮
H	0				1

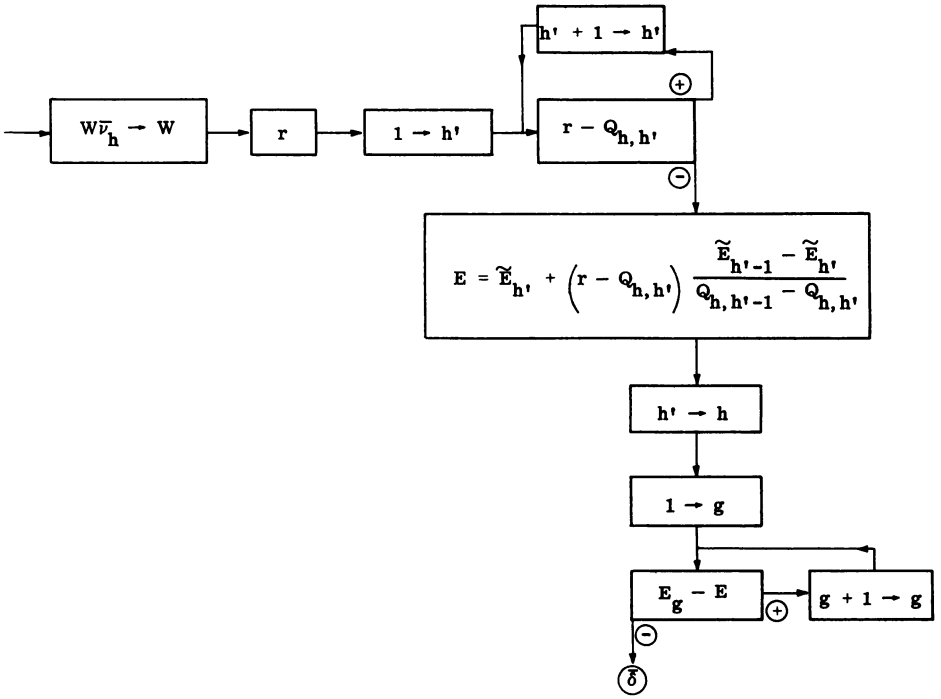

Fig. 42

13. Collisions shattering a nucleus. We consider in this section a type of collision in which a neutron of rest-mass m_1 and velocity V_1 enters a nucleus of rest-mass m_2 and velocity $V_2 = 0$, resulting in a shattering of the neutron + nucleus system into a set of fragments of masses n_j and velocities W_j, $j = 1,2,\dots$, the total rest mass $n = \Sigma n_j$ of the fragments being greater than $m = m_1+m_2$. We treat the mechanics of the collision non-relativistically, using the formula $\frac{1}{2} mV^2$ for kinetic energy of a particle of rest mass m, and velocity V, and we suppose that $m = n$ at various points of the argument. The actual mass-difference $n - m$ corresponds to an energy $\epsilon = (n - m)c^2$, where c is the velocity of light, and in order for the process to occur, part of the kinetic energy of the neutron must be used to supply this energy ϵ.

Proceeding as in §§3 and 9 of the present chapter, we have the general equations

$$P = mV \qquad Q = mW$$

$$k = k' + \frac{1}{2} mV^2 \qquad \ell = \ell' + \frac{1}{2} mW^2$$

(note the assumption $m = n$), and the conservation laws now read

$$P = Q$$

$$k = \ell + \epsilon$$

As usual, $V = W$, and so $k' = \ell' + \epsilon$. Just as in §9, we find that in order for the reaction to take place, we must have $k' = m_2 m^{-1} E \geqq \epsilon$

or

$$E \geqq m\, m_2^{-1} \epsilon$$

Assuming such an incident energy E, the conditions on the relative velocities W_j' of the fragments are

$$\begin{cases} \Sigma \frac{1}{2} n_j W_j'^2 = \ell' = m_2 m^{-1} E - \epsilon \geqq 0 \\ \Sigma n_j W_j' = 0 \end{cases}$$

In contrast to the situation in §9, these relations do not determine the $W_j'^2$ if more than two fragments exist (including the original neutron). We propose instead to single out an arbitrary one of the fragments n_J and discover the maximum relative energy with which it can emerge.

We adopt the convention that Σ' refers to summation on all $j \neq J$. Thus we define $n' = \Sigma' n_j$ to be the mass of the remaining fragments, and $n' W_R = \Sigma' n_j W_j$ defines the velocity W_R of their own center of mass. Now $W_R' = W_R - W$ denotes as usual the velocity of the residual center of mass R relative to that of the whole system. Moreover, we define $W_j'' = W_j - W_R = (W_j' + W) - (W_R' + W) = W_j' - W_R'$ for all $j \neq J$. Now the above system becomes

$$\left.\begin{aligned} \tfrac{1}{2} n_J W_J'^2 + \Sigma' \tfrac{1}{2} n_j W_j'^2 = \ell' \\ n_J W_J' + \Sigma' n_j W_j' = 0 \end{aligned}\right\} \qquad (9)$$

But observe that the following relations hold for the residual system:

$$\Sigma' n_j W'_j = \Sigma' n_j (W'_R + W''_j) = n' W'_R + \Sigma' n_j W''_j \tag{10}$$

$$\Sigma' \frac{1}{2} n_j W'^2_j = \Sigma' \frac{1}{2} n_j (W'_R + W''_j)^2 = \frac{1}{2} n' W'^2_R + W'_R \Sigma' n_j W''_j + \Sigma' \frac{1}{2} n_j W''^2_j \tag{11}$$

Now we know by definition that

$$\Sigma' n_j W_j = n' W_R$$

so that

$$\Sigma' n_j (W + W'_j) = n' (W + W'_R)$$

and hence

$$\Sigma' n_j W'_j = n' W'_R \tag{12}$$

Reference to (10) yields

$$\Sigma' n_j W''_j = 0$$

and this result with (11) gives us the familiar

$$\Sigma' \frac{1}{2} n_j W'^2_j = \frac{1}{2} n' W'^2_R + \Sigma' \frac{1}{2} n_j W''^2_j \tag{13}$$

Now to return to the system (9), its second relation together with (12) tells us that

$$n' W'_R = -n_J W'_J$$

so that $\frac{1}{2} n' W_R'^2 = (n_J/n')(\frac{1}{2} n_J W_J'^2)$. We may therefore rewrite (13) as

$$\Sigma' \frac{1}{2} n_j W_j'^2 = (n_J/n')(\frac{1}{2} n_J W_J'^2) + \Sigma' \frac{1}{2} n_j W_j''^2$$

The latter, substituted into the first member of the system (9), gives us finally

$$(m/n')(\frac{1}{2} n_J W_J'^2) + \Sigma' \frac{1}{2} n_j W_j''^2 = \ell'$$

It follows that the maximum relative energy of n_J must be $(n'/m)\ell' = (n'/m)(m_2 m^{-1} E - \epsilon)$.

Thus, in summary, if the incident energy E exceeds the minimal energy $m\, m_2^{-1} \epsilon$ required for the process, the maximal relative speed of any fragment J is given by

$$\bar{w}_J = \sqrt{\frac{2n'm_2}{m^2 n_J} (E - m\, m_2^{-1} \epsilon)}$$

Suppose that we now construct the laboratory velocity W_J and the corresponding laboratory deflection angle ψ_J by the usual addition $W_J = W + W_J' = V + W_J'$. Reference to Fig. 43 makes it clear that the possible end points of the vectors W_J occupy the sphere of radius $\bar{w}_J$ about the end point of V. Moreover, it is apparent that three essentially different cases arise, depending on the relative magnitudes of $\bar{w}_J$ and $|V|$, or, equivalently (using the above formula for $\bar{w}_J$), the relative magnitudes of E and $\tilde{\epsilon} \equiv n'\epsilon/(m_2 - n_J)$. If we are interested only in neutron masses n_J, the latter reduces to $m_2\epsilon/(m_2 - m_1)$.

Case 1. $\bar{w}_J < |V|$ or $E < \tilde{\epsilon}$. The angle ψ_J is limited to the range $0 \leqq \psi_J \leqq \arcsin(\bar{w}_J/|V|)$, and the possible speeds $|W_J|$ corresponding to any given ψ_J on this range are bounded from zero.

Case 2. $\bar{w}_J = |V|$ or $E = \tilde{\epsilon}$. The angle ψ_J is limited to the range $0 \leqq \psi_J \leqq \pi/2$ but for a given such ψ_J the possible $|W_J|$ range from 0 to a maximum.

Case 3. $\bar{w}_J > |V|$ or $E > \tilde{\epsilon}$. The angle ψ_J has its full range $0 \leqq \psi_J \leqq \pi$, and $|W_J|$ for a given ψ_J ranges from 0 to its upper bound.

In any case, the maximum speed w_J associated with a given possible ψ_J is given by the greater root of the quadratic equation

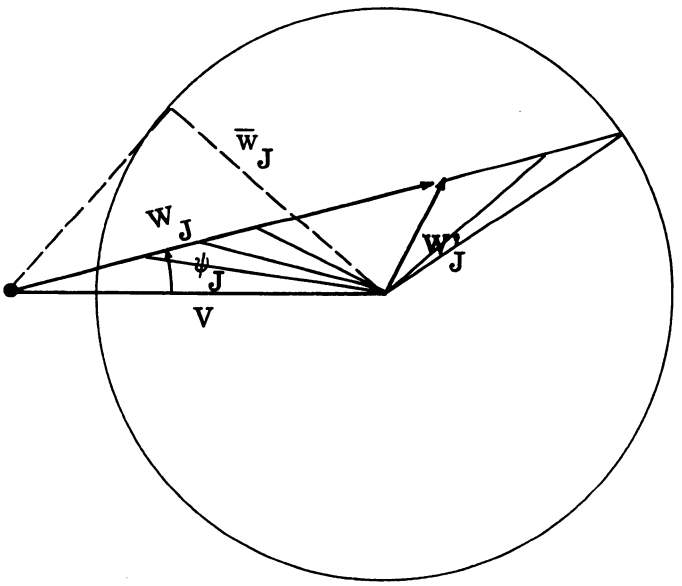

Fig. 43

$\bar{w}_J^2 = w_J^2 + V^2 - 2\, w_J |V| \cos \psi_J$. Substituting for $\bar{w}_J$ and writing ϵ_J for the maximal laboratory energy $\frac{1}{2} n_J W_J^2$ of the J^{th} fragment associated

with the laboratory deflection angle ψ_J, we obtain

$$\epsilon_J - [2m^{-1}(m_1 n_J E)^{1/2} \cos\psi_J]\,\epsilon_J^{1/2} + m^{-1}[n'\epsilon - (m_2 - n_J)E] = 0$$

If we apply this to any neutron n_J, we have $n_J = m_1$ and $n' = m_2$, so that finally

$$\epsilon_J - (2m^{-1}m_1\sqrt{E}\cos\psi_J)\,\epsilon_J^{1/2} + m^{-1}[m_2\epsilon - (m_2 - m_1)E] = 0$$

The discussion of this section thus serves to show why the inelastic cross section $\sigma_E(\text{in.})$ for such a process becomes zero for incident energies E below $m\,m_2^{-1}\epsilon$, and how the energy range of neutrons emerging from the reaction depends on the incident energy and the cosine of the laboratory angle ψ_J.

14. The (n-2n) reaction in deuterium. As an example of the preceding theory, we consider the reaction

$$n + {}_1H^2 \longrightarrow {}_1H^1 + 2n$$

in which a neutron disrupts the deuterium nucleus into its constituent proton and neutron.

Adopting the atomic masses of the following table

neutron	1.00893
${}_1H^1$	1.008123
${}_1H^2$	2.014708

we find an excess of .002345. This gives an actual mass of

.002345/A gm per deuterium atom. Multiplying by c^2 and dividing by the number 1.60203×10^{-6} of erg per Mev (Chapter II, §3) gives $\epsilon = 2.184$ Mev. Hence $m\, m_2^{-1}\epsilon = 1.5\,\epsilon$ is the minimal energy for the process to occur, and the three cases mentioned in the preceding section depend on the relative sizes of E and $m_2\epsilon/(m_2 - m_1) = 2\epsilon$.

We will suppose that a "cross section" $\tau_E(E', \psi)$ is defined in such a way that

$$2\pi\, \tau_E(E', \psi)\, dE'\, d(\cos\psi)\, \frac{N\Delta\ell}{\alpha}\, \alpha \cdot B$$

is the expected number of neutrons of energies between E' and $E' + dE'$, and directions between ψ and $\psi + d\psi$ resulting from such inelastic collisions of a beam of B neutrons of energy E traversing a medium of numerical density N and thickness $\Delta\ell$. (Contrast Chapter III, §1.) Now

$$2\alpha_E(\text{in.})\, N\Delta\ell \cdot B$$

is the total expected number of neutrons in this traversal, since each such collision produces two neutrons.

Hence we have

$$2\pi \int_{-1}^{1} \int_{\epsilon_1(E,\psi)}^{\epsilon_2(E,\psi)} \tau_E(E', \psi)\, dE'\, d(\cos\psi) = 2\sigma_E(\text{in.})$$

where the $\epsilon_i(E, \psi)$ are the upper and lower energy bounds referred to in the preceding section.

Moreover,

$$\pi \sigma_E^{-1}(\text{in.})\, \tau_E(E', \psi)\, dE'\, d(\cos\psi)$$

is the probability of an emergent neutron being in the range $(E, E + dE)$ and $(\psi, \psi + d\psi)$, assuming such a collision occurs.

The Monte Carlo procedure is therefore clear. We decide in the usual way whether the collision is of this kind by reference of a random number to $\sigma_E(\text{in.})/\sigma_E(\text{tot.})$. If r is less than this ratio, inelastic collision occurs. We then double the weight W of the incident neutron and determine its $\cos\psi = a$ and its energy E' from the above probability distribution. We may do this in two steps, using first the probability density function

$$P_E(a) = \pi \sigma_E^{-1}(\text{in.}) \int_{\epsilon_1}^{\epsilon_2} \tau_E(E', \psi)\, dE'$$

to determine the $a = \cos\psi$, and then finding the energy E' using the density function for E':

$$q_E(a, E') = \tau_E(E', \psi) \Big/ \int_{\epsilon_1}^{\epsilon_2} \tau_E(E', \psi)\, dE'$$

for the $a = \cos\psi$ determined.

A more complicated example involving an energy cutoff and critical angles in the same way as indicated in §7 of this chapter may be found in LA-1606 (not available).

15. An (n-2n) reaction on heavy nuclei. As a further illustration of the use of weights, consider a collision of a 14 Mev neutron with a heavy nucleus which results in the emission of a pair of neutrons, isotropically distributed in the laboratory system, one neutron being in the energy distribution

$$E' \exp(-E'/T_1)\, dE' , \quad 0 \leqq E' \leqq \epsilon , \quad T_1 < \epsilon$$

and the other in a similar distribution

$$E' \exp(-E'/T_2)\, dE' , \quad 0 \leqq E' \leqq \epsilon , \quad T_2 < \epsilon$$

where ϵ, T_1, T_2 are constants.

Let $A_i = \int_0^{\epsilon} E' \exp(-E'/T_i)\, dE' = T_i^2 \left\{ 1 - \left(1 + \frac{\epsilon}{T_i}\right) \exp(-\epsilon/T_i) \right\}$

for $i = 1,2$. We have then

$$p_i(E')\, dE' = A_i^{-1} E' \exp(-E'/T_i)\, dE'$$

for the probability of the i^{th} neutron emerging between E' and $E' + dE'$. Since the expected number of neutrons in the latter range, per collision, is $p_1(E')dE' + p_2(E')dE'$, we may properly assume one neutron of weight W suffering such a collision gives rise to a neutron of weight $2W$, chosen in the energy distribution

$$p(E')dE' = \frac{1}{2} \left[p_1(E') + p_2(E') \right] dE'$$

Since the maximum $\max p(E')$ on the range $0 \leqq E' \leqq \epsilon$ can be computed in advance, we may use the von Neumann device of Chapter I, §5, followed by an induction loop for determining the new energy group, and the procedure of Chapter VII, §5, for the final direction parameters.

16. Capture in a small zone. Certain problems involve determination of absorption in a small zone of material, surrounded by a relatively large system of moderator, which slows down neutrons by scattering on light nuclei. The slim chance of a neutron hitting this small capture zone may be improved by various devices, of which we indicate only one.

Suppose for simplicity that a spherically symmetric system contains a small central core of capture material of radius R_1. Let $R^* > R_1$ be chosen comparatively close to R_1. If a neutron undergoes collision at a point of radius $R > R^*$ we may proceed as usual. However, if $R \leqq R^*$, we may process from this point to termination $\bar{m}$ neutrons each of weight $W/\bar{m}$, instead of the customary single neutron of weight W. If the multiplicity $\bar{m}$ is sufficiently large and $R^* - R_1$ sufficiently small, some of the $\bar{m}$ descendants are very likely to hit the absorbing core.

Such a scheme requires modification of the over-all flow diagram. We call attention especially to the following changes: (a) the source routine (σ) sets a new parameter $m = 0$ for each fresh neutron leaving the source; (b) the (β) or (β_0) routine exits, in event of collision, to a new entry ($\bar{\gamma}$) which is preliminary to the usual capture routine (γ);

(c) the $(\bar{\gamma})$ routine, in case the multiplication trick is indicated, stores all parameters R, w, E, g, W,... of the "parent" neutron at the point of collision in new positions designated by $\tilde{R}$, $\tilde{w}$, $\tilde{E}$, $\tilde{g}$, $\tilde{W}$,... for reference in processing each of the $\bar{m}$ progeny from this point to termination; (d) the (α) entry, to which one returns on termination of any particle, is modified to order complete processing of $\bar{m}$ progeny before starting out a new source neutron. The parameter $m = 1,2,\ldots \bar{m}$ indicates the number of the descendant being processed. The following flow diagram (Fig. 44) includes the essential modifications.

Note that the entry $(\bar{\gamma})$ excludes using the multiplication trick on a descendant. That is, we do not iterate the process. In practice the device is usually of a more elaborate nature, using different multiplicities $\bar{m}$ for different critical radii R^*. Moreover, the capture cross section of the core usually becomes significant only at low energies, so that the multiplication decision may also rest upon a decision on $E - E^*$ where E^* is some stipulated low energy.

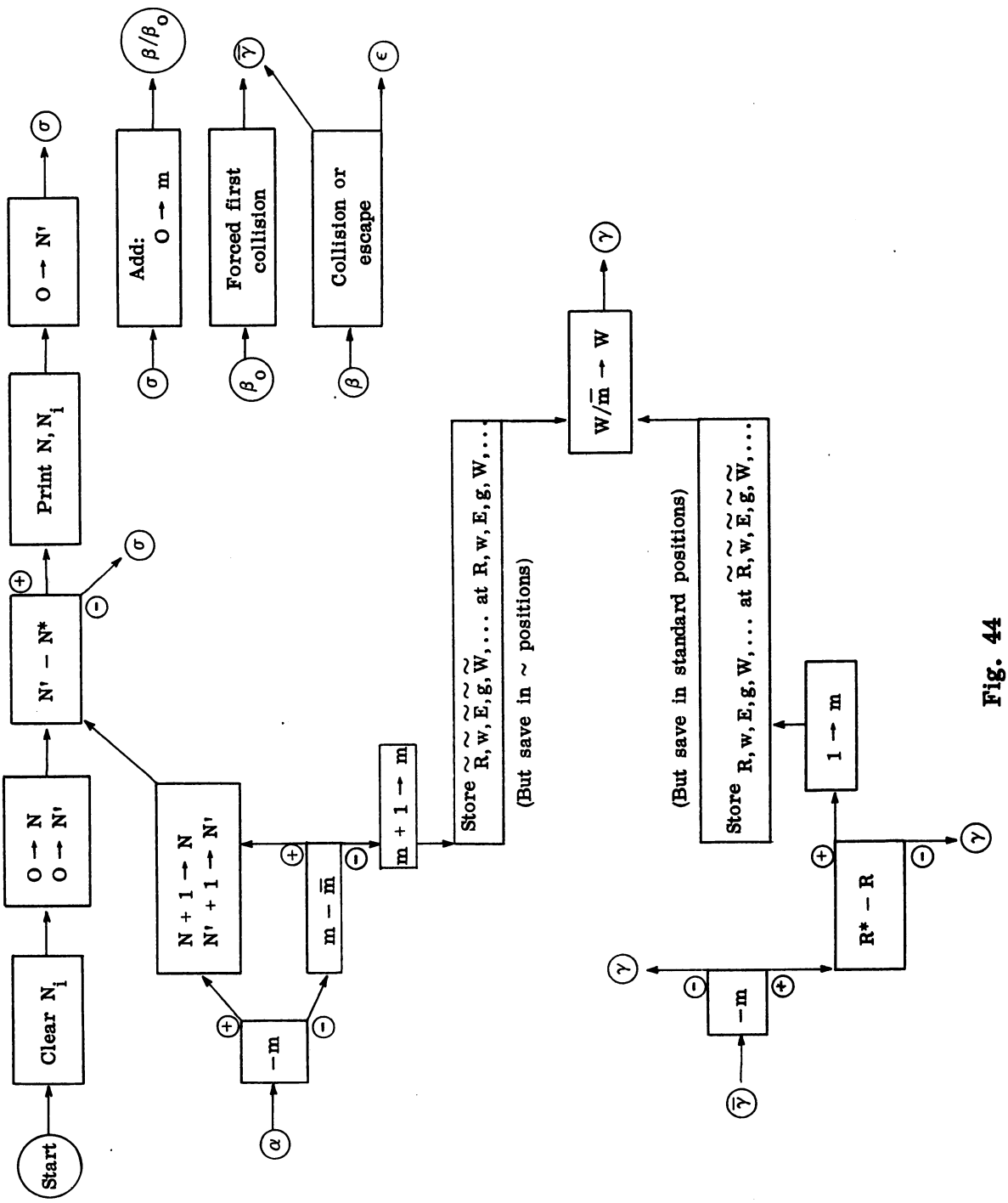

Fig. 44

17. Capture by a "point" detector. The method of the preceding section may be ineffective if the capture zone is extremely small. The present section presents a much simplified example of such a case.

Consider a spherical shell (radii $R_1 < R_2$) of a single light element which can be considered (perhaps by use of transport cross sections) to scatter neutrons isotropically in the laboratory system. Suppose further that a detector of very small radius $R_o << R_1$ is located at the center of the hole (vacuum), and it is desired to find the distribution into energy groups of neutrons impinging on the detector, considered as a perfect absorber.

Specifically, let $E_o > E_1 > \ldots > E_G$ denote the bounds of the energy groups adopted, E_G being the "cutoff" energy, below which neutrons are lost to a category L_E. Consider a collision C at x, y, z, R, $R_1 \leq R < R_2$ of a neutron with incident direction u, v, w. The fraction f of total solid angle subtended at C by the detector is $\frac{1}{2}(1 - \cos\sigma) \cong \frac{1}{2}(1 - (1 - \frac{1}{2}\sigma^2)) = \frac{1}{4}\sigma^2 \cong \frac{1}{4}\sin^2\sigma = \frac{1}{4}R_o^2/R^2$, where σ is defined by $\sin\sigma = R_o/R$. Observe that we are only considering a case where these approximations are very good.

Let the direction from C to the origin be denoted by u", v", w", and let $\eta = u\,u" + v\,v" + w\,w"$ be the cosine of the angle between this direction and the incident direction. Finally, let E" be that new energy which would result from a scattering from the direction u, v, w to the direction u", v", w".

We proceed in two essentially different ways according as this energy E'' is below or above E_G. If below, we allow the colliding neutron of weight W to scatter isotropically in the laboratory system into a new direction u', v', w'. If the new line of flight cuts the detector, or if it falls outside of the solid angle subtended at C by the detector and corresponds to a scattered energy below cutoff, we deposit the weight W in L_E. Otherwise, we follow the scattered neutron further to escape or its next collision by the usual (β) routine. It will be seen that this is the orthodox way of treating a collision, except that we assume that directions within the very small detector solid angle have the same behavior as the direction u'', v'', w'' insofar as resultant energy is concerned.

However, in case the energy E'' corresponding to u'', v'', w'' is above cutoff, we deterministically add a weight Wft to the category D_j, which records neutrons impinging on the detector with energies in the group containing the energy E''. Here f has its assigned meaning and $t = \exp\left\{-(R - R_1)/\lambda(E'')\right\}$ is the transmission for neutrons of energy E'' in the direction toward the center of the detector. We then allow an isotropic scattering into the direction u', v', w'. If this direction falls within the counter solid angle, we force a first collision of weight $W(1 - t)$ at $x + u''\ell$, $y + v''\ell$, $z + w''\ell$, where $\ell = -\lambda(E'')\ln[1 - r(1 - t)]$. (Cf. Chapter III, §5.) If the scattered direction $u'v'w'$ is outside this solid angle, we determine the corresponding new energy E' and deposit weight W in L_E if E' is below the cutoff E_G or follow the weight W further in the usual (β) routine if E' is above E_G.

In a large number N of collisions of the second kind ($E'' > E_G$) the expected number hitting the detector will be NWft (with the proper energy distribution), as it should be. Moreover (Nf) neutrons will scatter into the detector direction, on the average, resulting in a total weight of (Nf) W (1 - t) = (NW) f (1 - t) having first collisions in this direction, and these are distributed spatially in the correct exponential distribution. Finally,an expected number N(1 - f) of neutrons will scatter outside the detector solid angle, with total weight N(1 - f) · W = (NW)(1 - f), and these are correctly processed in their subsequent history.

The method has the great virtue of deterministically contributing a correct positive weight to the detector on <u>every</u> collision of the second kind. (Collisions of the first kind ($E'' < E_G$) cannot do so physically.)

A flow diagram covering the method is given in Fig. 44a. For the μ formula, one may refer to §6 of the present chapter. The computational parameter Ω is set to zero at the source (δ).

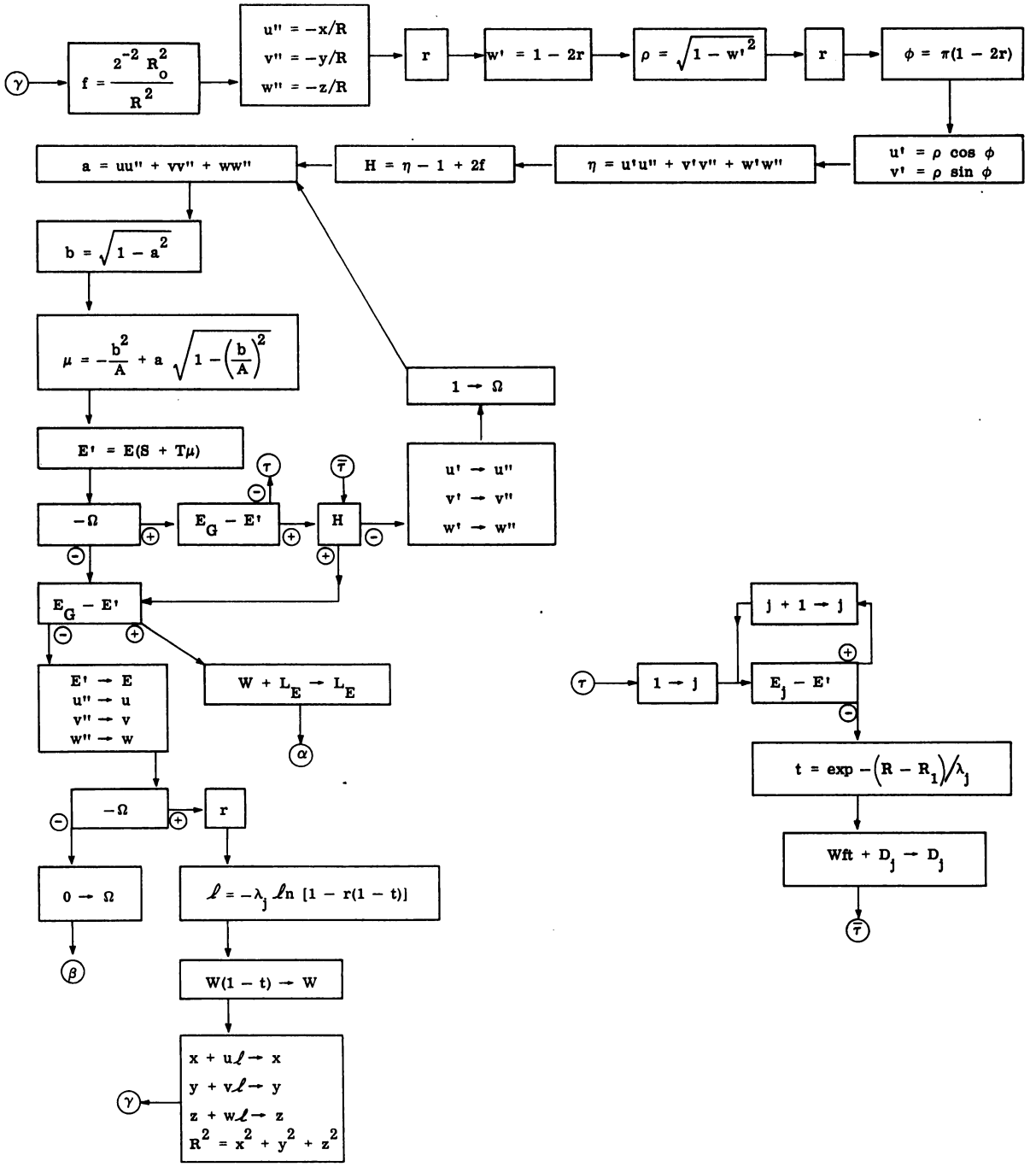

Fig. 44a

18. Remarks on thermal neutrons. In all neutron problems with which we are concerned, the energy range of neutrons actually followed is bounded from zero by some minimum energy $E^* > 0$. This bound may be some stipulated energy E^* above the mean thermal energy of the medium, neutrons with energies falling below this upon any collision being of no interest in the particular problem. The energy E^* then serves as the lower bound E_G of the lowest energy group for which cross sections are stored.

However, when neutrons are to be followed down to the mean thermal energy of the medium, this energy serves as the minimum E^*, and several remarks are in order. All cross section considerations and scattering formulas have been based on the assumption of target nuclei which are at rest in the laboratory system. It is clear that our procedure is unjustified in that part of the energy range approaching the thermal energy in the case of light elements. Moreover, if the mean energy of the medium is in the range below the molecular binding energies involved, simple nuclear cross sections may no longer be applicable.(11)

If neutrons reaching "thermal energy" are dropped, we again have $E^* = E_G$ as above, neutrons with energies below E^* being thrown into a counter L_E for losses to cutoff.

When the problem necessitates actually following neutrons which have reached the thermal energy range, we require a lowermost energy

---

(11) Cf. S. Glasstone, M. C. Edlund, The Elements of Nuclear Reactor Theory, D. Van Nostrand Company, Inc., Princeton, N. J., 1952, on thermal neutron cross sections.

group for such "thermal neutrons," a suitable "average free path," and differential scattering laws for this group, as well as probabilities for different types of reactions. It is impractical to deal with the actual case of a distribution of neutron energies in the thermal range, and all methods assume neutrons within this group have a fixed energy and upon elastic collision retain this energy. For heavy elements, isotropy in the laboratory system seems to be a valid assumption for elastic scattering. However, the choice of proper averages for the other nuclear constants referred to depends on the elements involved and on complicated questions of the actual energy distributions obtaining, which are non-Maxwellian in media with strong thermal capture.

19. Remark on determination of photon sources. Collisions of neutrons with particular types of nuclei may result in the production of γ-rays; radiative capture and certain (n-n) inelastic processes are examples. One of the applications of Monte Carlo to neutronics problems which is becoming of increasing importance is the determination of photon production by neutrons in shields. The latter information may be used in turn for the input energy and spatial distribution in the Monte Carlo treatment of photon diffusion, discussed in the following chapter.

Insofar as the neutronics of such shielding media is concerned, one need only record as they occur the number of radiative captures, and the number of (n-n)radiative collisions caused by incident neutrons of energy group g, in each of a set of spatial zones.

This, together with a knowledge of the γ energies produced in capture and the production cross sections for γ's by neutrons of energy group g in (n-n) reactions, yields the desired distributions for the source in the related photon problem.

CHAPTER VI

PHOTON COLLISIONS

1. Introduction. The procedures discussed in the present manual are adapted to problems involving the scattering of photons on electrons and nuclei insofar as photons may be considered as "particles" subject to mean free path and differential scattering laws. It is for this reason that we speak of particles in the text. It is only in the collision routine (γ) that the physical character of the particles need be distinguished. We have discussed many of the collision processes for neutrons with nuclei in Chapter V. We now turn to problems involving photons. The principal types of photon-electron collisions are: (1) Compton scattering, which is the strict analogue of elastic scattering of neutrons on nuclei; (2) pair-production; (3) photoelectric effect. These we proceed to discuss from the point of view of the Monte Carlo technique.

2. Basic concepts and constants. We shall use

$c = 2.99776 \times 10^{10}$ cm sec^{-1} for the velocity of light in vacuo

$h = 6.624 \times 10^{-27}$ erg sec for Planck's constant

$m_o = 9.10658 \times 10^{-28}$ gm for the rest-mass of the electron, and

$e = 4.8025 \times 10^{-10}$ esu for the electronic charge

A photon is characterized (for the purposes of this chapter) by its energy ϵ (ergs). To such a photon is ascribed a frequency ν (sec^{-1}) by means of the relation $\epsilon = h\nu$ and a wave-length λ (cm) by the equation $\lambda\nu = c$. The "equivalent mass" m (gm) of such a photon is defined by $mc^2 = \epsilon$. The speed of all photons in vacuum being c, we may assign to a photon a momentum (vector) mV, where V is the velocity vector of the photon in the laboratory system. Then

$|V| = c$, and $|mV| = mc = h\nu/c$

An electron is characterized for our purposes by its charge e (esu), rest-mass m_o (gm), and its velocity vector V. Its mass is then $m = m_o/\sqrt{(1 - \beta^2)}$ where $\beta = |V|/c$. The momentum vector of the electron is mV and its <u>total</u> energy mc^2.

It is customary to express photon energies by means of a dimensionless parameter $E = h\nu/m_oc^2$, which gives the ratio of photon energy to the rest-mass energy of the electron, namely, $m_oc^2 = .81837 \times 10^{-6}$ erg or .51083 Mev, recalling that 1 Mev is 1.60203×10^{-6} erg (Chapter II,§3). This parameter E is the one we adopt for photon energy in the remainder of the chapter.

3. <u>Compton collisions</u>. A Compton collision is by definition a collision of a photon with an electron (the latter assumed free and

at rest in the laboratory system), with preservation of total momentum (vector) and total energy. We may, therefore, proceed in much the same way as we did in the case of elastic collision between neutron and nucleus (Chapter V, §3), except that we do not introduce a center of mass. We agree on the notations and relations of the following table:

	Before collision		After collision	
	Photon	Electron	Photon	Electron
Mass	$m_1 = h\nu/c^2$	$m_2 = m_o$	$n_1 = h\nu'/c^2$	$n_2 = m_o/\sqrt{1-\beta^2}$ $\beta = w_2/c$
Velocity	V_1	$V_2 = 0$	W_1	W_2
Speed	$\lvert V_1\rvert = c$	$\lvert V_2\rvert = 0$	$\lvert W_1\rvert = c$	$\lvert W_2\rvert = w_2$
Momentum	m_1V_1	m_2V_2	n_1W_1	n_2W_2
Total energy	$\epsilon = h\nu = m_1c^2$	m_2c^2	$\epsilon' = h\nu' = n_1c^2$	n_2c^2

We have the two conservation laws:

$$m_1V_1 + m_2V_2 = n_1W_1 + n_2W_2$$
$$m_1c^2 + m_2c^2 = n_1c^2 + n_2c^2$$

or equivalently,

$$\begin{cases} (h\nu/c^2)\, V_1 = (h\nu'/c^2)\, W_1 + n_2W_2 & (1) \\ h\nu = h\nu' + c^2\,(n_2 - m_2) & (2) \end{cases}$$

Introducing the energy parameters $E = h\nu/m_oc^2$ and $E' = h\nu'/m_oc^2$, we read

$$\begin{cases} EV_1 = E'W_1 + W_2/\sqrt{1-\beta^2} & (3) \\ E - E' = 1/\sqrt{1-\beta^2} - 1 & (4) \end{cases}$$

remembering that, contrary to our usual practice, the capitals E, E' represent scalars.

From (4) it follows that

$$[1 + (E - E')]^2 - 1 = 2(E - E') + (E - E')^2 = \beta^2/(1-\beta^2) \quad (5)$$

while from (3) we obtain

$$E^2V_1^2 - 2EE' |V_1||W_1|\cos\psi_1 + E'^2W_1^2 = W_2^2/(1-\beta^2)$$

where ψ_1 is the deflection angle from V_1 to W_1. Hence,

$$(E^2 + E'^2 - 2EE'\cos\psi_1) = (E - E')^2 + 2EE'(1 - \cos\psi_1)$$

$$= \beta^2/(1-\beta^2) \quad (6)$$

Eliminating $\beta^2/(1-\beta^2)$ from the two equations (5) and (6),

$2(E - E') + (E - E')^2 = (E - E')^2 + 2EE'(1 - \cos\psi_1)$ or

$$E - E' = EE'(1 - \cos\psi_1)$$

Thus we have finally the relation

$$E' = E/[1 + E(1 - a)]$$

where we use $a = \cos\psi_1$, as usual for the laboratory deflection cosine of the incident particle. This is the analogue of the neutronics relation $E' = E(S + T\mu)$ of Chapter V, §3.

It is noted that, as in the case of neutrons scattering on nuclei heavier than hydrogen, there is a positive minimal energy $E'_{min} = E/1 + 2E$ for the scattered photon, attained for $a = \cos\psi_1 = -1$.

As a side remark, observe that the relation

$$E - E' = EE'(1 - \cos\psi_1)$$

leads at once to the familiar wave-length relation

$$\lambda' - \lambda = \left(\frac{2h}{m_o c}\right) \sin^2\left(\frac{\psi_1}{2}\right)$$

if we first write

$$\frac{1}{E'} - \frac{1}{E} = 2 \sin^2\left(\frac{\psi_1}{2}\right)$$

and use the relations $E = h\nu/m_o c^2$ and $\nu\lambda = c$ for both primed and unprimed variables E, ν, λ. The "Compton wave length" λ_o is defined to be $h/m_o c = .024264$ Å (1 Å = angstrom unit = 10^{-8} cm), and the relation is sometimes written

$$\Delta\lambda = 2\lambda_o \sin^2\left(\frac{\psi_1}{2}\right)$$

We have seen how $a = \cos\psi_1$ determines E', the resulting energy of the photon. We have still to show how the kinetic energy and defection cosine $\cos\psi_2$ of the scattered electron are found in terms of E and E'.

To be sure, equation (2) answers the first question, since $c^2(n_2 - m_2) = h\nu - h\nu' = m_o c^2(E - E')$; thus the kinetic energy of the scattered electron is

$$E_e = .51083\ (E - E')\ \text{Mev}$$

We use equation (3) to determine cos Ψ_2 as follows:

$$\cos \Psi_2 = W_2 V_1 / |W_2||V_1| = \sqrt{1 - \beta^2}\ V_1(EV_1 - E'W_1)/w_2 c$$

$$= \sqrt{1 - \beta^2}\ (EV_1^2 - E' |V_1| |W_1| \cos \Psi_1)/w_2 c$$

$$= \sqrt{1 - \beta^2}\ (E - E'a)/\beta$$

$$= (E - E'a)/(\beta / \sqrt{1 - \beta^2})$$

where $\beta/\sqrt{1 - \beta^2}$ is known from either equation (5) or (6).

Summarizing the results of this section, we have

photon deflection cosine $a = \cos \Psi_1$

scattered photon energy $E' = E/[1 + E(1 - a)]$ (units of $m_o c^2$)

recoil electron K.E. $E_e = .51083\ (E - E')$ Mev

electron deflection $\cos \Psi_2 = (E - E'a)/(\beta / \sqrt{1 - \beta^2})$

$$\beta/\sqrt{1 - \beta^2} = \sqrt{[(E - E')^2 + 2(E - E')]}$$

As an example, suppose an 8 Mev photon scatters at an angle of $\Psi_2 = 60^\circ$. Then

$$a = \frac{1}{2}$$

$$E = 15.661 \text{ (8 Mev)}$$

$$E' = 1.7735 \text{ (.90596 Mev)}$$

$$E_e = 7.09404 \text{ Mev}$$

$$\beta/\sqrt{1 - \beta^2} = 14.854$$

$$\cos \psi_2 = .99464$$

$$\psi_2 = 5^\circ 56'$$

4. The Klein-Nishina differential cross section.[12] This is the differential cross section $\sigma_E(\Omega)$ in cm^2/steradian which governs the distribution of $a = \cos \psi_1$ for the scattered photon in the Compton effect, and is the photon analogue of the neutron cross section of Chapter V, §§4 and 6. It is defined by the formula

$$\sigma_E(\Omega)d\Omega = \left(\frac{1}{2} r_o^2\right) \cdot \frac{1 + a^2}{[1 + E(1 - a)]^2} \left\{1 + \frac{E^2(1 - a)^2}{(1 + a^2)[1 + E(1 - a)]}\right\} d\Omega \quad (7)$$

where[13] $r_o = e^2/m_o c^2 = .28183 \times 10^{-12}$ cm.

Now we might proceed just as in the case of elastic collision to determine a by (say) von Neumann's device (Chapter I, §5) and then E' from E and a using the relation

---

(12) For an account of this and related functions see R. Latter and H. Kahn, Gamma-Ray Absorption Coefficients, Project RAND, R-170 (1949) and the National Bureau of Standards Circular 542, Graphs of the Compton Energy-Angle Relationship and the Klein-Nishina Formula from 10 Kev to 500 Mev.

(13) This is the classical Thomson radius of the electron which enters into the electron cross-section formula $(8/3)\pi r_o^2 = .6654 \times 10^{-24}$ cm^2 (= .6654 barns).

$$E' = E/[1 + E(1 - a)] \tag{8}$$

of the preceding section. In view of the complexity of (7) it is fortunate that a simpler alternative exists. We describe this in the following section.

5. The photon energy distribution and Compton cross section. In order to prepare for the alternative method, we first determine the differential cross section $\tilde{\sigma}_E(E')$ from the relation

$$\tilde{\sigma}_E(E')dE' = \sigma_E(\Omega)d\Omega = -\sigma_E(\Omega) \cdot 2\pi(da)$$

Using the preceding equation (8) in the form

$$a = 1 + \frac{1}{E} - \frac{1}{E'}, \tag{9}$$

we obtain the result

$$\tilde{\sigma}_E(E') = \frac{\pi r_o^2}{E^2}\left\{\frac{E'}{E} + \left(\frac{2}{E} + \frac{1}{E^2}\right) + \left(E - \frac{2}{E} - 2\right)\left(\frac{1}{E'}\right) + \left(\frac{1}{E'}\right)^2\right\}$$

We may obtain easily from this the total cross section for Compton scattering as follows:

$$\sigma_E(\text{Compton}) = \int_{\frac{E}{1+2E}}^{E} \tilde{\sigma}_E(E')dE'$$

$$= 2\pi r_o^2\left\{\frac{1+E}{(1+2E)^2} + \frac{2}{E^2} + \frac{E^2 - 2E - 2}{2E^3}\ln(1+2E)\right\}$$

which is graphed in the National Bureau of Standards Circular 542 (1c) and may be used to compute free paths $\lambda_g = 1/N_e \sigma_g$ (Compton) for a suitable set of energy groups (assuming N_e is the numerical density of free electrons and no other processes exist).

We will actually use the Monte Carlo procedure

$$r = P_E(E') \equiv \int_{E'}^{E} \bar{\sigma}_E(E')dE' \Big/ \sigma_E(\text{Compton})$$

to determine E' from E and random number r, since a sufficiently accurate fit for the inverse function is given by[14]

$$E' = \frac{E}{1 + \alpha r + (2E - \alpha)r^3}$$

where $\alpha = E/(1 + .5625\ E)$, and $E \leqq 4$ ($\sim$2 Mev). Addition of a term

$$\frac{1}{2}(E - 4)\ r^2\ (1 - r)^2$$

yields a reasonably good fit on the range $4 < E \leqq 10$.

The equation (5) above then permits determination of a from E and E'.

Thus a Compton collision with incident energy E not exceeding 5 Mev may be satisfactorily handled by the flow diagram of Fig. 45.

---

[14] Bengt Carlson, The Monte Carlo Method Applied to a Problem in γ-ray Diffusion, Los Alamos Scientific Laboratory, AECU-2857, 1953. Cf. H. Mayer, C. A. Burton, Tables of the Compton Effect Cross Sections and Energies, LAMS-1199, Los Alamos Scientific Laboratory, 1953, for goodness of fit.

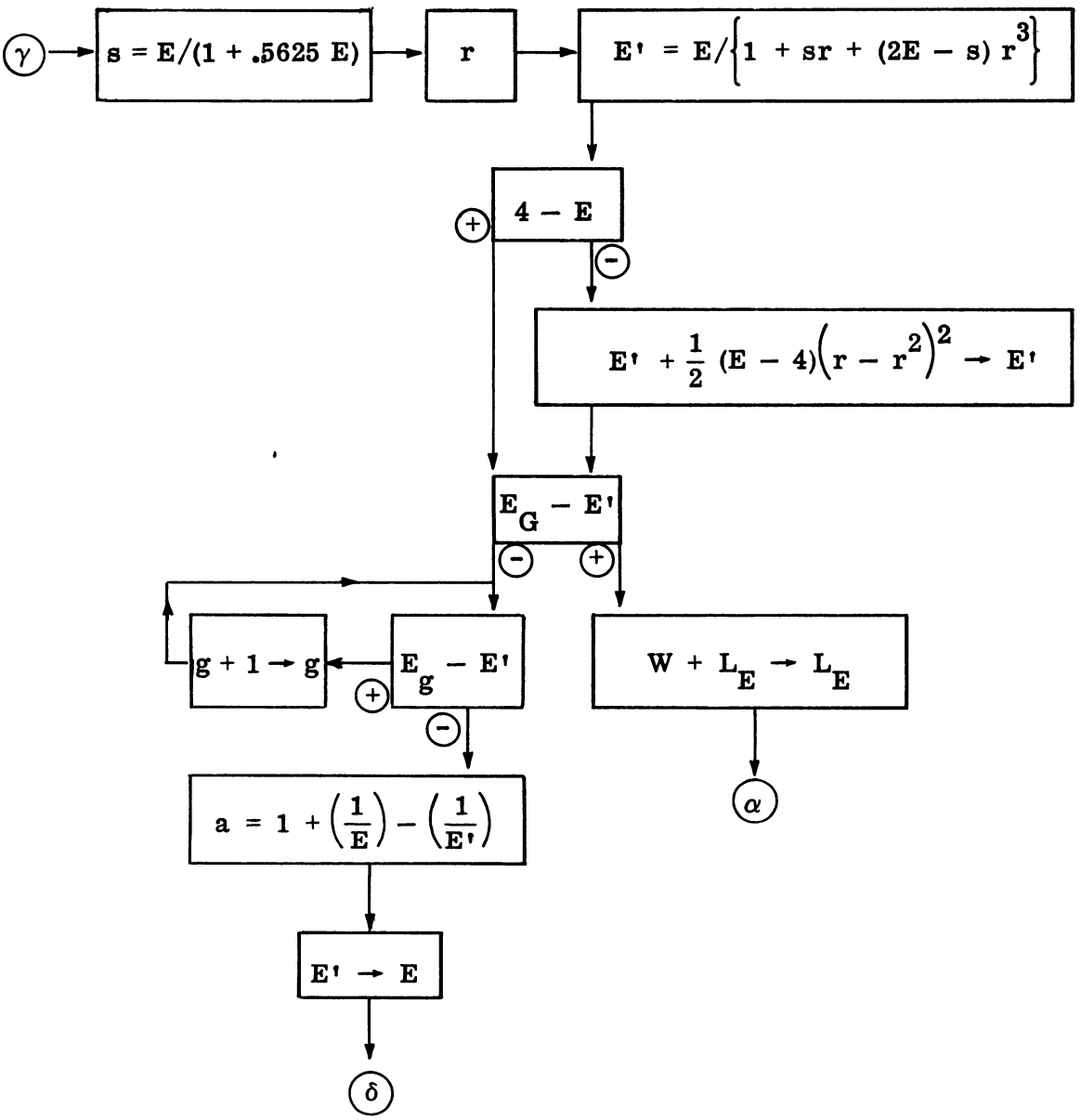

Fig. 45

6. Photoelectric effect and pair production. We have discussed the Compton collision for photons with electrons and noted that it corresponds to the elastic collision in neutronics. If a medium consists of elements A, B,..., the contribution of the Compton effect to the "total cross section" Σ (cf. Chapter III, §2) is $N\sigma_E(\text{Compton})$, where $N = N_A Z_A + N_B Z_B + \ldots$ is the total numerical electron density. Here N_A denotes the number of atoms of element A per cm^3 and Z_A is the atomic number (= number of electrons per atom) of element A.

In determining the "total cross section" all collision processes must be taken into account, and one must consider in this connection the further contributions $N_A \sigma_E^A(\text{pe}) + \ldots \equiv \sum_E(\text{pe})$ of the photoelectric effect and $N_A \sigma_E^A(\text{pp}) + \ldots \equiv \sum_E(\text{pp})$ of pair production. Cross sections for these processes for elements with $4 \leq Z \leq 92$ and $.10 \leq E \leq 20$ $(m_o c^2)$ may be found in the RAND report R-170 referred to before. Thus the free path determining collision positions is given by

$$\lambda = 1/\Sigma$$

where

$$\Sigma = N\sigma_E(\text{Compton}) + \sum_E(\text{pe}) + \sum_E(\text{pp})$$

In the present report we regard pair production and photoelectric effect as absorptions, and have therefore, upon any collision, an absorption probability $[\Sigma - N\sigma_E(\text{Compton})]/\Sigma$, which may be dealt with by the alternative methods discussed in Chapter II, §2.

It must be remembered that secondary photons (X-rays) may result from the photoelectric effect in heavy elements, and that the electron and positron born in pair production produce bremsstrahlung while being slowed down by ionization of the medium. Moreover, the inverse photoelectric effect may come into play, and the positron is finally annihilated with an electron to produce still further γ-rays. If the energy cutoff of the problem is not sufficiently high to exclude consideration of these secondary photons, one must include in the output of the original problem sufficient information to determine source distributions for such secondary radiation. We do not deal with this case in the present manual.

CHAPTER VII

DIRECTION PARAMETERS AFTER COLLISION

1. Introduction. The purpose of the present chapter is to develop formulas for the final direction parameters of a particle after scattering through an angle Ψ_1 of cosine a, in the laboratory system, from an incident direction u, v, w (or w alone). While these formulas are somewhat long, they may be derived from the simple principle of elementary complex variables which states that $(x + iy)(\cos\Theta + i \sin\Theta)$ is a complex number whose vector is rotated through an angle Θ from that of $x + iy$.

2. Formulas for the final direction cosines. Let $\bar{u} = \cos\bar{\alpha}$, $\bar{v} = \cos\bar{\beta}$, $\bar{w} = \cos\bar{\gamma}$ be the direction cosines of the incident line of flight. Consider $(\bar{u}, \bar{v}, \bar{w})$ as a point on the unit sphere $u^2 + v^2 + w^2 = 1$ in direction space U, V, W (cf. Fig. 46). Letting $\bar{\rho}, \bar{\phi}$ be the polar coordinates in the U, V plane of the point $(\bar{u}, \bar{v}, o)$ we see that

$$\bar{\rho} = \sin \bar{\gamma} = \sqrt{1 - \bar{w}^2}$$

$$\cos \bar{\phi} = \bar{u}/\bar{\rho}$$

$$\sin \bar{\phi} = \bar{v}/\bar{\rho}$$

Our first objective is to derive formulas for a particle rotation of U,V,W space into itself which takes the point (0,0,1) into $(\bar{u},\bar{v},\bar{w})$; namely, that resulting from iteration of two simple rotations: the first about the V-axis through the angle $\bar{\gamma}$, followed by a second rotation through the angle $\bar{\phi}$ about the W-axis.

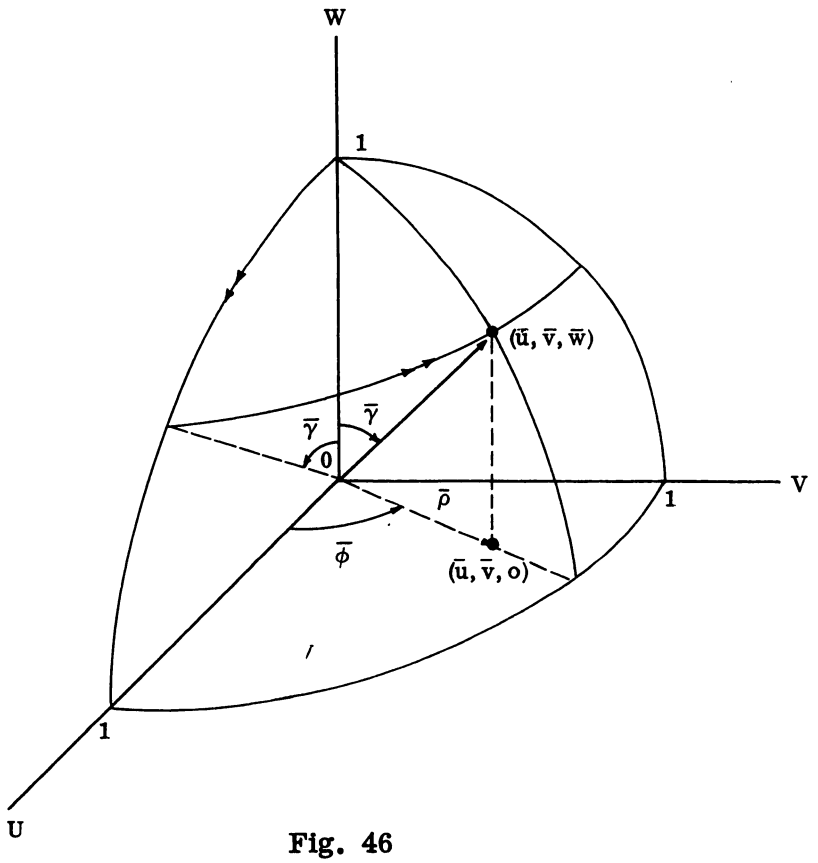

Fig. 46

We have for the first rotation

$$\left.\begin{aligned} w' + iu' &= (w + iu)(\cos \bar{\gamma} + i \sin \bar{\gamma}) \\ v' &= v \end{aligned}\right\} \qquad (1)$$

and for the second

$$\left.\begin{aligned} u'' + iv'' &= (u' + iv')(\cos \bar{\phi} + i \sin \bar{\phi}) \\ w'' &= w' \end{aligned}\right\} \qquad (2)$$

Separating real and imaginary parts, we read

$$\left.\begin{aligned} u' &= u \cos \bar{\gamma} + w \sin \bar{\gamma} \\ v' &= v \\ w' &= -u \sin \bar{\gamma} + w \cos \bar{\gamma} \end{aligned}\right\} \qquad (3)$$

$$\left.\begin{aligned} u'' &= u' \cos \bar{\phi} - v' \sin \bar{\phi} \\ v'' &= u' \sin \bar{\phi} + v' \cos \bar{\phi} \\ w'' &= w' \end{aligned}\right\} \qquad (4)$$

Substitution of (3) into (4) yields

$$\left.\begin{aligned} u'' &= u \cos \bar{\gamma} \cos \bar{\phi} - v \sin \bar{\phi} + w \sin \bar{\gamma} \cos \bar{\phi} \\ v'' &= u \cos \bar{\gamma} \sin \bar{\phi} + v \cos \bar{\phi} + w \sin \bar{\gamma} \sin \bar{\phi} \\ w'' &= -u \sin \bar{\gamma} + w \cos \bar{\gamma} \end{aligned}\right\} \qquad (5)$$

Replacing the functions of $\bar{\gamma}$, $\bar{\phi}$ by their values in terms of $\bar{\rho} = \sqrt{(1 - \bar{w}^2)}$, $\bar{u}$, $\bar{v}$, and $\bar{w}$, we obtain from (5)

$$\left.\begin{aligned} u'' &= (u\,\bar{w}\,\bar{u} - v\,\bar{v})/\bar{\rho} + w\,\bar{u} \\ v'' &= (u\,\bar{w}\,\bar{v} + v\,\bar{u})/\bar{\rho} + w\,\bar{v} \\ w'' &= -u\,\bar{\rho} + w\,\bar{w} \end{aligned}\right\} \qquad (6)$$

Under this rotation (6) it is evident that $(u,v,w) = (0, 0, 1)$ goes over into $(u'', v'', w'') = (\bar{u}, \bar{v}, \bar{w})$.

Now we know that the direction $(\bar{\bar{u}}, \bar{\bar{v}}, \bar{\bar{w}})$ of the deflected line of flight makes an angle ψ_1 of cosine a with the direction $(\bar{u}, \bar{v}, \bar{w})$ of the incident line of flight. It is clear that this restricts the former to a cone of directions of opening ψ_1 about the latter direction, and the directions on this cone are all equally likely. We adopt the following arbitrary convention for fixing the deflected direction; namely, we always consider first a cone of opening ψ_1 about the W-axis OW, and a point $P = (\sin\psi_1 \cos\delta, \sin\psi_1 \sin\delta, \cos\psi_1)$ located on this cone and the unit sphere, determined by an azimuthal angle of δ uniformly distributed on $-\pi \leqq \delta \leq \pi$ (Fig. 47).

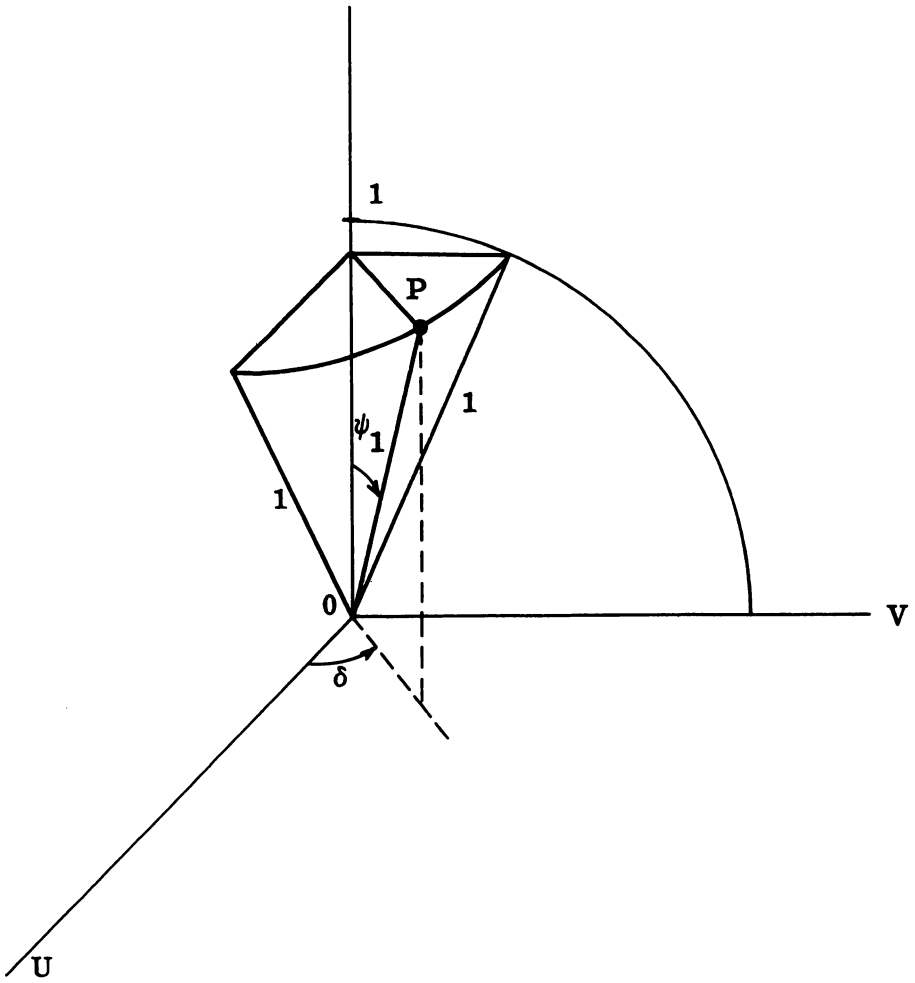

Fig. 47

We then agree that the final direction $(\bar{\bar{u}}, \bar{\bar{v}}, \bar{\bar{w}})$ is the image under rotation (6) of the point P so constructed. It should be clear that this is an appropriate convention for our purpose.

For simplicity we adopt the further notation

$$a = \cos \psi_1$$
$$b = \sin \psi_1 = \sqrt{(1 - a^2)} \qquad 0 \leqq \psi_1 \leqq \pi$$
$$c = \cos \delta$$
$$d = \sin\delta = (\operatorname{sgn} \delta)\sqrt{(1 - c^2)} \qquad -\pi \leqq \delta \leqq \pi$$

In this notation, the point P = (bc, bd, a) = (u, v, w) goes over into

$$\left.\begin{aligned} \bar{\bar{u}} &= (bc\bar{w}\bar{u} - bd\bar{v})/\bar{\rho} + a\bar{u} \\ \bar{\bar{v}} &= (bc\bar{\bar{w}}\bar{v} + bd\bar{u})/\bar{\rho} + a\bar{v} \\ \bar{\bar{w}} &= -bc\bar{\rho} + a\bar{w} \end{aligned}\right\}$$

Summarizing the results of the present section, we have

$$\left.\begin{aligned} u' &= (bcwu - bdv)/\sqrt{(1 - w^2)} + au \\ v' &= (bcwv + bdu)/\sqrt{(1 - w^2)} + av \\ w' &= -bc\sqrt{(1 - w^2)} + aw \end{aligned}\right\} \qquad (7)$$

where

u, v, w are direction cosines of the incident line of flight

u', v', w' are direction cosines of the deflected line of flight (lab.)

$a = \cos \psi_1$, where ψ_1 is the angle between the two

$b = \sqrt{1 - a^2}$

$c = \cos \delta$, where $-\pi \leqq \delta \leqq \pi$ uniformly

$d = (\operatorname{sgn} \delta)\sqrt{1 - c^2}$

Note that these formulas should not be used if $|w|$ is too close to unity. They are then poor computationally and indeterminate at $|w| = 1$. In such a case it is better to by-pass the rotation (6) and use for

u', v', w' the coordinates

$$\begin{cases} u' = bc \\ v' = bd \\ w' = aw \end{cases}$$

where a, b, c, d have the definitions above.

3. Subroutine for the final direction cosines. We incorporate these results into the (δ) routine of Fig. 48. The power 2^{-n} used to determine whether the incident direction should be considered vertical may well depend on the accuracy required and on the number of "bits" afforded by the particular machine being used.

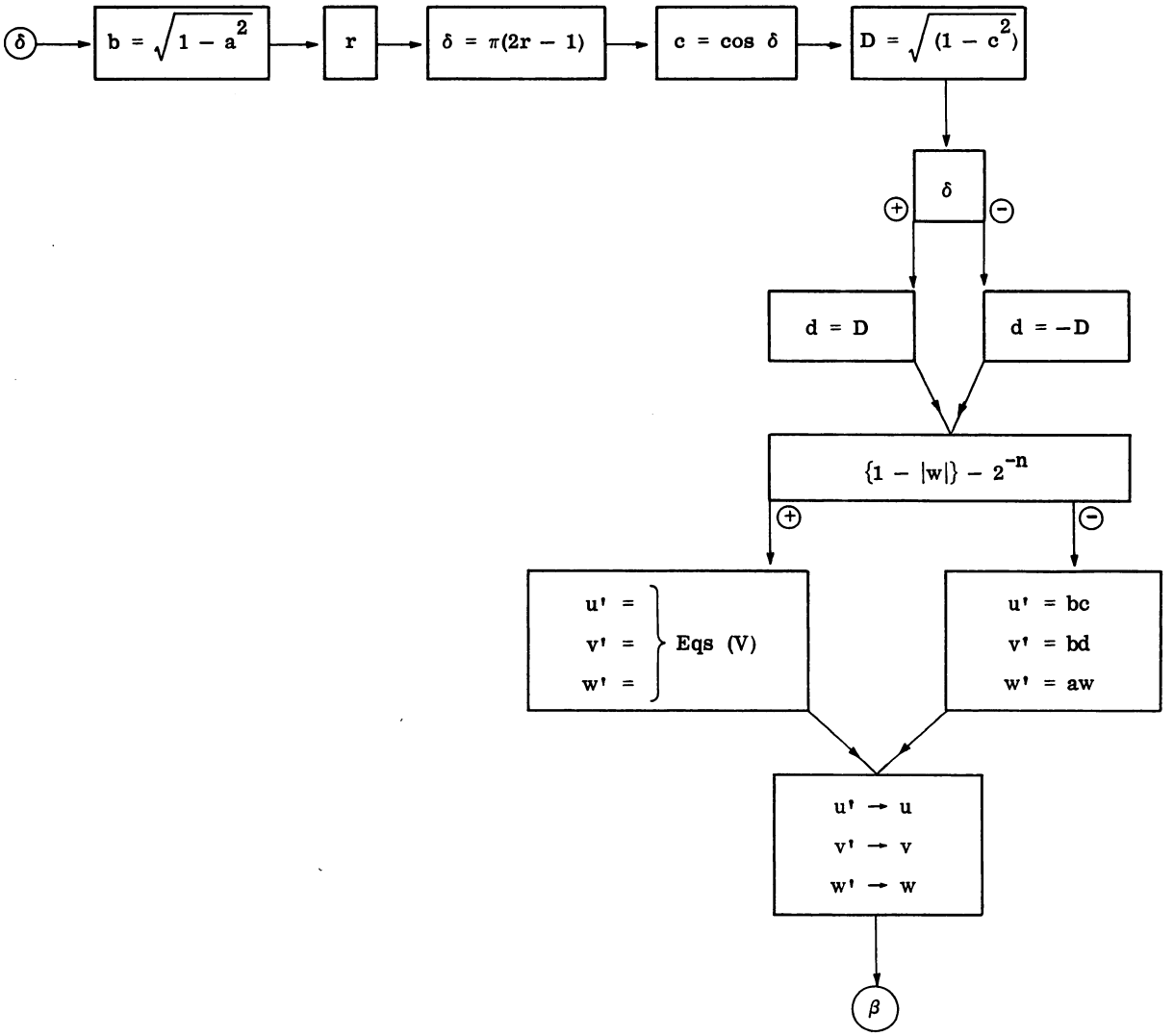

Fig. 48

4. Final direction w in slab or spherically symmetric case.

The present section is concerned with determination of the final direction cosine $w' = \cos \gamma'$ of the scattered line of flight as it exists at the point of collision, in terms of the cosine a of the laboratory angle Ψ_1 determined in (γ), as required in both slab geometry and spherically symmetric geometry. (Cf. Chapter II, §2, and Chapter IV, §8.) We recall that, in the spherical case, the cosine $w = \cos \gamma$ of the angle γ which the incident line of flight makes with the radius vector as it exists at the point of collision has already been prepared (Chapter IV, §3) and stored as w before entry at (δ).

It is immediately evident that the w' formula of equations (7), in §2 of the present chapter,

$$w' = -bc\sqrt{1 - w^2} + aw$$

applies to the slab case, where a, b, and c have the definitions given there. Note that the formula is independent of the u, v used in the derivation, as it should be.

But it will also be clear that the identical formula applies to the spherical case, if we imagine for the moment that OW represents the outwardly directed radius vector direction and u, v, w the direction of the incident line of flight relative to the radius vector, the u,v being immaterial.

In both applications, it will be observed that the angle δ involved in $c = \cos \delta$ may be limited to the range $0 \leqq \delta \leqq \pi$, since $\cos -\delta = \cos \delta = c$ is the only function of δ appearing in the w' formula.

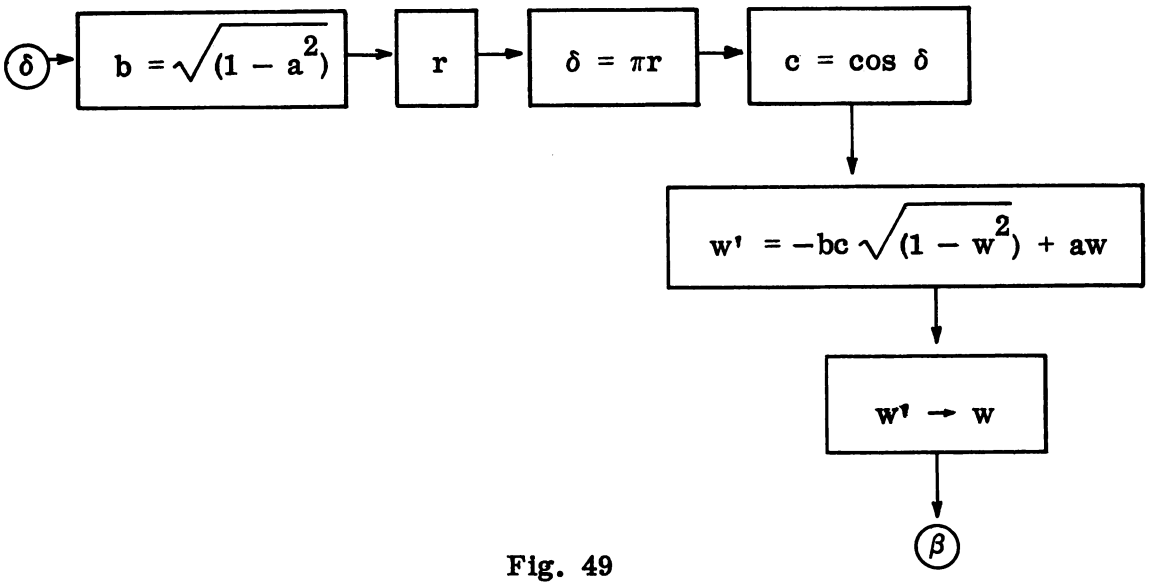

Fig. 49

In both cases, therefore, we have the simple routine of Fig. 49.

5. Scattering isotropic in the laboratory system. In any case where particles emerge from a collision in a distribution isotropic in the laboratory system, it is patently foolish to determine a = 2r - 1 for the deflection cosine relative to the line of flight and then determine the final direction cosines by means of the preceding two sections. It is simpler to assign the direction of the deflected line of flight by the same method we used to set up an isotropic source in Chapter II, §5a, c, ignoring the incident direction completely. Thus the ($\bar{\delta}$) routine referred to is simply that of Fig. 10, with exit to (β) for the u, v, w case, and, still more simply, boxes r and w = 2r - 1 for the slab and spherical case.

CHAPTER VIII

TERMINAL CLASSIFICATION

1. Introduction. We have already indicated various terminal events in the history of a particle, e.g., transmission, capture, loss to energy cutoff, and so on. We must still consider some of the many ways in which it may be desired to classify a particle which escapes the system. This is the general function of the (ϵ) routines previously referred to. Such routines invariably exit to (α) for the introduction of a new source particle. Of these many kinds of classification, we can hope to give only a brief indication, since the demands of physicists on this score are frequently involved and exacting. Indeed, it is the ability of Monte Carlo methods to provide answers to the most intricate questions of this kind which makes them an indispensable tool in design.

2. Classification of escapes on number of collisions. As the simplest example, we may refer to a problem whose purpose it is to determine the distribution of escaping neutrons with respect to the number of collisions suffered within the system. Suppose we agree to keep storage registers N_ν, $\nu = 1, 2, \ldots, 10$ for the total weight of

neutrons escaping with $\nu \leqq 10$ collisions, and N_{11} for those escaping with $\nu \geqq 11$. We suppose that the forced first collision device has been used so that the transmission counter T records the weight escaping with $\nu = 0$ automatically (cf. Ch. III, §4). We may, therefore, follow the routine of Fig. 50.

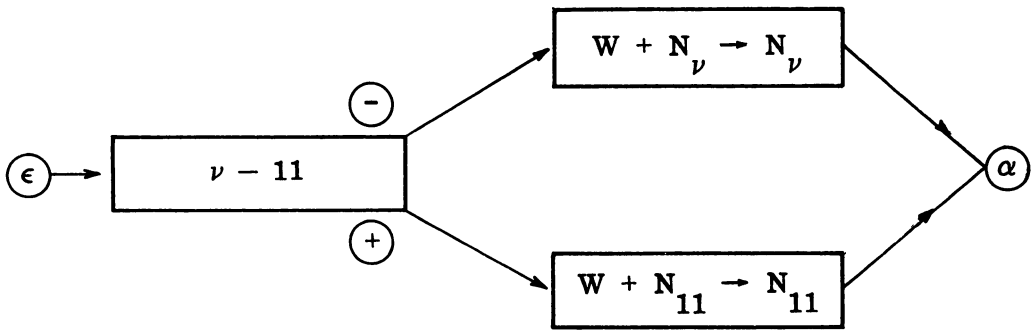

Fig. 50

3. Energy and angle distributions of escape. Consider a problem with a source direction $u = 0$, $v = 0$, $w = 1$ in which one desires the correlated distribution of escapes in energy and angle with the source direction. There must be provided in permanent storage a suitable set of cosines $C_1 > C_2 > \ldots > C_J = -1$ and energy bounds $\epsilon_1 > \epsilon_2 > \ldots > \epsilon_H = E_G$, which need not be the same as those used for other purposes, while in dynamic storage, we reserve JH positions $N_{j,h}$ for the total weights escaping in the corresponding categories. In such a problem, an escaping neutron enters (ϵ) with a known weight W, direction cosine w, and energy E, and is classified as indicated in Fig. 51.

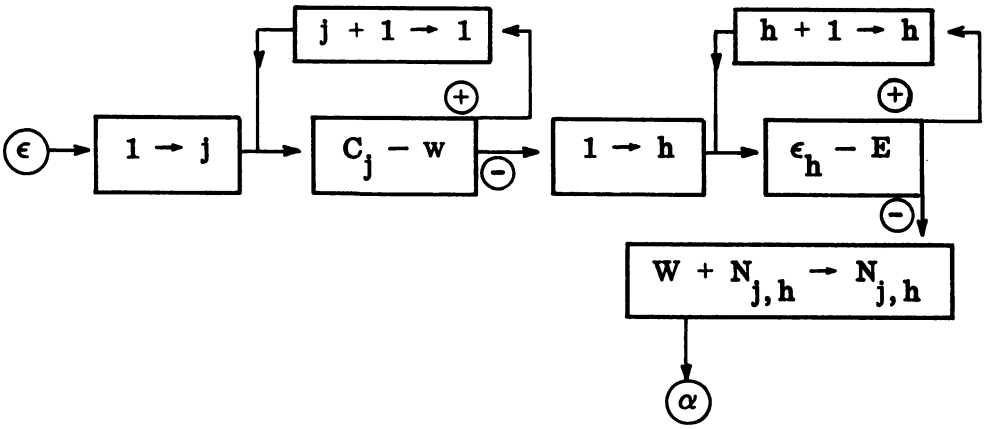

Fig. 51

Such a classification in angle is appropriate in a case like that of Fig. 52, where a detector band is at essentially infinite distance from a scattering medium symmetric about the Z-axis. Here infinite distance means that all particles escaping from any point of the medium surface in the same direction hit the band in the same angular zone. Then the number $N_{j,h}$ referred to is the number of h-group escapes in the solid angle $2\pi(C_j - C_{j-1})$, so that $N_{j,h}/2\pi(C_j - C_{j-1})$ is the number in this category escaping per steradian, and the number hitting a detector of given area on the circle indicated in the figure can be predicted.

If the source direction is again $u = 0$, $v = 0$, $w = 1$, and the scattering medium is symmetric about the Z-axis, ensuring symmetry of escape about this axis, but the detector is not at infinity in the

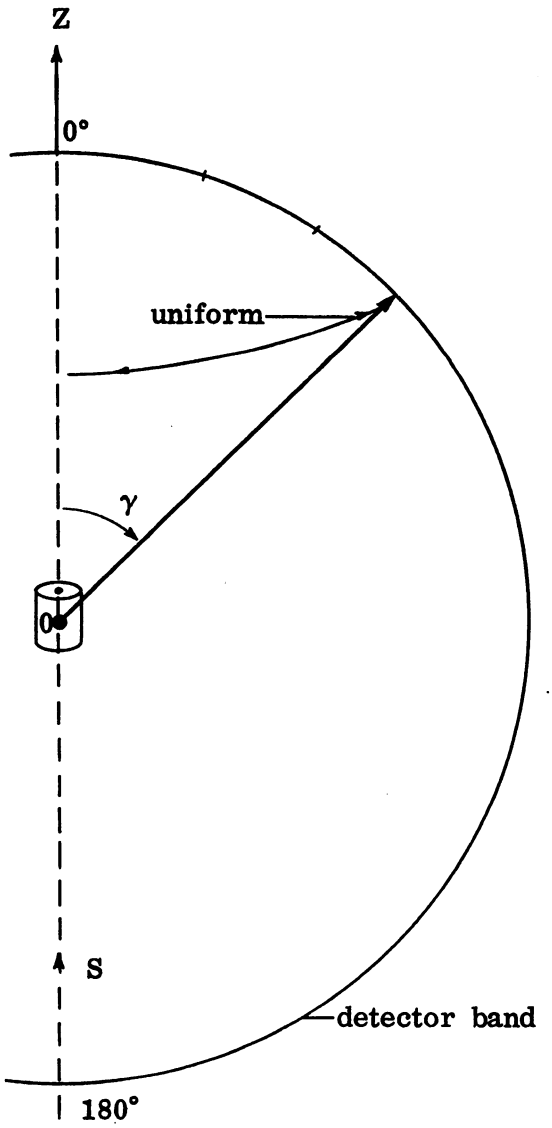

Fig. 52

sense referred to, it is necessary to take into account the distance d_B from center 0 to the detector band as indicated in Fig. 53 and Fig. 54. In the latter, the exit leads to the previous classification routine of Fig. 51 and thence to (α). At entry to the routine of Fig. 54, the x,y,z parameters are those of the last point of departure before escape. Again the results may be normed to number per steradian and interpreted with reference to the detector band indicated.

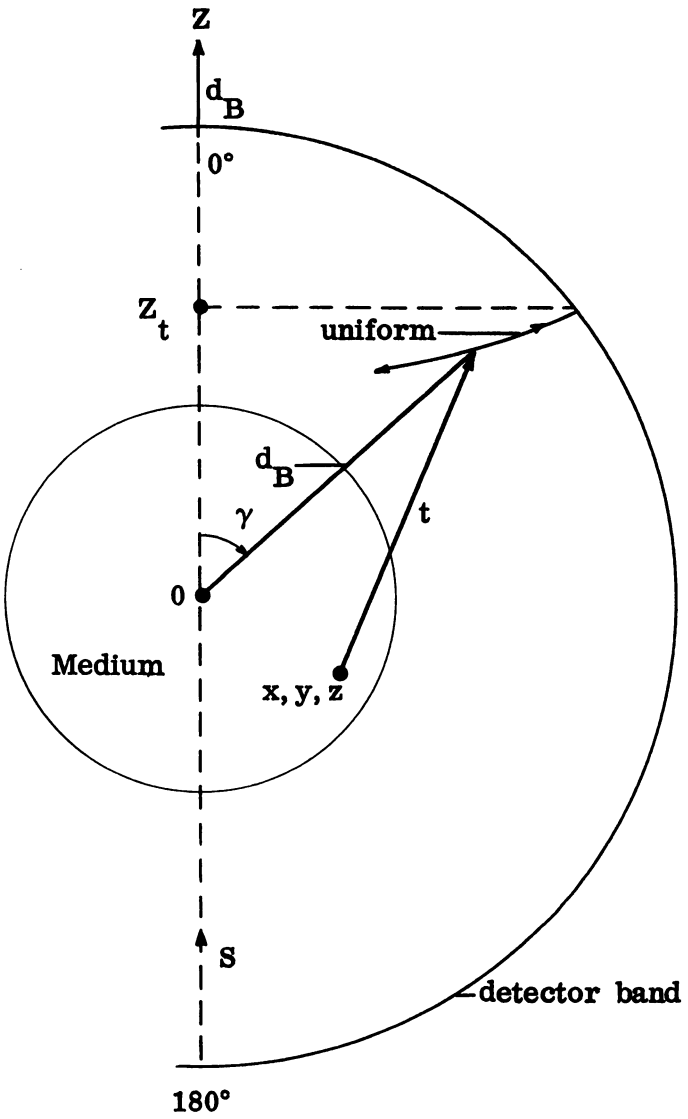

Fig. 53

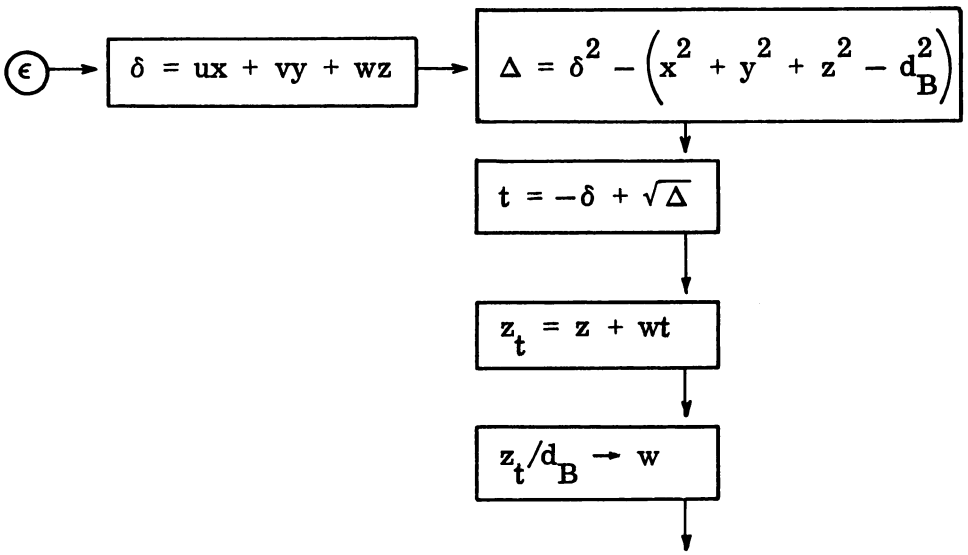

To Fig. 51

Fig. 54

The preceding discussion is limited to systems symmetrically distributed about the source (+Z) direction. Problems of this kind have the great advantage, from the Monte Carlo standpoint, that no escaping particles are lost to classification.

Unfortunately, there are experimental considerations which, in many cases, dictate a geometry in which such symmetry is lacking. Consider, for example, the situation in Fig. 55, in which a source with direction $u = 0$, $v = 0$, $w = 1$ impinges on the lateral surface of a cylinder with axis on the X-axis. It is desired to count the numbers N_j hitting a coaxial band zone j upon escape, the detector band having radius d_B and height h. Since the cylinder

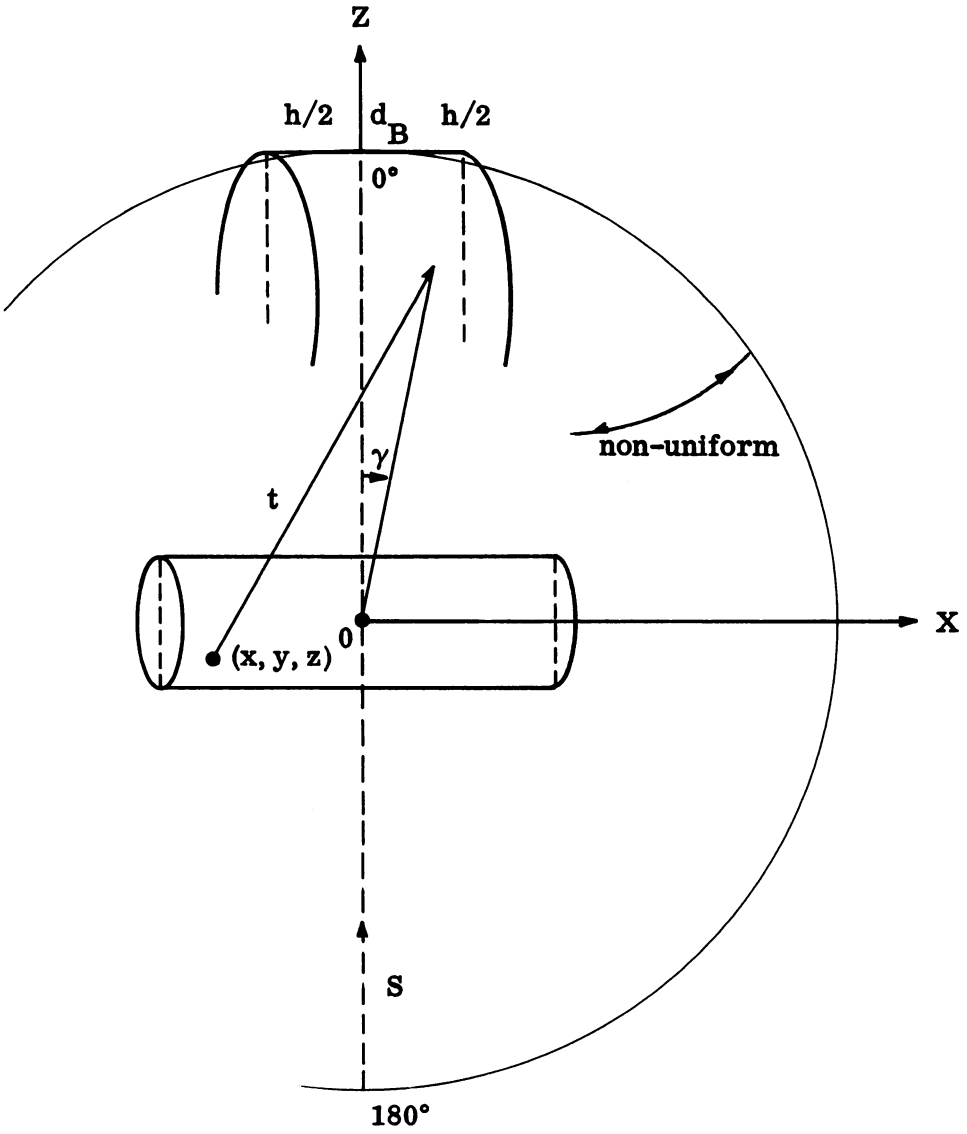

Fig. 55

lacks symmetry about the Z-axis, it is no longer possible to classify escaping particles according to the cosine w of the angle γ of the line from origin to the point of intersection of the line of flight with the sphere of radius d_B, since the escapes with this direction are non-uniform about the Z-axis. Without rather complicated devices for prejudicing scattering in the band direction, which we shall not discuss, all one can do is to submit to running very much larger samples in order that the rather small solid angle actually subtended by the band shall receive a sufficient number of escapes to render the N_j statistics reliable. This is a real difficulty, and it would be of great value for experimentalists contemplating the use of Monte Carlo methods for thick target corrections to consider the feasibility of the symmetric geometry in the experimental setup.

A suitable routine for the case cited, without any special importance sampling devices, is given in Fig. 56, the exit again referring to the routine of Fig. 51. The category L_B refers to all escapes failing to hit the band. In computing the distance t to the (infinite) cylindrical surface $y^2 + z^2 = d_B^2$, one avoids the $1 - u^2 \cong 0$ catastrophe, as indicated in Ch. IV, §6 (end of section).

Consider finally a case where it is desired to classify a particle escaping with direction u,v,w from the lateral surface of a cylinder $x^2 + y^2 = R^2$ according to the angle measured from the normal to the surface. If (x_t,y_t,z_t) is the point of escape, determined in the usual manner from u,v,w,R, and the position x,y,z of

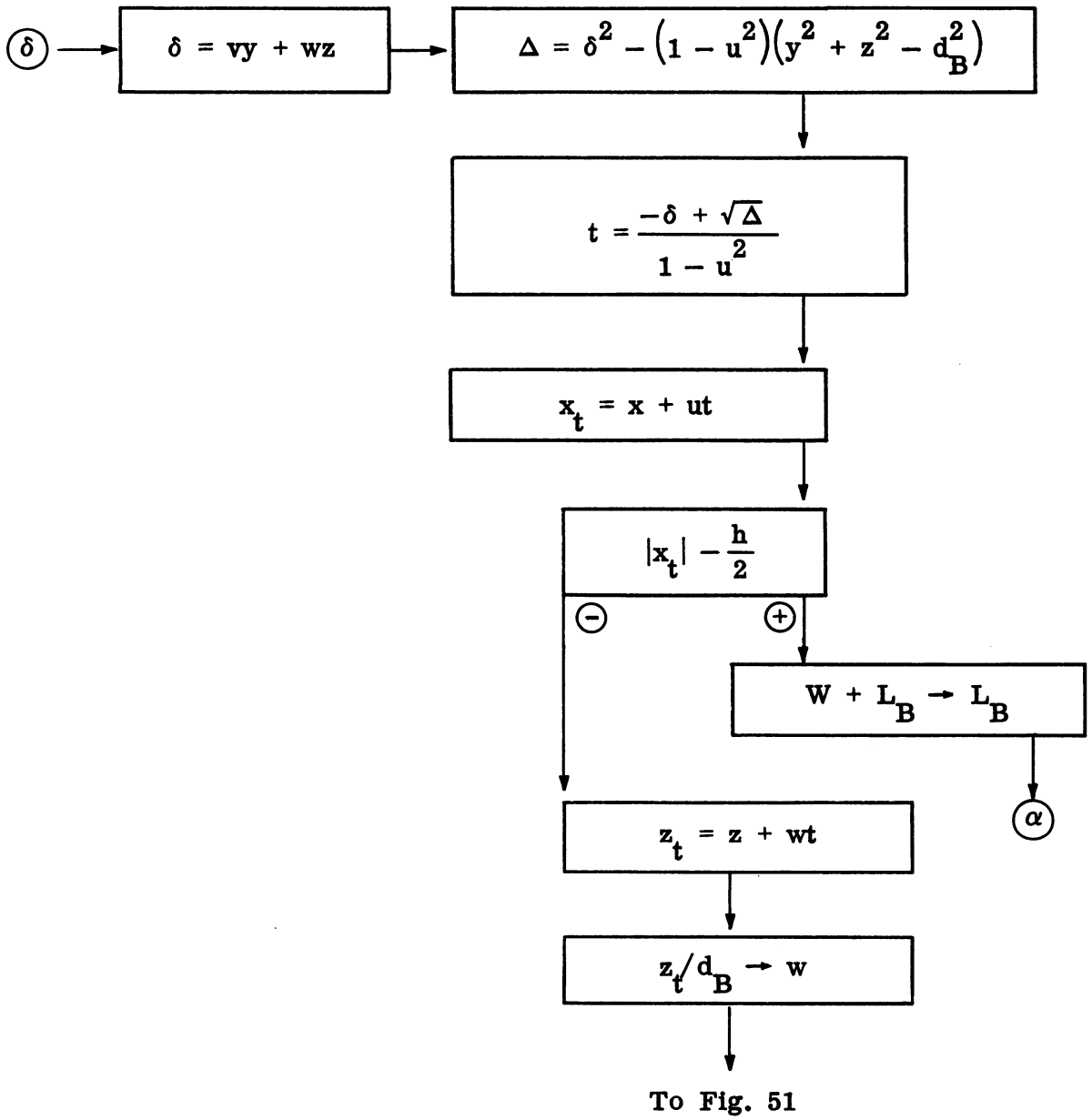

Fig. 56

last departure, then the direction of the normal at this point is given by

$$\frac{x_t - 0}{R}, \quad \frac{y_t - 0}{R}, \quad \frac{z_t - z_t}{R}$$

and the cosine w of the angle of escape with the normal is

$$w = \frac{x_t u + y_t v + z_t \cdot 0}{R} = (x_t u + y_t v)/R$$

CHAPTER IX

REMARKS ON COMPUTATION

1. Scaling. If the machine employed lacks the "floating decimal" feature or if considerations of machine speed exclude its use, all computations indicated in the flow diagram at each step must be planned in advance to remain on the interval $-1 < x < 1$. The formulas and flow diagrams of the present text are unscaled and are expressed in the usual physical units. The scaling procedure in Monte Carlo problems usually causes no difficulties, and may be left to the imagination, with the reminder that one must be careful to avoid the loss of accuracy which attends over-scaling. Remarks are made about scaling at various points in the present chapter as it enters into special subroutines, such as $\exp(-x/y)$ where x may exceed y, in the $\ell n\ x$ routine where x may be as small as 2^{-23}, and in the cosine routine for $-\pi \leqq x \leqq \pi$.

2. Debugging. When a problem is ready for actual running by the machine, some method of detecting the inevitable human errors which may enter at all phases of the coding must be employed to assure all

concerned that the machine will perform exactly the routine intended. It goes without saying that all permanent storage constants should be printed out at various intervals and checked against the original list, certainly at the beginning and end of the problem. Moreover, it is sometimes possible to build in a sum check of all code orders and permanent constants which will automatically detect any changes due to electronic misbehavior once the machine is running. We refer here rather to the question of ensuring that the code itself is correct. This question presents rather greater difficulties in Monte Carlo problems than in other types of computation because of the complexity of decisions involved.

We have found that the most convincing guarantee of faithfulness of code to flow diagram consists in the preparation by hand of a deterministic sequence of numbers $r_1, r_2, r_3, \ldots$ designed to process automatically a hand-picked set of particles which are so chosen that every logically possible path through the flow diagram is traversed at least once with non-trivial parameters. A special debug routine may be used for this purpose which instructs the machine to follow the code precisely except that, upon call for the next random number, the random number routine is by-passed, and the prepared list is consulted for the next number r_n of the hand-picked sequence. At every list consultation the machine prints out all significant variables of the problem, the printout then being compared with the hand-computed particle histories.

This is a laborious process in the hand-computing phase, but is well worth doing, even though, in complicated problems, the processing of 50 particles or so may be necessary.

3. Special subroutines. We include a number of special subroutines for some of the functions commonly occurring in Monte Carlo calculations. No claim is made that these are the best available; they are only given for completeness in case the reader knows of no better one.

a. A random number routine. We have used in all problems the sequence $r_1, r_2, r_3, \ldots$ of 38 bit diadic numbers, generated by the algorithm defining r_{n+1} to be that 38 bit number corresponding to the middle 38 bits of the square of r_n, where r_1 is the 38 bit number defined by 10 BBB FA4DE in the system with base 16, with the decimal after the first bit. Thus r_1 = 0.001, 0000, 1011, 1011, 1011, 1111, 1010, 0100, 1101, 111$\emptyset$, the final zero being ignored. The sequence automatically terminates in zero at about n = 750,000 and has been thoroughly tested, not only for the usual statistical features but by its actual use in many problems. The Monte Carlo use of the sequence is of a very peculiar and unpredictable kind. If one fixes attention on any particular random number box of the flow diagram, it appears that the numbers actually selected from the sequence for use in this box are a subsequence selected from the main sequence by completely inscrutable rules depending on the sequence itself. Whenever a probability of some terminal event (e.g., transmission) was known, the corresponding N_i/N

for that category agreed even better than one might expect it to on the basis of a truly random sequence.

b. Shifted random numbers. An average problem may involve 20,000 source particles, each with perhaps five collisions, and each collision may involve three or four random numbers. It is clear that one may expect to exhaust the random number sequence in many problems if it is used in this simple way. It is true that the same sequence may safely be used over again without repetition of results provided the initial r_1 is not used at the identical place it was first called in the flow diagram, and indeed, such re-use of the sequence may be resorted to.

We may mention however that the usual problems do not require anything like 38 bit resolution, and the number of random numbers available may be increased by a factor 2 or even 4 by a shifting routine, which is incidentally faster than squaring and so helps to reduce machine time. This consists in using in sequence not only r_n, but also the fractional parts of $2^{\alpha_1} r_n$, $2^{\alpha_2}(2^{\alpha_1} r_n)$, etc., as random numbers, before squaring r_n to obtain the next r_{n+1}. For example, if three random numbers are to be obtained from r_n, one might use the fractional parts of r_n, $2^{12} r_n$, and $2^{12}(2^{12} r_n)$. The sequences obtained by such extensions of the basic routine have also been tested and proved satisfactory.

c. A logarithm routine. From the usual series

$$\ell n(1 + x) = x - x^2/2 + x^3/3 - x^4/4 + \ldots \qquad |x| < 1$$

one obtains

$$\ell n(1 - x) = - x - x^2/2 - x^3/3 - x^4/4 - \ldots \qquad |x| < 1$$

and hence

$$\ell n \left(\frac{1-x}{1+x}\right) = - 2\left\{x + x^3/3 + x^5/5 + \ldots\right\} \qquad |x| < 1$$

which, under the transformation $y = \frac{1-x}{1+x}$ becomes

$$\ell n\, y = 2\left\{\left(\frac{y-1}{y+1}\right) + \frac{1}{3}\left(\frac{y-1}{y+1}\right)^3 + \frac{1}{5}\left(\frac{y-1}{y+1}\right)^5 + \ldots\right\} \qquad y > 0$$

Convergence of the latter series is rapid enough for the range $\frac{1}{2} < y < 1$ to permit use of a moderate number of terms; five should suffice for most purposes.

Now suppose ξ is a number on the range $2^{-23} \leqq \xi < 1$ for which $\ell n\ \xi$ is to be computed. We determine that integer n for which

$$2^{-23} \leqq 2^{-(n+1)} \leqq \xi < 2^{-n} \leqq 1$$

Then $2^{-1} \leqq 2^n \xi \equiv \eta < 1$ and $\ell n\ \xi = -n\ \ell n\ 2 + \ell n\ \eta$, where $\ell n\ \eta$ can be obtained from the series.

Now $-\ell n\ 2^{-23} = 23\ \ell n\ 2 < 23(.694) < 16$, so that $|2^{-4}\ \ell n\ \xi| < 1$ for ξ on the range $2^{-23} \leqq \xi < 1$. Hence a routine suitable for a scaled problem is given by Fig. 57.

Our only use for the ℓn function has been in collision-distance formulas such as

$$\ell = -\lambda\ \ell n\ r = -2^4\ \lambda\ (2^{-4}\ \ell n\ r)$$

Limitation of random numbers entering this formula to the range $r \geqq 2^{-23}$ means that we <u>force</u> a collision within 16 free paths. This is inaccurate to the extent that e^{-16} is the chance of collision at a still further distance, which is an acceptable error in most cases. In problems involving systems so large that such errors are significant, probably some type of importance sampling will be used in place of the simple formula above. In any case it is clear how to modify the routine for higher powers, 2^{-23} being quite arbitrary.

For the routine as given, it is clear that if all distances (cm) are scaled down by a factor exceeding 16 times the greatest free path λ occurring in the problem, one is safe so far as this particular formula is concerned.

Input ξ on $2^{-23} \leqq \xi < 1$
Stored constant $\alpha = 2^{-4} \ln 2$

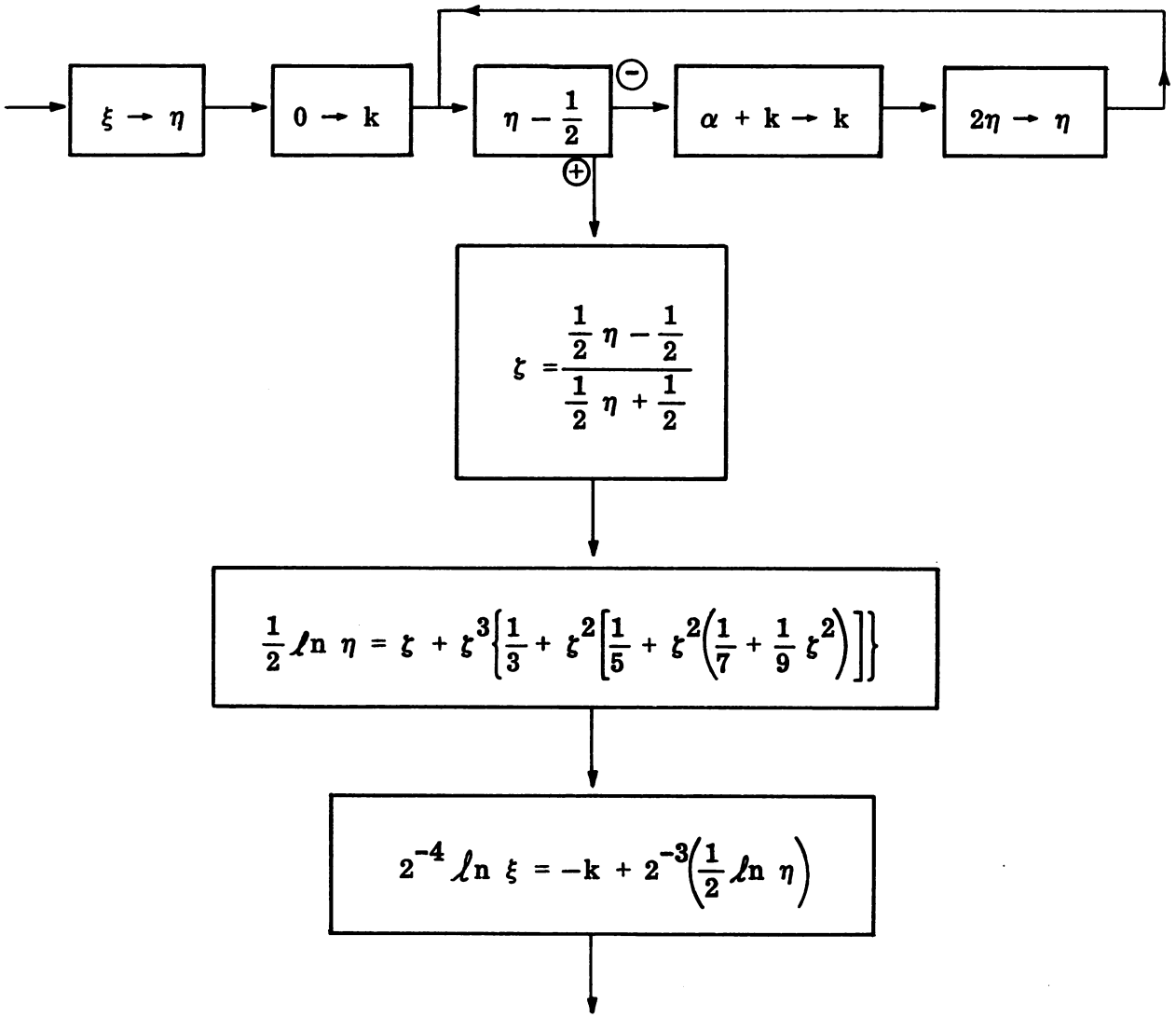

Fig. 57

d. The exponential $\exp(-x/y)$. It is frequently necessary to compute the value of $\exp(-x/y)$, where $0 \leqq x < 1$, $0 < y < 1$. Even though x and y are scaled, the quotient x/y may exceed unity and cannot be dealt with directly by fixed decimal point machines. There are excellent polynomial approximations[15] to $\exp(-\rho)$ for $0 < \rho \leqq \ell n\, 2$, so that we may define the integer n by

$$n\, \ell n\, 2 < x/y \leqq (n+1)\, \ell n\, 2$$

and ρ on the prescribed range by $\rho = (x/y) - n\, \ell n\, 2$. We shall therefore have

$$\exp(-x/y) = 2^{-n}\, e^{-\rho}$$

where $e^{-\rho} \cong a_o + \rho\,(a_1 + \rho\, a_2)$ with

$$a_o = 1$$

$$a_1 = -.9664279798$$

$$a_2 = .3535763634$$

is usually sufficiently accurate for our purposes.

---

[15] B. Carlson and M. Goldstein, "Rational Approximation of Functions," Los Alamos Scientific Laboratory, LA-1943, 1955. Gives polynomials of various degrees with bounds on the errors involved.

We may therefore proceed as in Fig. 58.

e. A cosine routine. We indicate a scaled routine for computing $\frac{1}{2}\cos\delta$, where δ is to be chosen uniformly on $-\pi \leqq \delta \leqq \pi$, as required by Ch. VII, § 3. It is based on the following series of formulas

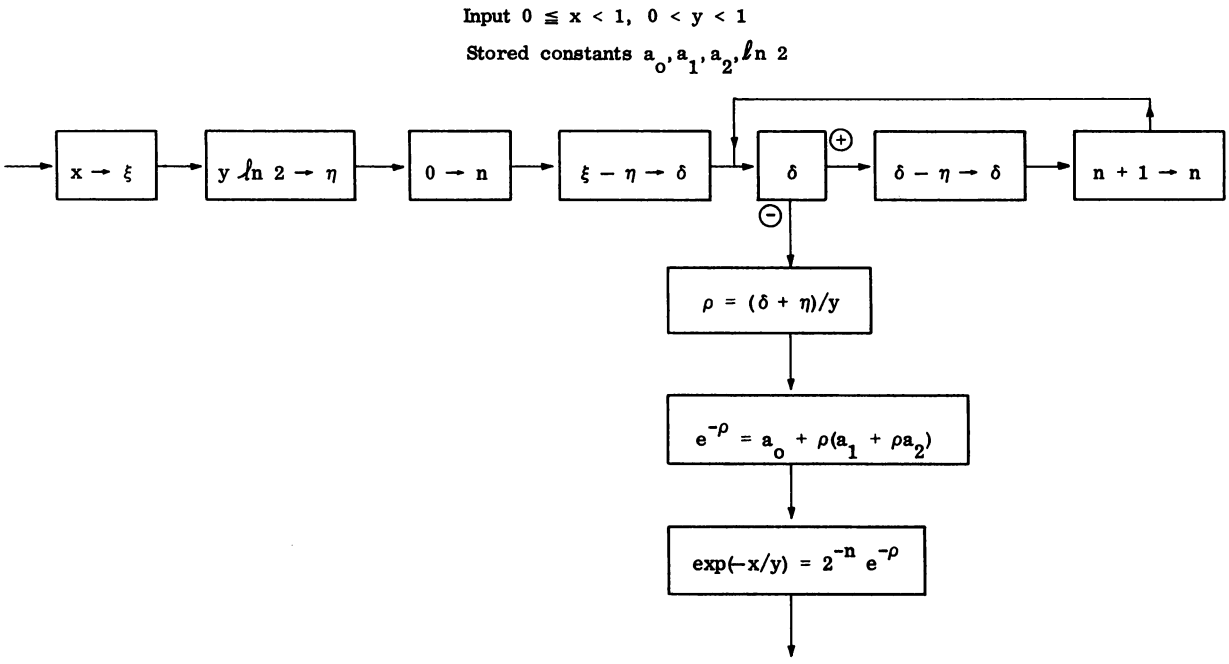

Fig. 58

$$\delta' = 2\left[\frac{\pi}{4}(r - \frac{1}{2})\right]$$

$$s = \sin \delta' = \delta' - \delta'^3\left\{\frac{1}{3!} - \delta'^2\left[\frac{1}{5!} - \delta'^2\left(\frac{1}{7!} - \frac{1}{9!}\,\delta'^2\right)\right]\right\}$$

$$\frac{1}{2}\cos \delta = 2^2\left\{2^{-3} - s^2 + s^4\right\}$$

the final formula arising from

$$\cos \delta = \cos 4\delta' = 2\cos^2 2\delta' - 1$$

$$= -1 + 2\left[1 - 2\sin^2 \delta'\right]^2$$

$$= 1 - 8s^2 + 8s^4$$

It may perhaps be mentioned here that for scaled machines the following procedure is somewhat shorter than that obtained by applying the preceding method to Fig. 49, the routine for slab and spherical final direction w'. In place of choosing δ uniformly on $0 \leqq \delta \leqq \pi$, we may introduce the angle $\tilde{\delta} = \delta - \pi/2$, choosing the latter uniformly on $-\pi/2 \leqq \tilde{\delta} \leqq \pi/2$. Thus we may proceed as follows:

$$\delta' = 2\left[\frac{\pi}{4}\left(r - \frac{1}{2}\right)\right]$$

$$s = \sin \delta' \text{ as above}$$

$$c = \cos \delta = \sin \tilde{\delta} = \sin 2\delta' = 2 \sin \delta' \cos \delta'$$

$$w' = aw - bc\sqrt{1 - w^2}$$

$$= aw - 2s\sqrt{(1 - a^2)(1 - s^2)(1 - w^2)}$$

We should therefore have in place of Fig. 49 the routine of Fig. 59. In this way we avoid the square root for $b = \sqrt{1 - a^2}$ and make use of only one double angle formula instead of two.

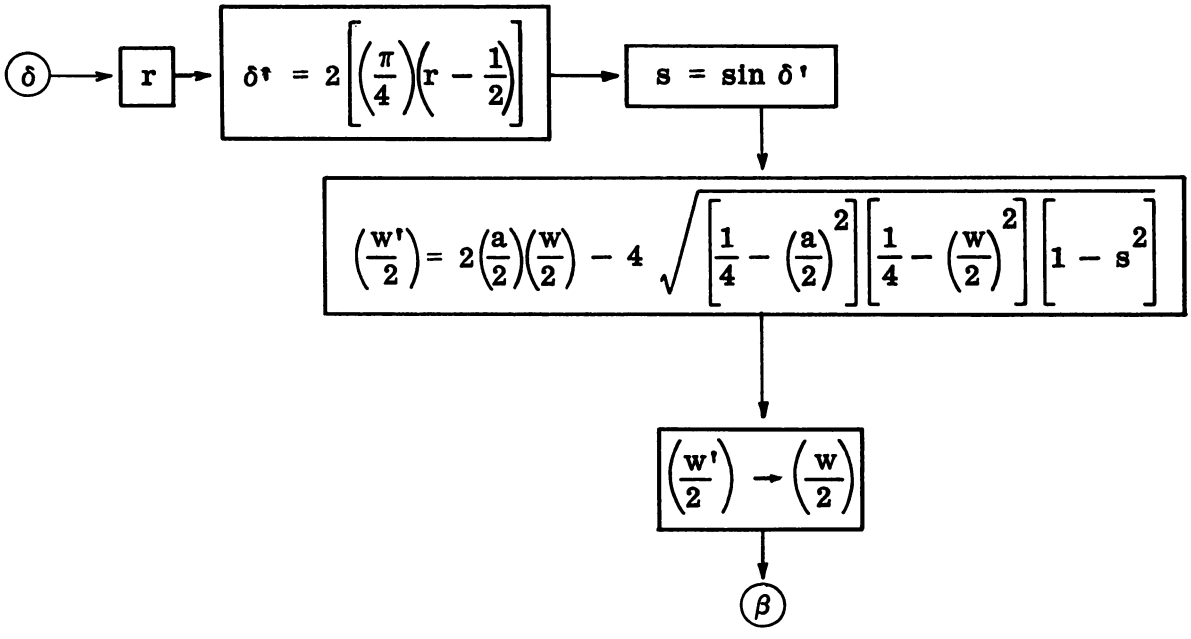

Fig. 59

4. A Monte Carlo device for $\sqrt{r}$. There are many ingenious devices for avoiding the computation of the value of various functions with arguments involving a random number. As a simple example,[16] the process

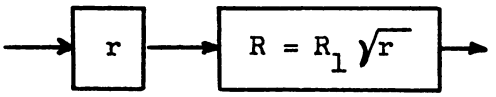

involved in throwing for the radius of a neutron in a source distributed uniformly in area on a disk of radius R_1 may be replaced by the following:

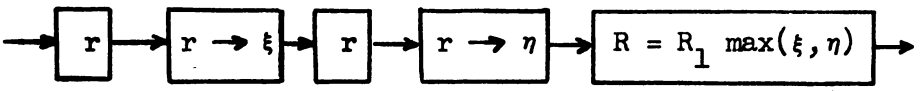

That is to say, one may use in place of the square root of one random number the larger of any two successive ones, for the equation $\xi = \sqrt{r}$ results from the standard Monte Carlo relation

$$r = \int_0^x 2\xi \, d\xi$$

and is thus equivalent to choosing ξ on the interval $(x, x + dx)$ with frequency $2x\,dx$. But the alternative of throwing points (ξ, η) into the unit square $0 \leq \xi \leq 1$, $0 \leq \eta \leq 1$ uniformly in area and choosing the larger of the coordinates automatically determines an $x \equiv \max(\xi, \eta)$

(16) Cf. J. W. Butler's paper in Symposium on Monte Carlo Methods, John Wiley & Sons, Inc., New York, 1956.

on $(\xi, \xi + d\xi)$ with this frequency, as is apparent from Fig. 59a.

5. A Monte Carlo device for the cosine of an equidistributed angle.[17] In various places we have needed the cosine and sine of an angle ϕ equidistributed on the interval $-\pi \leqq \phi \leqq \pi$, and have heretofore given a rather cumbersome but straightforward method involving series, square root, and, in case of fixed decimal requirements, a multiple angle formula. We give in Fig 59b an alternative method, easily scaled if necessary and avoiding series and square root routines.

One observes that the desired determination of $c = \cos\phi$ and $d = \sin\phi$ is equivalent to choosing a point (c,d) uniformly on the unit circle. This in turn is tantamount to throwing points (ξ,η) uniformly in the square $-1 \leqq x, y \leqq 1$, rejecting those lying outside the unit circle $x^2 + y^2 = 1$, and taking for c and d the values $\xi/\sqrt{\xi^2+\eta^2}$ and $\eta/\sqrt{\xi^2+\eta^2}$, for the retained points (ξ,η) are uniformly distributed in area in the unit circle and hence their projections (c,d) on the unit circle are uniformly distributed also. But these square roots may be avoided by limiting the selection procedure to the first quadrant and using double angle formulas to obtain (c,d) uniformly on the upper half-circle. Finally an additional random number can be used to change the sign of d with probability 1/2. The efficiency of the retention of random number pairs is $\pi/4$.

---

(17) The method is described by von Neumann in U. S. Department of Commerce, National Bureau of Standards, Applied Mathematics Series #12, Monte Carlo Method, Washington, D. C., 1951. Cf. footnote (1).

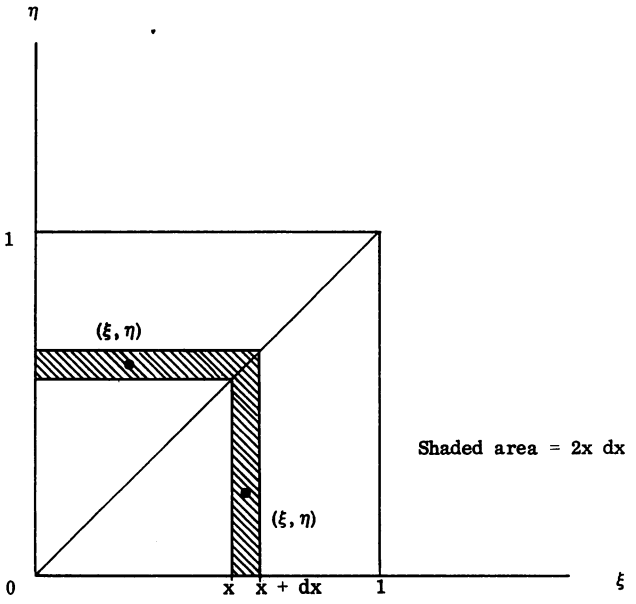

Fig. 59a

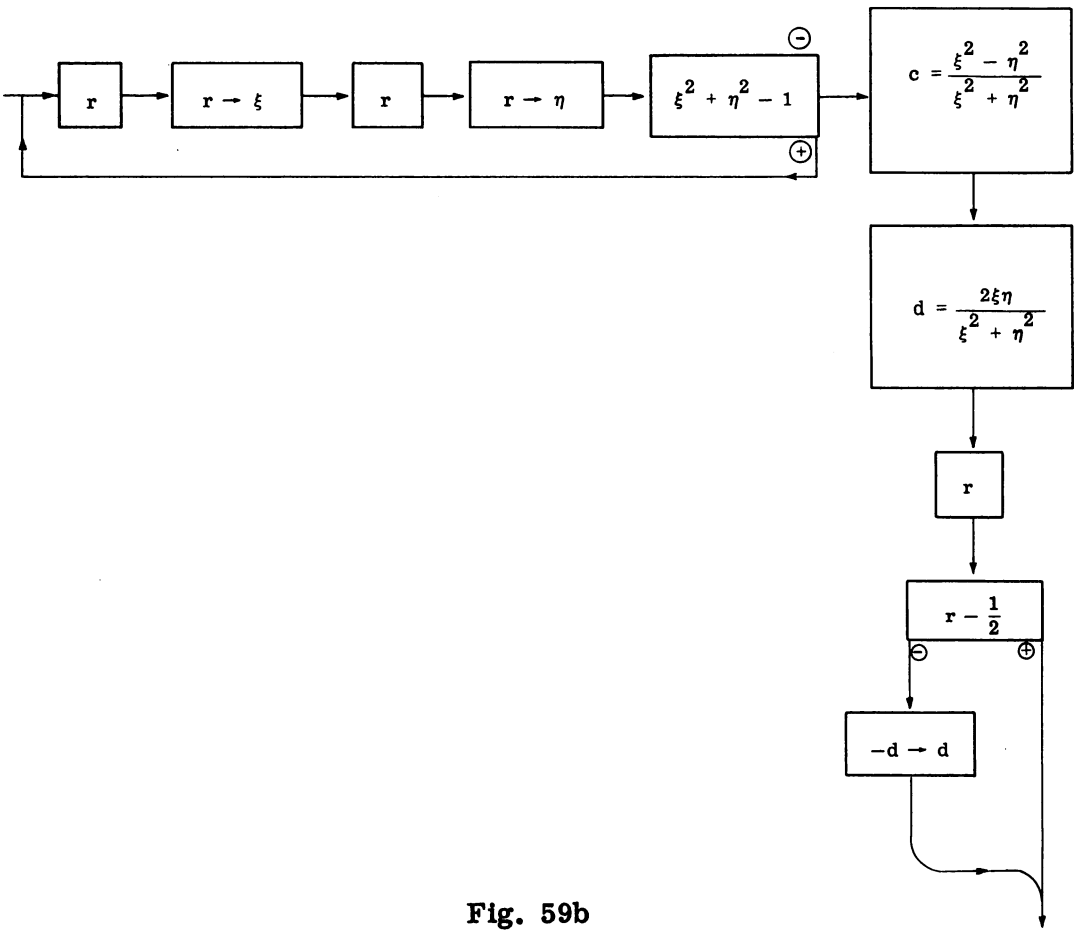

Fig. 59b

CHAPTER X

STATISTICAL CONSIDERATIONS

1. The limit theorem in the Bernoulli case. Suppose that a certain experiment can result in c ways of which a are favorable to an event E_1 while $b = c - a$ result in the event E_o (not E_1). Consider the set of all sequences of N trials of this experiment. In this set of c^N sequences, the number of sequences resulting in exactly M occurrences of E_1 is clearly

$$C_M^N a^M b^{N-M}$$

where C_M^N is the number of combinations of N things taken M at a time. Hence, the probability of exactly M occurrences of E_1 in a sequence of N trials is

$$P_M^N = C_M^N a^M b^{N-M}/c^N = C_M^N p^M q^{N-M}$$

where $p = a/c$ and $q = b/c$ are the probabilities of E_1 and E_o, respectively.

It is meaningful, therefore, to speak of the probability that, in a sequence of N trials of this experiment, the number M of "successes" E_1 shall lie between two given bounds; indeed,

$$P(\alpha < M < \beta) = \sum_{\alpha < M < \beta} P_M^N$$

There is a fundamental probability theorem[18] which states that

$$P\left(\left|\frac{M}{N} - p\right| \leq \epsilon\right) = \sqrt{\frac{2}{\pi}} \int_0^t e^{-u^2/2}\, du + R$$

where $t = \epsilon \sqrt{\frac{N}{pq}}$ and

$$|R| < \frac{e^{-t^2/2}}{\sqrt{2\pi Npq}} + \frac{.2 + .25\,|p - q|}{Npq} + e^{-(3/2)\sqrt{Npq}}$$

2. Application to the terminal ratios. The output of a non-multiplicative[19] Monte Carlo calculation without weights gives the

---

[18] J. V. Uspensky, Introduction to Mathematical Probability, McGraw-Hill Book Company, Inc., New York, 1937, p. 130.

[19] I.e., not involving fission, (n-2n) reactions, etc., in which a particle gives rise to more than one particle.

number M out of N source particles which terminate in each of a set of all-inclusive, mutually disjoint categories C. If we fix attention upon some particular category C, we may regard the processing of a source particle as an experiment which has as its outcome either the event E_1 of termination in this category or E_0 of non-termination therein.

Now in any actual problem, there is a definite upper bound ℓ on the number of random numbers needed to process a particle due to the existence of cutoffs based on energy, time, weight, number of collisions, etc. We may then consider the class of all γ sequences of ℓ random numbers. All these sequences are equally likely, and a certain $\underline{\alpha}$ of them determine a history terminating in category C. We may, therefore, say that the probability of termination in C is $p = \alpha/\gamma$.

To be sure, this probability p of E_1 is unknown; indeed, its determination is precisely the object of the problem. We may, however, gain some idea of the statistical reliability of the Monte Carlo result by tentatively taking for p the value of M/N at some late stage of the problem, when the latter ratio appears to have settled down, and define $q = 1 - (M/N)$. Then the preceding theory states that the ratio of the number of sequences of N trials resulting in a ratio of $\frac{M}{N}$ satisfying the inequality

$$\left|\frac{M}{N} - p\right| < \epsilon$$

to the totality of all possible sequences of N trials is approximately

$$f(t) = \mathrm{erf}(t/\sqrt{2})$$

where $t = \epsilon\sqrt{\frac{N}{pq}}$ and $\mathrm{erf}(x)$ is the well-tabulated "error function"

$$\mathrm{erf}(x) \equiv \frac{2}{\sqrt{\pi}} \int_0^x e^{-x^2}\, dx$$

for which we include a brief table.

x	erf x
0	0
.2	.2227
.4	.4284
.6	.6039
.8	.7421
1.0	.8427
1.2	.9103
1.4	.9523
1.6	.9763
1.8	.9891
2.0	.9953
2.2	.9981
2.4	.9993
2.6	.9998
2.8	.9999

Fig. 60

By assigning to ϵ the maximum error to be tolerated and to N the number of source particles processed, one finds from the value of the integral the approximate chance of an error not exceeding ϵ, which should be close enough to unity for comfort and which approaches unity with increasing N.

As an example, suppose a Monte Carlo run of 50,000 neutrons shows a capture of 5000 neutrons in a certain zone, and the probability p of capture in this zone is desired with 5% accuracy. Let $p = .1$, $\epsilon = .05p = .005$. Then $t = 3.72678$ and $f(t) = \text{erf}(t/\sqrt{2}) = \text{erf}(2.635) > .9998$. The error $|R|$ in using $f(t)$ for $P(|M/N - p| < \epsilon)$ does not exceed .0001.

This is, of course, far higher probability of safety than one can usually hope for. Consider for contrast the extreme case of a capture p of about .01 with a maximum error of 1%. Then $\epsilon = 10^{-4}$, and for $N = 50,000$, $t = .225$, and $f(t) = \text{erf}(t/\sqrt{2}) = \text{erf}(.175) \cong .18$, with $|R| < .018$. Here it appears that a simple-minded Monte Carlo is quite ineffective. To be sure, these requirements are far more stringent than are usually encountered, but such problems do arise, notably in counter design, and one sees clearly the necessity for very large samples combined with ingenious devices for improving statistics by use of weights in such cases.

3. The central limit theorem. The preceding remarks apply strictly only to Monte Carlo procedures of the most straightforward kind where no weights are employed, and a single, non-multiplying source particle is followed until it ends its history in some terminal category.

By assigning to ϵ the maximum error to be tolerated and to N the number of source particles processed, one finds from the value of the integral the approximate chance of an error not exceeding ϵ, which should be close enough to unity for comfort and which approaches unity with increasing N.

As an example, suppose a Monte Carlo run of 50,000 neutrons shows a capture of 5000 neutrons in a certain zone, and the probability p of capture in this zone is desired with 5% accuracy. Let $p = .1$, $\epsilon = .05p = .005$. Then $t = 3.72678$ and $f(t) = \text{erf}(t/\sqrt{2}) = \text{erf}(2.635) > .9998$. The error $|R|$ in using $f(t)$ for $P(|M/N - p| < \epsilon)$ does not exceed .0001.

This is, of course, far higher probability of safety than one can usually hope for. Consider for contrast the extreme case of a capture p of about .01 with a maximum error of 1%. Then $\epsilon = 10^{-4}$, and for $N = 50,000$, $t = .225$, and $f(t) = \text{erf}(t/\sqrt{2}) = \text{erf}(.175) \cong .18$, with $|R| < .018$. Here it appears that a simple-minded Monte Carlo is quite ineffective. To be sure, these requirements are far more stringent than are usually encountered, but such problems do arise, notably in counter design, and one sees clearly the necessity for very large samples combined with ingenious devices for improving statistics by use of weights in such cases.

3. The central limit theorem. The preceding remarks apply strictly only to Monte Carlo procedures of the most straightforward kind where no weights are employed, and a single, non-multiplying source particle is followed until it ends its history in some terminal category.

It may then be considered as a physical particle undergoing an experiment insofar as the random numbers employed may be regarded as truly random.

However, we have mentioned many devices employing weighted particles. In such cases, it is clear that the total weight M terminating in a given category C after such procedures no longer represents the number of successes out of N trials, that is, out of the processing of N source particles, each initially of weight 1, and we can no longer apply the theorem of §1. There is, however, a well-known generalization called the central limit theorem, of which we shall give here a very special case,[20] which does apply to the weight method.

Instead of the simple experiment which results in 1 with probability p and in 0 with probability q, let us consider an experiment which can result in K different ways, to which we assign definite real numbers $W_1, \ldots, W_K$, with probabilities $p_1, \ldots, p_K$, respectively, $p_1 + \ldots + p_K$ being unity. In a single trial of the experiment, therefore, we may say that W_k has probability p_k, $k = 1, \ldots, K$. In such a case, we define the mean $a = \Sigma\, p_k W_k$ and the dispersion $b = \Sigma\, p_k (W_k - a)^2 = \Sigma\, p_k W_k^2 - a^2$. Suppose now that N trials are made of this experiment, and M is the sum of N weights so determined. Then our theorem states that the probability

$$P\left(\left|\frac{M}{N} - a\right| < \epsilon\right) = \operatorname{erf}(t/\sqrt{2}) + \rho_N$$

---

[20] J. V. Uspensky (1c), page 294; cf. footnote (18).

where $t = \epsilon\sqrt{\frac{N}{b}}$ and $\rho_N \to 0$ as $N \to \infty$. The estimation of ρ_N is given in terms of the third moment of the W-distribution.

Notice that the Bernoulli case is contained in this, since for that case, we have $p_1 = p$, $W_1 = 1$; $p_2 = q$, $W_2 = 0$, $a = p \cdot 1 + q \cdot 0 = p$, $b = (p \cdot 1^2 + q \cdot 0^2) - a^2 = p - p^2 = p(1 - p) = pq$, and the sum M of the weights 1 and 0 recorded in the N trials is simply the number of 1's (successes) in this sequence.

4. Application to problems using weights. Consider now a perfectly general Monte Carlo problem(21) in which weighted particles may be used, each particle leaving the source with weight 1. For simplicity, we consider the weights limited to a finite set of numbers, which is, in fact, the case in machine computation. Each possible history assigns a definite weight W_k to the particular terminal category C. Moreover, it is clear that each such weight W_k has a definite probability p_k of realization upon the trial of a random source particle, namely, the probability of a history which assigns W_k to C. Thus the mean $a = \Sigma\, p_k W_k$ is the expected weight terminating in C per source particle. If we process N particles in a Monte Carlo problem, tallying the weight $W^{(\tau)}$ contributed to category C by each trial particle $\tau = 1, 2, \ldots, N$, the final sum $\Sigma W^{(\tau)}$ is the M of the theorem, and M/N may be used as an approximation to a. The difficulty in applying

(21) Multiplicative processes are not excluded. When they are involved, we speak of the "expectation" a of termination in category C rather than the probability whether weights different from unity are used or not.

the theorem lies in the fact that we do not ordinarily have at hand an estimate for the dispersion b. In the simple Bernoulli case, we saw that b was expressible in terms of p, but, in general, a does not determine b. Since $b = \Sigma p_k W_k^2 - a^2$, we could use $\sum_{\tau=1}^{N} (W^\tau)^2/N - (M/N)^2$ as a guess for b if we had provided in the problem for tallying the $(W^\tau)^2$ as well as the (W^τ) for each trial particle $\tau = 1, \ldots, N$.

Note that in case of capture, one squares the <u>total</u> of capture contributions from all collisions of the particle; it is not correct to simply cumulate the squares of each weight captured.

In a problem which does not involve multiplication (fission, (n-2n) reactions, etc.), the weight procedure is better than that not employing weights, at a given stage N, and for a given error ϵ, to the extent that the upper limit of integration $\epsilon\sqrt{\frac{N}{b}}$ exceeds $\epsilon\sqrt{\frac{N}{pq}}$, the probability in the left member being identical, that is, the gain is based on the degree to which b is less than pq. Now $b = \Sigma p_k W_k^2 - a^2$, $pq = p - p^2$, and the expectation of category C in such a problem is its probability, i.e., $a = p$. Hence, finally the improvement rests on the fact that

$$\Sigma p_k W_k^2 \leqq p = a = \Sigma p_k W_k$$

which is clear since $W_k \leqq 1$ for all k. However, the degree of improvement can be calculated only in the most trivial examples. It is at least clear why the improvement is so great in cases of small quantities, since, then, the W_k are quite small and $W_k^2 << W_k$.

It may also be remarked that the theorem of section (3) applies perfectly well in finding the expected number a (per source particle) of particles terminating in a particular category C, while the theorem of § 1 does not. The unfortunate feature involved in the application of the former theorem is that one has no simple way of knowing the dispersion b. Problems of the complexity in practice usually forbid complete tabulations of W^2's for purely statistical studies. Actually one provides the best weight tricks one can think of and tries to judge the reliability of an output ratio by its convergence and stability as N increases.

5. Illustrative examples. We include some extremely trivial examples which nevertheless may help to fix the ideas involved in the preceding sections.

(1) Consider the non-multiplicative problem defined by the following flow diagram:

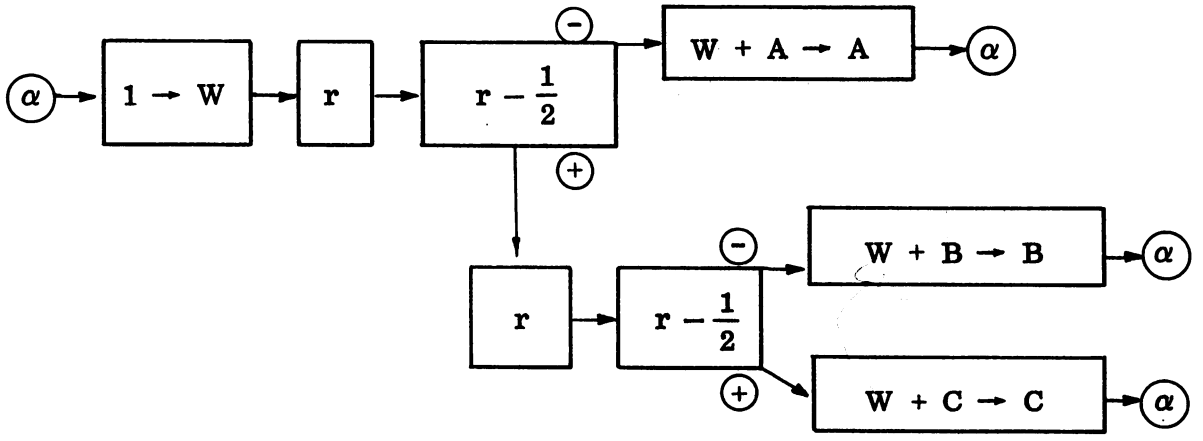

We may limit random numbers to be either 0 or 1. The upper bound ℓ on lengths of sequences of random numbers required is 2, and the total number γ of such sequences is $2^2 = 4$. In fact, we have the following results:

00 implies termination in A

01 implies termination in A

10 implies termination in B

11 implies termination in C

If we fix attention on C, we find that the number α of sequences favorable to C is 1, and the probability of termination in C is $\alpha/\gamma = 1/4$. Hence, relative to this category, we have $p = 1/4$ for $W = 1$ and $q = 3/4$ for $W = 0$, with dispersion $pq = 3/16$.

Suppose for comparison that we decide to use a weight method for this problem as indicated below.

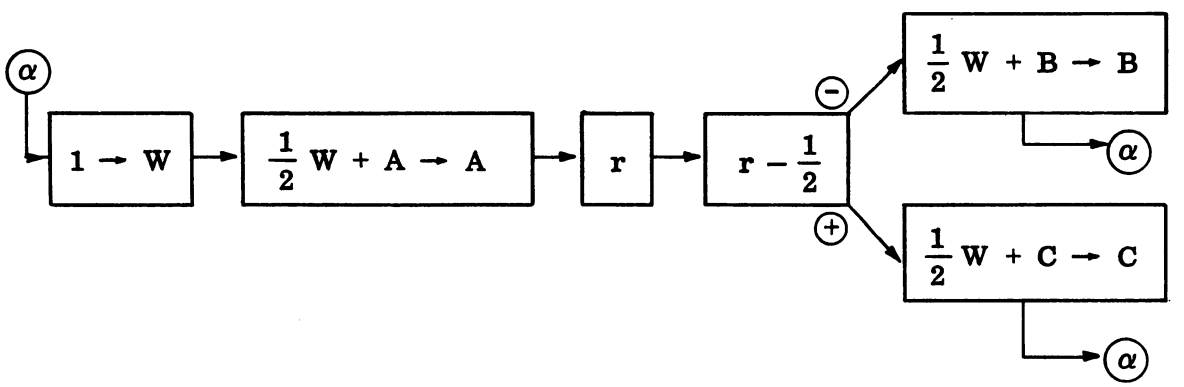

Now sequences of random numbers are limited to length $\gamma = 1$, and we have the results

$$0 \quad \text{implies} \quad A = 1/2 \quad B = 1/2$$

$$1 \quad \text{implies} \quad A = 1/2 \quad C = 1/2$$

Again fixing attention on C,

$$p_1 = 1/2 \quad \text{for} \quad W_1 = 0$$

$$p_2 = 1/2 \quad \text{for} \quad W_2 = 1/2$$

and

$$a = p_1 W_1 + p_2 W_2 = 1/4$$

$$b = p_1 W_1^2 + p_2 W_2^2 - a^2 = 1/16 < pq = 3/16$$

which illustrates in this very trivial example the type of improvement discussed in the preceding section.

(2) Now suppose we have the simple multiplicative system indicated by the following scheme:

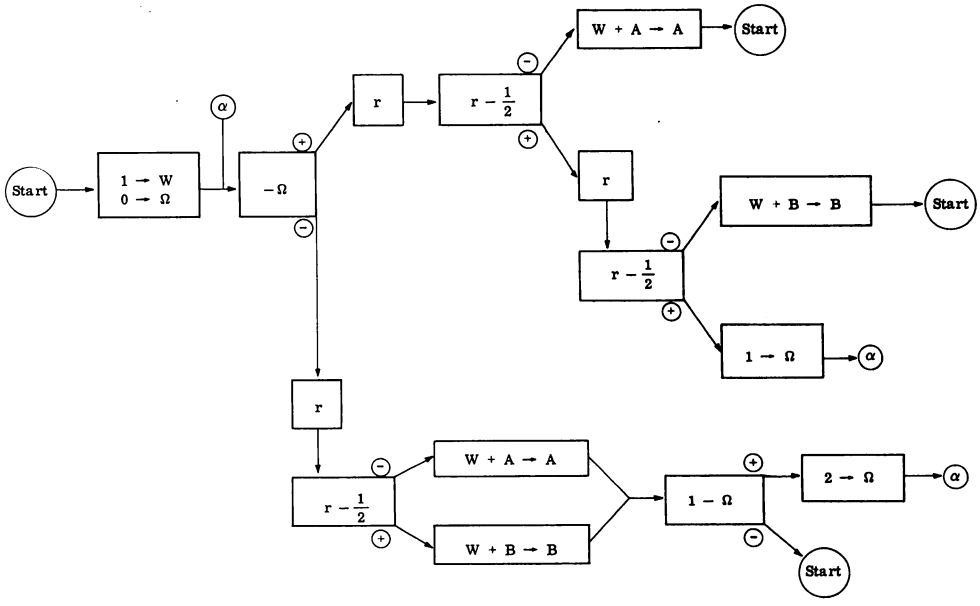

Thus a source particle may terminate in A with probability 1/2 or, in the contrary case, it may either terminate in B with probability 1/2 or produce two particles with probability 1/2. The two progeny thereupon have equal chances of terminating in A or B.

Here the maximum length ℓ of random number sequences of 0's and 1's is 4, $\gamma = 2^4 = 16$, and we have the following correspondence between random number sequences and terminal weights:

0000	A = 1	B = 0
0001	A = 1	B = 0
0010	A = 1	B = 0
0011	A = 1	B = 0
0100	A = 1	B = 0
0101	A = 1	B = 0
0110	A = 1	B = 0
0111	A = 1	B = 0
1000	A = 0	B = 1
1001	A = 0	B = 1
1010	A = 0	B = 1
1011	A = 0	B = 1
1100	A = 2	B = 0
1101	A = 1	B = 1
1110	A = 1	B = 1
1111	A = 0	B = 2

Let us consider only category B. We have by inspection the weights and corresponding probabilities

$$p_o = 9/16 \qquad W_o = 0$$

$$p_1 = 6/16 \qquad W_1 = 1$$

$$p_2 = 1/16 \qquad W_2 = 2.$$

The expectation and dispersion are

$$a = \Sigma\, p_k\, W_k = 1/2$$

$$b = \Sigma\, p_k\, W_k^2 - a^2 = 3/8$$

Let us compare this procedure with one which, in the event of multiplication, processes one particle of weight 2 rather than two particles each of unit weight, as indicated below.

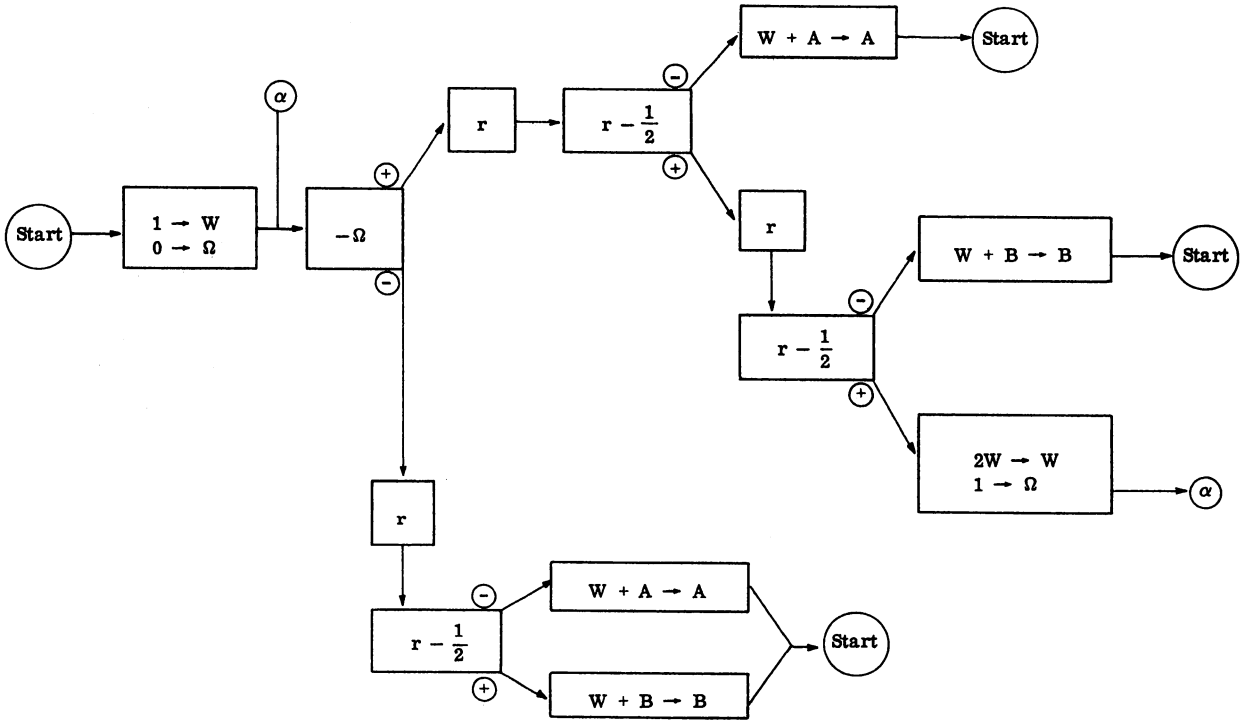

We now obtain the results

000	A = 1	B = 0
001	A = 1	B = 0
010	A = 1	B = 0
011	A = 1	B = 0
100	A = 0	B = 1
101	A = 0	B = 1
110	A = 2	B = 0
111	A = 0	B = 2

and for category B,

$$p_o = 5/8 \qquad W_o = 0$$

$$p_1 = 2/8 \qquad W_1 = 1$$

$$p_2 = 1/8 \qquad W_2 = 2$$

$$a = \Sigma\, p_i\, W_i = 1/2$$

$$b = \Sigma\, p_k\, W_k^2 - a^2 = 1/2$$

It will be noted that the revision has resulted in <u>increasing</u> the dispersion. That this is not an inevitable consequence of employing weighted multiplication, the reader may verify by observing that the dispersion for category B becomes 0 in the following treatment of the same problem:

APPENDIX

SUMMARY OF CERTAIN PROBLEMS RUN ON MANIAC I

Introduction. We conclude this report with a very brief summary of some of the Monte Carlo type problems which we have set up and run on the MANIAC I at Los Alamos during the past three years. The coding for these problems has been done by some extremely rapid and resourceful coders at Group T-7 of this laboratory, whom we wish to thank collectively, and to whom we refer individually in this appendix and LA-2121.

It is hoped that the reader unfamiliar with the method will find in this brief list of problems some indication of the actual situations in which the methods of the text find application. It may also perhaps help those contemplating use of the method in problems of their own to form some judgment of its possibilities.

The collection included here naturally omits the many classified problems which have been completed.

Problem 1

COMPTON COLLISIONS IN A SPHERICAL SHELL

Coder: R. G. Schrandt

Requester: G. H. Best and H. C. Hoyt

Medium: Free-electron "gas" in spherical shell of radii $R_o < R_1$.

Source: Monoenergetic photons directed radially outward from R_o. Various initial energies were studied.

Photon parameters: x, y, z, u, v, w, E, g.

Physical processes: Compton collisions of photons with free electrons.

Output: Correlated energy and angle distribution of photons escaping R_1, together with totals lost to core and lost to energy cutoff. Any photon impinging on the inner boundary R_o was considered absorbed.

Remarks: "Forced first collision" device was used. The angular distribution desired was that of Ch. VIII, Fig. 53.

Problem 2

COMPTON COLLISIONS IN A SOLID SPHERE

Coder: R. G. Schrandt

Requester: G. H. Best and H. C. Hoyt

Medium: Free electron gas in solid sphere of radius R_1.

Source, photon parameters, and physical processes: As in Problem 1.

Output: As in Problem 1 with exception of core losses.

Remarks: It was desired to study the effect of the core on the escape distribution by comparison of the results of Problems 1 and 2. Actually, by suitable devices in the flow diagram, it was possible to combine the two problems into a single code, keeping two sets of terminal category registers and following a photon path further for purposes of Problem 2, after it had hit the core and been lost for Problem 1. This is a device which cuts machine time almost in half.

Problem 3

NEUTRONS IN A SPHERICAL SHELL

Coder: J. M. Kister

Requester: J. R. Beyster

Medium: Hollow spherical shell of heavy nuclei.

Source: Monoenergetic isotropic point source at center of sphere.

Neutron parameters: R, w, ν.

Physical processes: Inelastic scattering, regarded as terminal, elastic scattering according to given lab. system differential cross section, attended by no energy loss.

Output: Number of neutrons lost to inelastic collision, number of neutrons escaping after ν collisions, $\nu = 0, 1, \ldots, 10$, and $\nu \geq 11$.

Remarks: The distribution function P_j was tabulated for scattering at a cosine $a \geq a_j$ for 32 strategically chosen intervals of the cosine range. The problem was run as a check on an analytic method of H. A. Bethe based on transport cross sections, the results of the latter being computed by J. R. Beyster. The Monte Carlo procedure was coded in two different ways, one using the weight method for inelastic termination, the other not. The results were in excellent agreement and checked Bethe's result. Transmission was obtained without forced first collision and agreed closely with the analytic value. The problem is written up in LA-1583, A Monte Carlo Determination of the Escape Fraction for a Scattering Spherical Shell with Central Point Source.

Problem 4

ENERGY INDEPENDENT SCATTERING IN A CYLINDER

Coder: R. L. Bivins

Requester: M. Walt

Medium: Solid cylinder of homogeneous material. Problem run for many heavy elements.

Source: Monoenergetic neutrons in parallel beam incident on lateral surface of cylinder in direction normal to axis.

Neutron parameters: x, y, z, u, v, w, W, ν.

Physical processes: Inelastic collision, treated as terminal, elastic scattering at source energy governed by differential cross section. No energy loss assumed on elastic scattering.

Output: Transmission, loss to inelastic collision, number of emergent scattered neutrons not hitting detector band, classification of neutrons hitting band zone i with $\nu = 1, 2, 3$, and $\nu \geq 4$ collisions. Detector band was coaxial with cylinder and calibrated in 5° zones. Geometry was that of Fig. 55.

Remarks: Weights were used for transmission and inelastic losses. Elastic scattering probabilities P_j were used as indicated in Problem 3. It will be noted that many of the problems included are of this general nature, the Monte Carlo results being used in correcting experimentally determined differential cross sections and cross sections of other processes for multiple collision effects in thick targets.

Problem 5

ENERGY DEPENDENT SCATTERING IN A CYLINDER

Coder: R. L. Bivins

Requester: M. Walt

Medium: Solid cylinder of homogeneous material. Many light elements were run.

Source: Same as Problem 4.

Neutron parameters: x, y, z, u, v, w, E, g, W, ν.

Physical processes: Inelastic collision regarded as terminal, elastic scattering governed by differential cross sections $\sigma_g(\mu)$ in C.M. system.

Output: Transmission, loss to inelastic collision, loss to energy cutoff, emergent neutrons failing to hit detector band (same geometry as in Problem 4 and Fig. 55), and those hitting band in zone i with $\nu \geq 1$, 2, and $\nu \geq 3$ collisions.

Remarks: Weights used for transmission (forced first collision device) and for inelastic losses. Differential elastic scattering handled by the von Neumann device using $\sigma^*(g,\mu) = A_g + B_g \mu + C_g \mu^2$ as indicated in Ch. V, §5. Tables stored for free path λ_g and for coefficients A_g, B_g, C_g for suitable energy groups g.

Problem 6

CYLINDRICAL SHELL WITH PARALLEL SOURCE

Coder: R. G. Schrandt

Requester: J. D. Seagrave

Medium: Cylindrical shell of homogeneous material. Problems run for CD_2, C, and CH_2 shells.

Source: Monoenergetic parallel beam of neutrons incident on lateral surface of cylinder in direction normal to axis. Various source energies were studied.

Neutron parameters: x, y, z, u, v, w, E, g, W, ν.

Physical processes: Elastic scattering on C, D, H according to C.M. differential cross sections $\sigma_g^e(\mu)$. Such scattering on H was assumed isotropic; C scattering was treated by a fit $\sigma^*(g,\mu) = A_g + C_g \mu^2$; while for D, the double interpolation method of Ch. V, §5 (Fig. 37) was used on the basis of a stored table $\sigma^*_{m,n}$.

Output: Transmission, loss of "degraded" neutrons to energy cutoff, emergent undegraded scattered neutrons failing to hit band, and classification of scattered undegraded neutrons hitting the band (geometry of Fig. 55) into the following categories:

(a) hits on band zone i with energy above given upper bound $\bar{\epsilon}_i$

(b) hits on band zone i with energy below given lower bound ϵ_i

(c) hits on band zone i with energy between ϵ_i and $\bar{\epsilon}_i$ with $\nu = 1$

(d) hits on band zone i with energy between ϵ_i and $\bar{\epsilon}_i$ with $\nu > 1$.

Problem 7

14 MEV NEUTRONS IN A CYLINDRICAL SHELL

Coder: R. G. Schrandt

Requester: L. Rosen and L. Stewart

Medium: Solid cylinder of homogeneous scattering material. Problems run for two heavy elements (Bi, Ta).

Source: Parallel beam of monoenergetic (14 Mev) neutrons incident on base of cylinder. Geometry of Fig. 52.

Neutron parameters: x, y, z, u, v, w, ν, E, f (group index for elastic scattering differential cross section purposes), g (group index for free path and probability of elastic scattering constants), h (group index for escape classification).

Physical processes: At most, two collisions were permitted, escape being forced after a second collision, with the direction obtaining as a result of that collision. The branching process of Fig. 61 was involved. The assumptions made for the types of collisions were as follows:

(a) Elastic collision: no energy loss, lab. differential cross sections $\sigma_f(a)$ for five energy ranges f.

(b) d-process. Energy of emergent neutron equidistributed between 5 and 12 Mev. Process occurs only at 14 Mev. One differential cross section given for lab. angle a.

(c) (n-2n) process. Two neutrons emerge with energy distributions $n_1 = E' \exp(- E'/T_1)$ and $n_2 = E' \exp(- E'/T_2)$ on $0 \leqq E' \leqq 5$. Isotropic emergence in lab. system. Process occurs only at 14 Mev. (Cf. Ch. V, §15, for method.)

(d) Inelastic collision. One neutron emerges, isotropically in lab. system, with energy distribution $n = E' \exp(-E/T)$ where $T = k\sqrt{(E/14)}$. Process occurs only below 12 Mev. (Cf. Ch. V, §11, for method.)

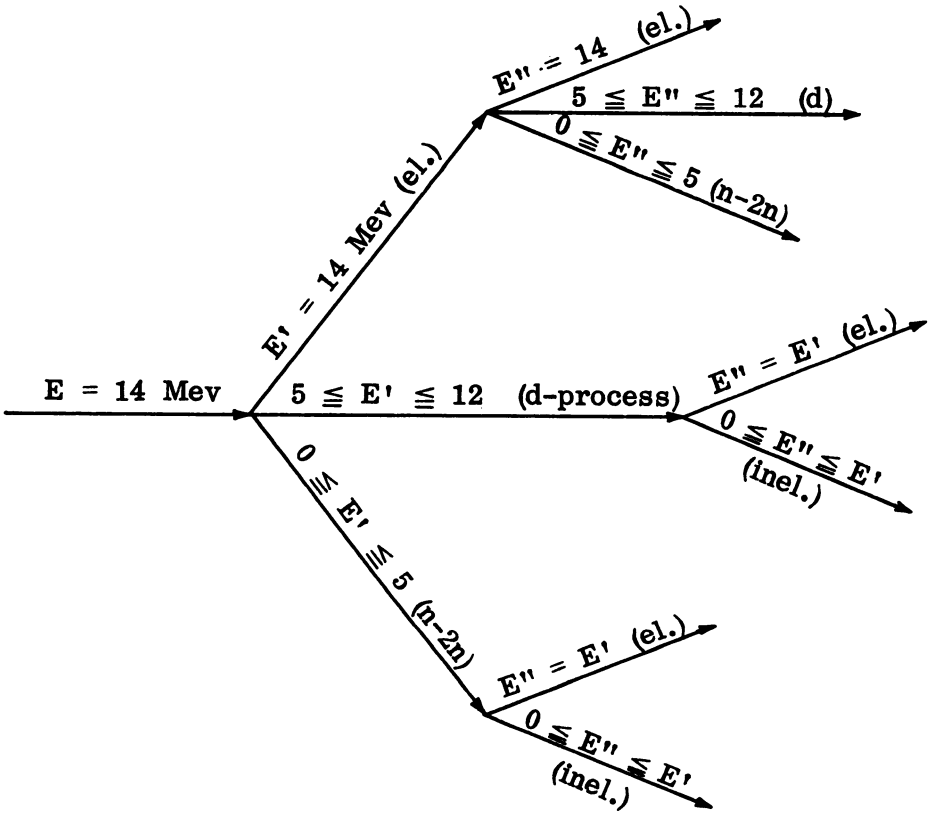

Fig. 61

Output: Energy and angle distribution of escape.

Remarks: Symmetry of system about source distribution obtains, and counter was at infinite distance so that the optimum conditions of Fig. 52 obtained. (Cf. discussion of Ch. VIII, §3.)

Problem 8

CYLINDRICAL SHELL WITH POINT SOURCE

Coder: R. L. Bivins

Requester: L. Cranberg

Medium: Cylindrical shell of homogeneous material. Various heavy elements run.

Source: Monoenergetic point source incident on lateral surface of cylinder from an external point midway between base planes. (Cf. Ch. II, §5d, and Fig. 11.)

Neutron parameters: x, y, z, u, v, w, E (three discrete values E_1, E_2, E_3).

Physical processes: A typical element (Bi) had two excited state energy levels at $\Delta_1 = .9$ and $\Delta_2 = 1.65$ Mev above the normal state. A neutron with energy E colliding with the nucleus can thus scatter elastically, with no energy loss, or inelastically, emerging with energy $E - \Delta_1$ if $E \geq \Delta_1$ or with energy $E - \Delta_2$ if $E \geq \Delta_2$. Since the source energy was 2.5 Mev, the histories of Fig. 62 were possible. Inelastic scattering was assumed isotropic in the lab. system, while elastic scattering was assumed to obey a given differential cross section $\sigma(a)$ applicable at all energies involved.

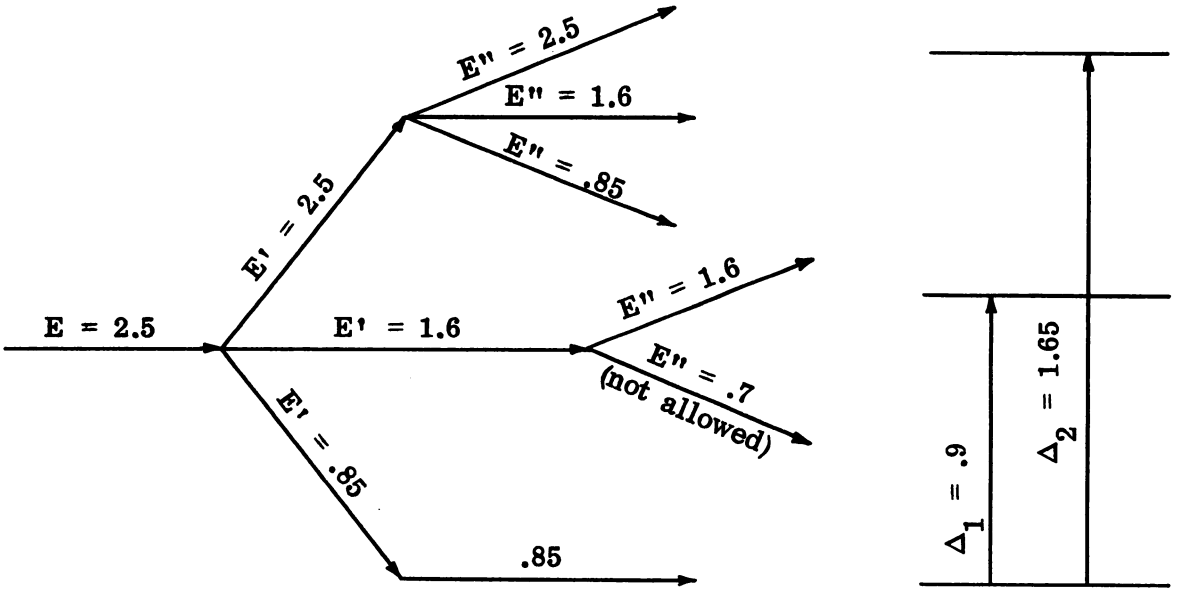

Fig. 62

Output: At most, two collisions were allowed. Neutrons having a third collision were classified in a terminal category L_3. At most, one inelastic collision was permitted. Neutrons suffering a second inelastic collision were classified in a terminal category I_2. Thus all escaping neutrons emerge with one of three possible energies E_1, E_2, E_3. Of these, the neutrons hitting the detector band (geometry of Fig. 55) in angular zone i and energy E were tabulated as $N_i(E)$ for each E.

Also recorded were the transmission, escapes not hitting the band, total hitting band after one elastic collision, and the total hitting the band after one collision of any kind.

Problem 9

A SCINTILLATION COUNTER

Coder: R. L. Bivins

Requester: R. F. Taschek and N. J. Terrell

Medium: Cylindrical shell containing various compounds of H, C, O, and Cd.

Source: Monoenergetic point source at center of cylindrical hole (vacuum) with various deterministic directions.

Neutron parameters: x, y, z, u, v, w, E, g.

Physical processes: H-capture, Cd-capture, elastic scattering isotropic in C.M. system for H, O, Cd, and according to a differential cross section $\sigma_g(\mu) = A_g + C_g \mu^2$ for C.

Output: Loss from shell surface, H-capture, Cd-capture, and losses to energy cutoff classified according to 6 radial and 12 height zones.

Remarks: The purpose of the problem was the determination of the space distribution of degraded neutrons referred to, for use as input in a subsequent age theory calculation (not performed by us) connected with sensitivity of a scintillation counter design.

Problem 10

A "LONG COUNTER"

Coder: R. L. Bivins

Requester: A. W. Schardt

Medium: Cd cylinder (medium m = 1, parts p = 1, 2, 4 of Fig. 63) containing B (gaseous boron compound under pressure) and vacuum space, and surrounded by a hydrocarbon (medium m = 2, parts p = 3,5) in cylindrical outer container as shown.

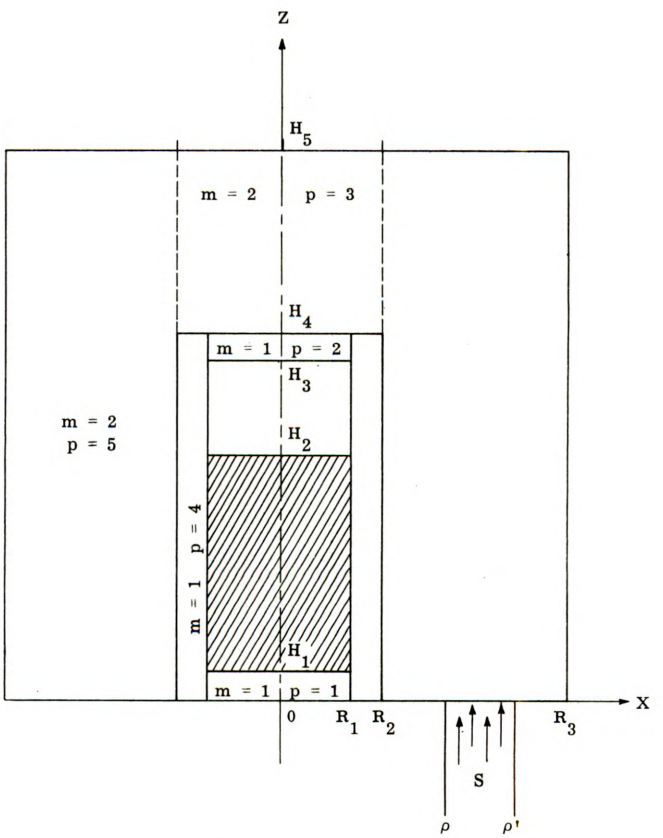

Fig. 63

Source: Monoenergetic neutrons in parallel beam impinging on various radial zones (ρ, ρ') of base of outer container. Various source energies studied.

Neutron parameters: x, y, z, u, v, w, E, g, W, m, p.

Physical processes: H-capture, Cd-capture, B-capture, elastic scattering on H, Cd isotropic in C.M. system, C as in Problem 9.

Output: Escape from Cd-base (p = 1, p = 4), escape from hydrocarbon surface (p = 3, 5), H-capture, Cd-capture, B-capture, losses to energy and weight cutoff.

Remarks: The purpose was to estimate the efficiency of B-capture as a function of source energy and distance from axis in connection with design of a long counter. Weights were used throughout, neutrons passing through B cylinder were attenuated exponentially, and the multiplication device of Ch. V, §16, was used. This problem probably represents the most demanding one statistically that we have set up. Enormous samples were involved, and the actual running of the machine was done by Schardt and co-workers.

Problem 11

A PROBLEM CONNECTED WITH NEUTRINO DETECTION

Coder: R. L. Bivins

Requester: F. Reines and C. L. Cowan

Medium: Plane slab of homogeneous $CH_{1.5}$ on the z-interval $-H \leqq z \leqq H$, with Cd-layer at z = 0. Two different thicknesses of Cd were studied. The slab thickness 2H was essentially infinite.

Source: Monoenergetic neutrons at various heights z and with various directions from OZ. A series of source energies was studied.

Neutron parameters: z, w, E, τ, W, and a parameter indicating the status of the neutron relative to two problems run simultaneously. (See Remarks.)

Physical processes: H-capture at thermal energy (only), Cd-capture, elastic scattering on H isotropic in C.M. system at energies above thermal, and isotropic in lab. system at thermal with no further energy loss. Elastic scattering on C was assumed isotropic in the lab. system with no energy loss at all energies.

Output: Classification of Cd-captures in .2 μsec intervals from time (t = 0) of leaving source to time cutoff of 30 μsec, 150 intervals in all, hydrogen capture, loss to time cutoff.

Remarks: The following conventions on Cd wall capture were adopted. The thicker wall captures all neutrons impinging on it at energies $< .4$ ev, while the thinner wall captures all neutrons impinging at energies $< .34$. The thick and thin Cd-wall problems were run simultaneously by keeping separate counters $N_1, \ldots, N_{150}$ and $N'_1, \ldots, N'_{150}$ for the two time distributions and following the path of a neutron further for purposes of the thin wall problem after it had been classified terminally as captured in the thick wall problem.

Problem 12

AN α DETERMINATION

Coder: J. M. Kister

Requester: R. B. Lazarus

Medium: Bare homogeneous Oy sphere.

Source: Initially an arbitrary distribution of neutrons in energy groups g = 1, 2, 3, radial zones z = 1, ..., 10, and cosine intervals j = 1, ..., 10, 300 categories in all.

Neutron parameters: R, w, V = $\sqrt{E}$, g.

Physical processes: The usual processes for a fissionable element were treated by the transfer matrix method of Ch. V, §12.

Output: The problem was run in cycles of fixed time length $\Delta\tau$, the output $N_{g,z,j}$ of one cycle serving as the number of neutrons to be processed in category (g,z,j) during the next. The problem run was close to critical, so that no re-normalization was involved. (Cf. Ch. II, §8, and Ch. IV, §9.)

Problem 13

NEUTRON FLUX IN AIR

Coder: R. G. Schrandt

Requester: J. Hall, R. G. Wagner, and G. M. Wing

Medium: Sphere of homogeneous air zoned for computational purposes by radii $R_1 < R_2 < R_3$.

Source: Monoenergetic isotropic point source at center R = 0. Various initial energies were studied.

Neutron parameters: R, w, E, g, W, z.

Physical processes: Elastic scattering on O and N assumed isotropic in C.M. system.

Output: Loss to energy cutoff in each zone, loss from system (at R_3), loss to weight cutoff. These were the only terminal categories. However, the purpose of the problem was to determine total flux at R_1, R_2, R_3. Counters were, therefore, provided to tally all neutrons crossing each boundary R_γ in each energy group g in outward direction and in inward direction. (Cf. Ch. IV, §4.)

Remarks: Weights were used in connection with the device discussed in Ch. V, §7, for avoiding loss of trajectories to energy cutoff. Thus no trajectory terminated until loss to weight cutoff or loss from R_3.

Problem 14

ESCAPE DISTRIBUTION FROM A CARBON SLAB

Coders: M. B. Wells and R. G. Schrandt

Requester: T. B. Taylor

Medium: Plane slab of C on $0 \leqq z \leqq Z$.

Source: Monoenergetic neutrons upwardly directed at z = 0 in cosine distribution.

Neutron parameters: z, w, E, g".

Physical processes: Elastic scattering on C governed by a differential cross section of form $\sigma^*(g,\mu) = A_g + C_g \mu^2$.

Output: 13 energy group classification escapes at z = 0 and z = Z. Energy cutoff losses classified according to position in five sub-intervals.

Problem 15

ESCAPE DISTRIBUTION FROM A SPHERICAL SHELL

Coders: M. B. Wells and R. G. Schrandt

Requester: C. L. Longmire

Medium: Spherical shell of hydrocarbon on $R_1 \leqq R \leqq R_2$.

Source: Monoenergetic neutrons directed into shell at R_1 in cosine distribution.

Neutron parameters: R, w, E, g".

Physical processes: Elastic scattering on H isotropic in C.M. system, on carbon as in Problem 14.

Output: 13 energy group classification of escapes at R_1, escapes at R_2, loss to energy cutoff.

Problem 16

A ROCKET MOTOR

Coder: R. L. Bivins

Requesters: G. I. Bell and C. L. Longmire

Medium: Cylindrical container of C, U, H, with C of uniform density, H and U of prescribed densities in each of a set of shell zones, defined by 7 radial and 15 height intervals. This cylinder was surmounted by a coaxial cyclinder of H and Be at specified densities, and these two cylinders were surrounded by a cylindrical shell of Be. The U-density distribution was subject to change from problem to problem, of which a whole series was run. (Cf. Fig. 64.)

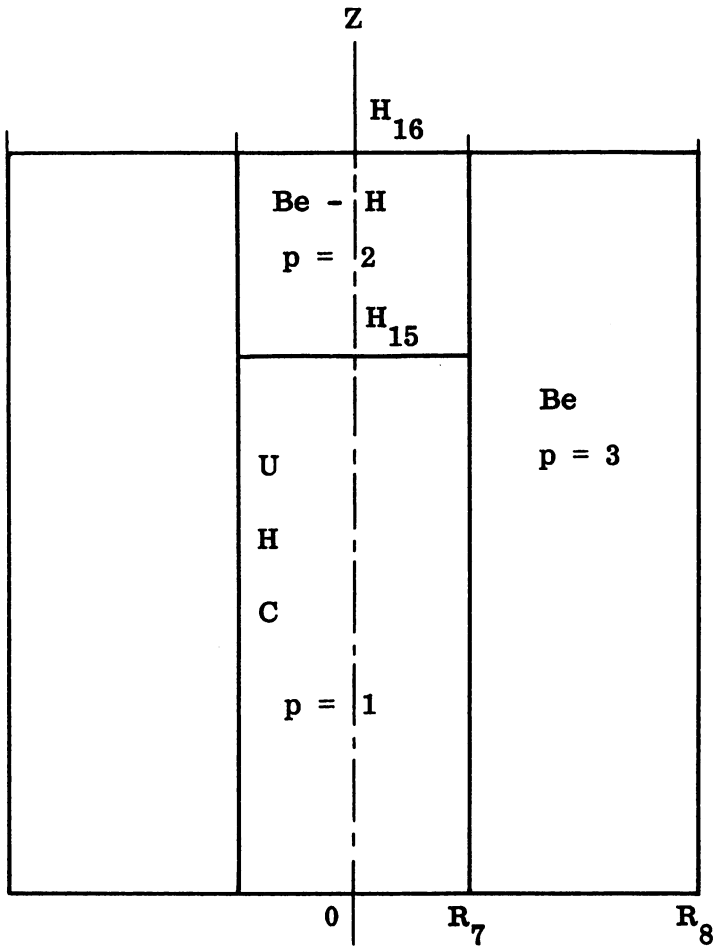

Fig. 64

Source: Isotropic source in fission energy spectrum, spatially distributed as prescribed among the 105 zones. The spatial distribution also varied with the problem and was so normalized that integral numbers N_γ of neutrons were involved in each source.

Neutron parameters: x, y, z, u, v, w, E, g, γ, W, and a sector parameter p = 1, 2, 3. (See Fig. 64.) The zone parameter γ is really a pair i,j which define the associated radial and height zones.

Physical processes: Be-capture at "thermal" energy; U-capture, fission, elastic and inelastic scattering; elastic scattering on C and Be assumed isotropic in lab. system, using transport cross sections for free path contributions but with correct energy losses. Elastic scattering on H isotropic in C.M. system.

Output: Losses from system classified according to surface of escape; Be-capture; U-capture; number N'_γ of fissions in each of the 105 spatial zones. Fission was regarded as a terminal event.

Remarks: There was no loss to energy cutoff; neutrons degrading to "thermal" energy were allowed to scatter isotropically in the lab. system without further loss of energy. A neutron was followed until capture, fission, or escape occurred. The purpose of the problem was to determine a U-density distribution together with a fission source distribution in space which would produce a steady state in the sense that the output N'_γ and input N_γ should satisfy the equations

$$N'_\gamma = \nu_o^{-1} N_\gamma$$

where ν_o is the fission multiplication constant. Such problems arise in the design of nuclear rocket motors, the hydrogen of the problem being present in the form of a propellant gas.

Problem 17

PHOTON DIFFUSION IN A REACTOR

Coder: R. G. Schrandt

Requesters: M. E. Battat and B. M. Carmichael

Medium: Cylindrical assembly consisting of inner fuel region, tamper, and top and bottom reflectors of given electron densities.

Source: Prompt γ-rays in exponential energy distribution $n(E)dE = k \exp(-1.01\,E)dE$, $.2 \leqq E \leqq 5$ Mev, isotropic in direction, and with given radial and heightwise photon density distributions throughout the fuel.

Photon parameters: x, y, z, u, v, w, E, g, m (medium index indicating region of occupancy: fuel, tamper, or reflectors), R'^2, R''^2, H', H" defining radial and height boundaries of region m.

Physical processes: Compton scattering of photons on electrons with energy losses due to such scattering and to cutoffs (varying with m) chosen at the point where the photoelectric effect becomes an effective absorption.

Output: Distribution in energy and angle of photons escaping each of outer surfaces, energy deposition within the system in 82 spatial regions.

Problem 18

A THICK Zr TARGET PROBLEM

Coder: R. G. Schrandt

Requesters: L. P. Stewart and L. P. Rosen

Medium: Solid Zr cylinder.

Source: Parallel beam of monoenergetic (14 Mev) neutrons incident on base of cylinder.

Neutron parameters: x, y, z, u, v, w, ν, E, f, g, h (cf. Problem 7).

Physical processes: Those of Problem 7 except that the (n-2n) process was replaced by a more general process involving production cross sections for neutrons in each of two energy distributions with a total expectation of 2.32 neutrons.

Output: As in Problem 7.

Remarks: The problem was handled by a revision of the code of the problem cited.

Problem 19

A THICK C TARGET PROBLEM

Coder: R. G. Schrandt

Requesters: L. P. Stewart and L. P. Rosen

Medium: Solid carbon cylinder.

Source: Monoenergetic (14.1 Mev) neutrons in parallel beam incident on base of cylinder.

Neutron parameters: u, v, w, x, y, z, E, g, ν.

Physical processes: Elastic scattering according to given differential cross sections curves on four ranges between 14 and 0 Mev; capture; inelastic scattering for levels 4.4, 7.6, 9.6, and 11.2 Mev (the latter an average for levels >9.6), inelastic scattering at 4.4 level for incident energy >10 Mev governed by given $\sigma(E,\theta)$, all other inelastic scattering assumed isotropic in C.M. system.

Output: Distribution in 28 energy groups and 10° angular intervals (with vertical) of neutrons escaping after one or two collisions, total number of second collisions.

Remarks: First collision forced, neutrons forced out after a second collision. Method of Ch. V, §9, used to determine parameters after inelastic collision.

Problem 20

HEAVY WATER EXPERIMENT

Coder: R. G. Schrandt

Requester: J. N. Grundl

Medium: Heavy water in (A) spherical shell, (B) hemispherical shell. Both problems run simultaneously. A series of runs involved various inner and outer radii.

Source: Isotropic point source at center of system in fission-neutron energy distribution, $.1 \leqq E \leqq 10$ Mev.

Neutron parameters: u, v, w, x, y, z, E, g, μ (parameter indicating trajectory lost relative to problem (B) or not).

Physical processes: Elastic scattering on D and O assumed isotropic in C.M. system; transport cross section based on this assumption used for free path.

Output: For problems (A) and (B), loss to outer surfaces, loss to energy cutoff, classification in 25 energy groups of neutrons re-entering central cavity with normal angles in each of four angular ranges.